Coordination Chemistry Reviews 253 (2009) 3015–3041

Contents lists available at ScienceDirect

Coordination Chemistry Reviews

journal homepage: www.elsevier.com/locate/ccr

Review

Optical properties and applications of hybrid semiconductor nanomaterials

Jinghong Li[a,*,1], Jin Z. Zhang[b,*]

[a] Department of Chemistry, Key Lab. of Bioorganic Phosphorus Chemistry & Chemical Biology, Tsinghua University, Beijing 100084, China
[b] Department of Chemistry and Biochemistry, University of California, 1156 High Street, Santa Cruz, CA 95064, USA

Contents

* Corresponding author. Tel.: +1 831 459 3776; fax: +1 831 459 2935.
E-mail addresses: jhli@mail.tsinghua.edu.cn (J. Li), zhang@chemistry.ucsc.edu (J.Z. Zhang).
[1] Tel. +1 86 10 62795290; fax: +1 86 10 62771149.

0010-8545/$ – see front matter
doi:10.1016/j.ccr.2009.07.017

ARTICLE INFO

Article history:
Received 12 February 2009
Accepted 23 July 2009
Available online 3 August 2009

Keywords:
Optical properties
Semiconductor nanomaterials
Hybrid nanomaterials
Composite nanomaterials
Hybrid semiconductor nanomaterials
Quantum dots
Metal nanoparticles
Solar cells
Sensors
Biomedical imaging
Cancer therapy
Photodynamic therapy
Photocatalysis
Photoelectrochemistry
Lasers
Light emitting diodes
Electroluminescence
Photochromism
Electrochromism
Light energy conversion
Hydrogen generation
Fuel cells
Water splitting
Solid state lighting
Chemical sensing

ABSTRACT

Hybrid semiconductor nanomaterials (HSNs) possess unique and interesting optical properties and functionalities that find important applications in emerging technologies. Compared to single component nanomaterials, hybrid nanomaterials offer the possibility and flexibility to control their properties by varying the composition of the materials and related parameters such as morphology and interface. Hybrid nanomaterials are essentially composite materials with relevant physical dimensions for the interface region between different components on the atomic up to nanometer scales, the same length scale of nanomaterials. This article provides an overview of some of the fundamental optical properties of hybrid semiconductor nanomaterials as well as their exploitation for potential applications in different fields. A number of examples from recent research are discussed to illustrate the points of interest and to highlight the salient features of HSNs.

1. Introduction

1.1. Motivation for hybrid semiconductor nanomaterials (HSNs)

Nanomaterials have interesting properties and useful functionalities that can differ substantially from their bulk counterparts. For instance, spatial quantum confinement effect results in significant change in optical properties of semiconductor nanomaterials. Likewise, the very large surface-to-volume (S/V) ratio has major influence on their optical and surface properties. As a result, semiconductor nanomaterials have attracted significant attention in research and applications in areas including energy conversion, sensing, electronics, photonics, and biomedicine. Parameters such as size, shape, and surface characteristics can be varied to control their properties for different applications of interest.

For many applications, it is highly desired to be able to control and alter the properties and functionalities of nanomaterials with greater flexibility and possibility. One approach is to use hybrid nanomaterials that have properties different from those of single component nanomaterials. The use of multiple components offers a higher degree of flexibility for altering and controlling properties and functionalities of nanomaterials. Hybrid nanomaterials can be generally defined as nanomaterials that contain more than one single component. Examples include doped nanomaterials and composite nanomaterials. For many emerging technologies, hybrid nanomaterials with improved optical and electronic properties are needed, including solar energy conversion, optical devices, optical imaging, and biomedical detection and therapy.

Hybrid nanomaterials have many different useful properties and applications. In this review, we focus on optical properties and related functionalities and applications. In principle, the constituting components can be insulators, semiconductors, or metals. The components can also be classified as inorganic, organic, or biological. Due to space limitation, we will further restrict ourselves to hybrid nanomaterials that contain an inorganic semiconductor as one of its components. Thus, the emphasis is on *optical properties and applications of hybrid semiconductor nanomaterials* (*HSNs*).

1.2. Energetic and structural nature of HSNs

The different components in HSNs have apparently different chemical and physical properties. Following the conventional classification of materials as metal, semiconductor and insulator, one can have hybrid nanomaterials with two components of metal–semiconductor, metal–insulator, semiconductor–insulator, and so on. They could also be composed of two different metals or two different semiconductors, etc. Of course, a hybrid system can also be composed of multiple components.

The difference in optical properties between hybrid nanomaterials and their constituent components depends largely on the chemical nature of each component as well as how the two or more components interact with each other. The interaction between the components depends strongly on characteristics such as interface, size, shape, and structure. In the extreme case of no or little interaction between the components, the optical properties of the composite should be equivalent to a simple sum of the optical properties of the individual components. In cases where the interaction between the components is strong, the optical properties of the composite system can differ substantially from the simple sum of the properties of the individual components. The characteristics of the individual components are lost and new feature arise as a result of the strong interaction. For example, new absorption and emission bands may appear in the absorption and emission spectra of hybrid nanomaterials as compared to the individual components. This can be rationalized by considering the interaction as a perturbation and the starting individual components as the zeroth-order system.

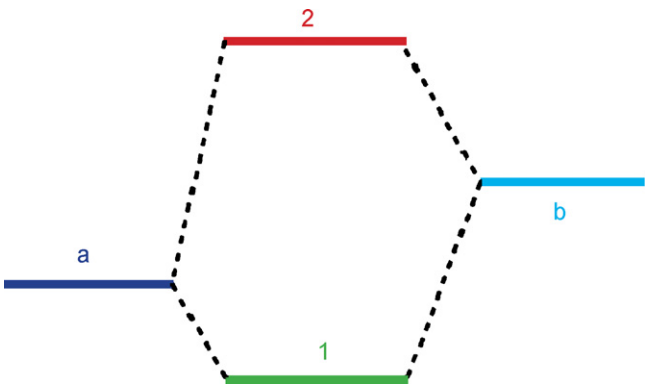

Fig. 1. Illustration of the energy levels of the zeroth-order systems, *a* and *b*, vs. those of the resulting hybrid material for a two-component system. The energy difference between 1 and 2 depends on how strong the interaction is between *a* and *b*; stronger interaction between *a* and *b* results in large energy difference between 1 and 2 and the new states for the composite are more dissimilar to the zeroth-order states *a* and *b*.

For example, in a simple two-component system consisting of two different materials *A* and *B*, their interaction can be considered as a perturbation or coupling energy *V*. If the zeroth-order wavefunctions are labeled as ψ_a and ψ_b and the new composite system wavefunctions labeled as ψ_1 and ψ_2 for the lower and higher energy states resulting from the two initial zeroth order states, applying perturbation theory then gives us the following:

$$\psi_1 = c_1\psi_a + c_2\psi_b \quad (1)$$

$$\psi_2 = c_1'\psi_a + c_2'\psi_b \quad (2)$$

The coefficients in the above two equations depend on the strength of perturbation *V*. This is similar to the treatment of molecular orbitals for a heterodiatomic molecule from atomic orbitals of two different atoms. In general, the stronger *V* is, the more different the new states from the zeroth-order states. Fig. 1 shows a schematic of the energy level involved in such a simple two-component system.

Most hybrid systems are featured with moderate interaction. In such cases, the optical properties of hybrid materials may still resemble those of the individual components while some changes may occur or new features may arise, but usually not to the degree as in the strongly interacting case. For example, absorption and/or emission bands of the hybrid system will likely exhibit modest changes compared to those of the original components, e.g. spectroscopic shift or line width broadening.

Since this review focuses on inorganic hybrid semiconductor nanomaterials, the systems to be discussed will have at least one component that is an inorganic semiconductor nanomaterial. We will exclude *alloys* that are atomic level hybrid materials. The hybrid systems to be discussed are made up of at least two components and each composite retains its chemical identity with physical dimension on the few to a few hundred nm scales. We further restrict to situations where at least one component is nanocrystalline, which is considered as the primary component. If non-crystalline components are present, e.g. passivating molecules, they will be considered as secondary components. By doing so, systems that are entirely amorphous, i.e. non-crystalline, on the atomic scale will be excluded. The electronic energy levels or structure in the hybrid system is dependent on the crystal structure of the individual components

Besides energetic properties, inter-component structural or morphological properties of hybrid nanomaterials are also important in determining their properties and functionalities. Fig. 2 shows an illustration of a simple two-component system in which each component is crystalline. Of course, most real hybrid nanomaterials have more complex compositions and structural features, with

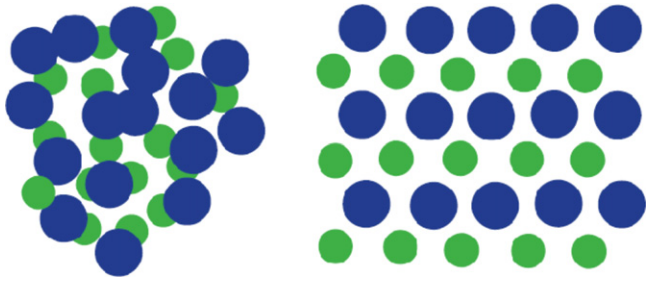

Fig. 2. Schematic of a two-component hybrid system with no structural order, e.g. aggregates (left), and with order, e.g. a superlattice (right), between the individual nanoparticles of the two components that are assumed to be spherical and crystalline. The ordered structure is basically a binary superlattice structure.

specific examples given later. The case on the left of Fig. 2 has no long-range order among the constituting nanoparticles while the case on the right does. The two systems illustrated can have quite different properties due to their difference in structure [1].

A special note should be made about the distinction between semiconductors and insulators, particularly when applied to metal oxides (MOs). Some MOs are insulators while others are considered as semiconductors, depending on their bandgaps. There is no clear-cut about what the bandgap energy should be in distinguishing semiconductors and insulators, even though 3.5–4.0 eV is usually chosen somewhat arbitrarily as the dividing point [1]. Materials with bandgap larger than this number are often considered as insulators while those smaller semiconductors. Sometimes, a given MO with a fixed bandgap can be considered as insulator or semiconductor, depending on the relevant context. Also, the bandgap energy could differ depending on if it is defined optically or electrically. For example, TiO_2 and ZnO are considered as insulators optically in most contexts due to weak or no visible absorption. However, they are often considered as wide bandgap semiconductors also because of their electrically semiconducting properties usually caused by doping. Furthermore, when they are hybridized with a small bandgap semiconductor such as ZnSe or metal such as gold, it is more convenient to treat TiO_2 and ZnO as insulators since the optical and electrical properties for such systems will be dominated by the small bandgap semiconductor or metal. In this article, we will consider MOs mainly as insulators since the focus is on optical properties and application. In some context, it is more appropriate to consider some MOs, such as TiO_2 and ZnO, as semiconductors and proper justification will be given when this occurs.

1.3. Synthesis of HSNs

In the interest to save space and stay focused, this review will not provide a detailed discussion of synthesis and characterization of nanomaterials including HSNs. However, a brief discussion is given to make the text self-contained and better connected to the discussion of optical properties and applications later. Synthesis of HSNS is presented next with characterization presented in the following section.

Methods for synthesis and fabrication of nanomaterials can be roughly divided into and gas- or vapor-based (chemical or physical) and solution-based (usually chemical). Gas- or vapor-based techniques include chemical vapor deposition (CVD), metal–organic CVD (MOCVD) [2–10], and molecular beam epitaxy [11,12]. Solution-based techniques include precipitated hydrolysis, melting and rapid quenching, hydrothermal, and thermal decomposition. In solution-based synthesis, two critical steps involved are initial nucleation and subsequent growth [13], which apply for metal, semiconductor or insulator. The properties of the nanomaterials

produced, e.g. size, shape, and crystal structure, can be varied by controlling the nucleation and growth processes.

For metal nanomaterials, the synthesis usually involves reduction of metal salts or metal ions by appropriate reducing agents in solution. Simple reduction reactions usually produce small nearly spherical nanoparticles [14–20]. For large nanoparticles, the technique of seed-mediated growth has been developed [21–25]. For more complex shaped structures, such as nanorods, aggregates, hollow nanospheres, nanowires, nanocages, nanoprisms, and nanoplates, the synthesis is typically more involved, including using surfactants such as cetyltrimethylammonium bromide (CTAB) [26–31] or galvanic replacement [32–37].

For semiconductor nanomaterials (quantum dots, QDs or nanocrystals, NCs), the synthesis methods vary depending on the nature of the semiconductor. For semiconductors such as Si and Ge that involve only one element, their synthesis usually involve reduction of a salt of the corresponding element with appropriate reducing agent or decomposition of precursor compounds, which is similar to the synthesis of metal nanomaterials [38–42]. In a typical synthesis of binary semiconductors such as II–VI and III–V semiconductors, reactants or molecular precursors containing the desired cation and anion components are mixed in an appropriate solvent to produce the nanostructures of interest [43–50]. Surfactant or capping molecules are often used to stabilize the nanoparticles or to direct particle growth along a specific crystal plane to produce nanospherical structures [51]. Nanoparticles in aqueous solutions tend to have a high density of defects or trap states and low overall photoluminescence (PL) yield. Their optical properties, especially PL, are usually sensitive to pH of the solution [52]. Recently, synthesis of semiconductor nanomaterials in organic solvents has produced various high quality nanoparticles in terms of size monodispersity, surface properties, and PL yield. The organic solvents are usually mixtures of long chain molecules, e.g. alkylphosphines, R_3P, alkylphosphine oxides, R_3PO (R = butyl or octyl), and alkylamines [43]. For instance, highly monodisperse and luminescent II–VI semiconductors such as ME (M for metal such as Cd and Zn and E for S, Se, and Te) have been synthesized by injecting liquid metal–organic precursors containing M and E into hot (around 150–350 °C) coordinating organic solvents [13].

For insulator nanomaterials, the general synthetic strategy is very similar to that used for synthesizing semiconductors. Most insulator nanomaterials are based on binary compounds, e.g. ZrO_2, and their synthesis in solution involves reaction between reactants containing the appropriate cation and anion components [53]. Solution methods, e.g. hydrolysis, are most commonly used for making MO nanoparticles or other shaped nanomaterials, e.g. TiO_2, ZnO, WO_3, and SnO_2 [54–59] As a complementary method, hydrothermal synthesis is also often used for making MO nanomaterials [60–65], which is particularly useful for making non-spherical particles such as one-dimensional (1D) nanostructures [66–68].

Specific for HSNs, the synthesis is usually based on either a sequential, step-wise approach or simultaneous, one-pot or one-step approach. In a sequential approach, the different components are synthesized first separately or in different steps, and the hybrid system is produced at the end. This is the more commonly used method. In the one-pot approach, all the reactants are added simultaneously and the different components are produced at the same time.

The sequential approach has often been used to make "core/shell" structures, a class of unique hybrid nanostructures that contain two different types of materials, one as the core and another as the shell. Various combinations of core/shell structures can result from using metal, semiconductor, or insulator for the core or shell, or just two different metals, semiconductors, or insulators for the core and shell [69–71]. The shell is usually used to alter the properties of the core for different applications of interest. For example, CdSe/ZnS was studied as a system to enhance PL stability and yield of CdSe as well as to lower the toxicity since ZnS is less toxic than CdSe [72–74]. The shell semiconductor is usually chosen to have larger bandgap and lower toxicity compared to the core semiconductor. For example, CdSe NCs were overcoated with a shell of ZnS [72–78], ZnSe [79], or CdS [47,80], which resulted in dramatic improvements in luminescence efficiency of CdSe [73]. More complex structures, such as core/shell/shell, can also be produced, e.g. CdS/HgS/CdS [81,82]. The detailed crystal structures of the shells are usually not as well identified as the core due to their thinness. In many cases, the shells are polycrystalline. Other examples of core/shell hybrid nanomaterials include CdS/TiO_2 [83], CdS/Au [84], TiO_2/Pt [85], TiO_2/Au [86], TiO_2/CdSe [87], CdSe/SiO_2 [88], CdTe/SiO_2 [89], and Au/SiO_2 [90–92]. In synthesis, the shell is produced after the core in a sequential manner.

Another use of the sequential approach is for surface modification of nanostructures post synthesis. One example is silanization, i.e. coating of a silica layer on the nanostructure surface [93–96]. Surface modification is often necessary for specific applications. For instance, while QDs synthesized in organic solvents tend to have higher quality in terms of lower density of surface trap states and thus higher PL yield, their hydrophobic surfaces are not compatible with applications that require QDs with hydrophilic surfaces, e.g. biological applications involving aqueous environment. In order to render QDs with hydrophobic surface hydrophilic, a number of strategies have been developed, including ligand exchange [97–100], silanization [101–103], and surface coating using amphiphilic polymers or surfactants such as phospholipids [104–107]. All these strategies for surface modification result in practically hybrid nanostructures with the primary component being a semiconductor, at least in terms of optical properties of interest.

For one-pot approach to synthesizing HSNs, a good example is synthesis of doped semiconductor nanomaterials [108]. Doping refers the process of intentionally introducing a small amount of a foreign or different element into a host material. For example, B or N can be introduced into Si as a way to alter its chemical composition and, more importantly, to influence its properties, e.g. optical and electronic. Another major use of doping is in phosphors based on binary semiconductors such as ZnS with dopants such as Cu, Mn, and Ag ions [108–119]. For doped nanomaterials, the method is often only slightly altered from that used for undoped semiconductor synthesis. The main modification is that the dopant element is introduced during synthesis. For doping to be successful, the dopant needs to be compatible to the host material. Similarly, many MO semiconductors and insulators have been successfully doped with different elements such as Gd^{3+} [55], N [120–124], C [125], and Tb^{3+} [126]. For example, Cu-doped ZnO NCs were synthesized using copper acetate and zinc acetate as the Cu and Zn sources, respectively, through hydrolysis using sodium hydroxide and with isopropanol as a solvent [127].

More complex nanostructures can also be produced but usually involve multiple steps and processes such as self-assembly [128–132]. Discussion of synthesis of such structures is beyond the scope of this review.

1.4. Characterization of HGNS

Many techniques have been employed to characterize nanomaterials including HSNs. Since HSNs are more complex than single component nanomaterials, their characterization usually demands a combination of techniques or more sophisticated techniques. In general, the characterizations are based on spectroscopy, microscopy or X-ray techniques.

Optical spectroscopic techniques are widely used in the study of optical properties of different materials including nanomateri-

als [133]. The different techniques are usually based on measuring absorption, scattering or emission of light that contains information about properties of the materials. Commonly used techniques include electronic absorption (UV–vis), photoluminescence (PL), infrared red (IR) absorption, Raman scattering, dynamic light scattering, as well as time-resolved techniques, such as transient absorption and time-resolved luminescence [133]. Other more specialized techniques include single molecular spectroscopy and non-linear optical techniques such as luminescence up-conversion. These different techniques can provide different information about the molecular properties of interest, including energy levels, surface, and structure. UV–vis and PL are sensitive probes of electronic transitions and electronic structures while IR and Raman are sensitive to vibration or phonon structures. Dynamic light scattering is useful for determining global structure of nanomaterials. Time-resolved techniques are used to determine dynamic properties such as charge carrier lifetimes [134].

Besides optical spectroscopy, a number of other experimental techniques are routinely used for characterizing nanomaterials, including electron microscopy, electrochemistry, X-ray-based methods such as X-ray diffraction (XRD) [13,45,135,136], XPS, and EXAFS. While microscopy techniques are usually used to reveal structural, morphological, and topological information, X-ray techniques are applied to gain information about structure, energetic, and surface characteristics [1,128,137–145]. X-ray based spectroscopies are useful in determining the chemical composition of materials. These techniques include X-ray absorption spectroscopy (XAS), extended X-ray absorption fine structure (EXAFS), X-ray absorption near edge structure (XANES), X-ray fluorescence spectroscopy (XRF), energy dispersive X-ray spectroscopy (EDX), and X-ray photoelectron spectroscopy (XPS) [146,147]. They are mostly based on detecting and analyzing radiation absorbed or emitted from a sample after excitation with X-rays, with the exception that electrons are analyzed in XPS. The spectroscopic features are characteristic of specific elements and thereby can be used for sample elemental analysis. Other related techniques include small angle X-ray scattering (SAXS) and wide angle X-ray scattering (WAXS) that are useful for structural determination [148–150]. SAXS arises from inhomogeneous electron density on different length scales ranging from angstroms to microns, while WAXS primarily arises from regular, periodic variations of electron density over length scales that are large compared to the repeat distance.

Scanning probe microscopy (SPM) represents a group of techniques, including scanning tunneling microscopy (STM), atomic force microscopy (AFM), and chemical force microscopy (CFM), that have been extensively applied to characterize nanostructures [137,143,144,151]. A common characteristic of these techniques is that an atomically sharp tip scans across the specimen surface and the images are formed by either measuring the current flowing through the tip or the force acting on the tip. SPM can be operated in a variety of environmental conditions and in different liquids or gases, allowing direct imaging of inorganic surfaces as well as organic molecules. It also allows manipulation of objects on the nanoscale. For non-conductive nanomaterials, AFM is a better choice [143–145]. AFM operates in an analogous manner as STM except the signal is the force between the tip and the solid surface. The interaction between two atoms is repulsive at short-range and attractive at long-range. The force acting on the tip reflects the distance from the tip atom(s) to the surface atom, thus images can be formed by detecting the force while the tip is scanned across the specimen.

Scanning electron microscopy (SEM) is a powerful and popular technique for imaging the surfaces of almost any material with a resolution down to about 1 nm [138,139]. The image resolution offered by SEM depends not only on the property of the electron probe, but also on the interaction of the electron probe with the specimen. Interaction of an incident electron beam with the specimen produces secondary electrons along with back-scattered electrons. While the secondary electrons detected in SEM provide primarily topographic information, e.g. surface texture and roughness, back-scattered electrons afford both topographic and compositional information [152,153]. Similarly, transmission electron microscopy (TEM) is a high spatial resolution structural and chemical characterization tool [154]. A modern high resolution TEM (HRTEM) has the capability to directly image atoms in crystalline specimens at resolutions close to 1 Å, smaller than the interatomic distance. This type of analysis is extremely important for characterizing materials at a length scale from atoms to hundreds of nanometers. TEM can be used to characterize nanomaterials to gain information about particle size, shape, crystallinity, and interparticle interaction [138,155].

2. Optical properties of HSNs

For convenience of discussion, we will divide the HSNs into different groups based on the chemical nature of their components. We will be concerned primarily with two-component systems, denoted as *A*–*B*, with one component (*A*) being a primary inorganic semiconductor. The other, secondary component (*B*) can be inorganic, organic, or biological. The following discussion will follow the classification of *A* being the primary semiconductor and *B* being the secondary component that can be an insulator (inorganic, organic, or biological), semiconductor (inorganic or organic), and metal (inorganic). In practice, *B* itself can be composed of more than one component and some examples will be given.

2.1. Inorganic semiconductor–insulator

2.1.1. Inorganic semiconductor–inorganic insulator

Inorganic semiconductors and insulators have often been used to produce hybrid materials for various applications including electronics and sensors as well as for exploration of potential new properties. For example, a film of SiO_2 nanoparticles with CdSe nanoparticles with good dispersion on the nanoscale would be considered as an inorganic semiconductor–insulator system. For such systems, the optical properties are usually dominated by the semiconductor, at least in the visible region, since the small bandgap of the semiconductor, compared to that of insulators, results in visible absorption and the insulator does not alter the semiconductor properties in a significant manner. However, if one considers the UV or VUV region, the insulator properties can be predominant. Therefore, the dominance of the component in the hybrid material properties depends on the energy or spectroscopic region considered. This is simply because different electronic transitions are involved in different energy regions.

The interaction between the semiconductor and insulator depends on how their lowest energy levels, e.g. valence and conduction band edges, are aligned. In a typical situation, the semiconductor has a smaller bandgap with bandedges fall within the bandgap of the insulator, as shown in Fig. 3. In such situations, the effect of the insulator on the electronic energy levels and thereby optical properties of the semiconductor is minimal. However, if the insulator helps to passivate the surface of the semiconductor as in a core/shell structures, the PL intensity of the semiconductor may be substantially enhanced by the presence of the insulator (Fig. 3(right)).

On the other hand, if the conduction or valence bandedge of the insulator happens to fall within the bandgap of the semiconductor, energy or charge transfer could occur when the hybrid system is subject to photoexcitation. In this case, the optical and photochemical properties of the hybrid system could differ substantially from

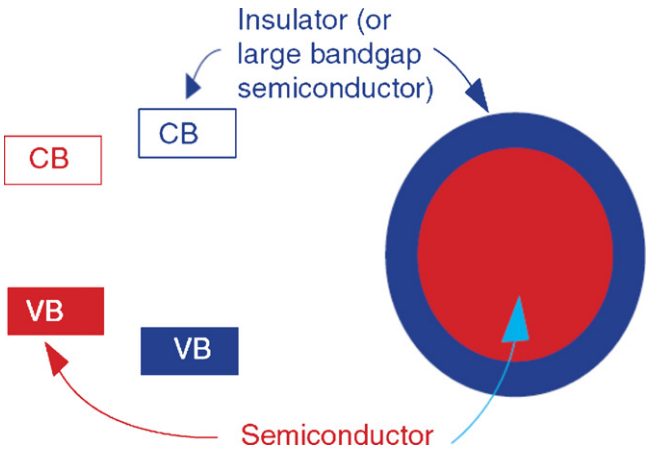

Fig. 3. Illustration of the energy levels (left) of a typical semiconductor–insulator hybrid system, exemplified by a core/shell nanostructure (right). The scenario could be for a small bandgap semiconductor (red, core) as the core and a larger bandgap semiconductor (blue, shell) as the shell. The difference is only quantitative in the bandgap for the insulator vs. the larger bandgap semiconductor. The relative band-edge positions will depend on the specific systems and could significantly affect the optical and electronic properties of the hybrid system. VB and CB are for valence band and conduction band, respectively. (For interpretation of the references to color in this figure legend, the reader is referred to the web version of the article.)

those of the semiconductor. Such situations are not as commonly encountered as the situation illustrated in Fig. 3.

Examples of inorganic semiconductor–inorganic insulator hybrid nanomaterials are numerous. We will provide two examples to highlight their optical properties. The first example is silica-coated CdSe/ZnS core/shell QDs useful for biolabeling and other applications [102]. In this case, the CdSe/ZnS core is considered as the primary semiconductor system, which by itself is a hybrid system composed of two semiconductors, as will be discussed further later. Fig. 4 shows some UV–vis and PL spectra of these silanized QDs. It was found that the silica coating does not significantly modify the optical properties of the nanocrystals. The silanized nanocrystals exhibit enhanced photochemical stability over organic dye molecules and display high stability in buffers at physiological conditions (>150 mM NaCl), which are desired for conjugation to biological molecules.

The second example is CdSe QDs embedded into TiO_2 matrix with TiO_2 essentially functioning as an insulator even though in some settings TiO_2 is considered as a semiconductor. This is because the bandgap of CdSe is much smaller than that of TiO_2 and there is weak electronic interaction between CdSe and TiO_2. Fig. 5 shows a schematic for the nanocompsoite synthesis (A), STEM (B), and UV–vis and PL (C and D) of the QDs before (C) and after (D) they are incorporated into TiO_2 [156]. A comparison of Fig. 5C and D clearly shows that TiO_2 has little effect on the absorption and PL of the CdSe QDs. This hybrid system exhibits good photostability and easy processibility for non-linear optical applications.

Similarly, CdSe–TiO_2 hybrid nanomaterials have been studied and explored as a potential system for solar energy conversion applications [157]. Electrically, TiO_2 can be considered as a semiconductor due to its role in charge transport. However, optically, it functions as an insulator since the visible absorption of interest is mainly due to CdSe. This is very similar to the system in which CdSe, in conjunction with N-doping, was used to sensitize TiO_2 nanoparticles to enhance visible absorption for solar energy conversion application [158]. Similar systems include TiO_2/CdS [159–161], TiO_2/CdSe [162], ZnO/CdS [163], SnO_2/TiO_2 [164], SnO_2/ZnO [165,166], SnO_2/CdSe [167], TiO_2/ZnO [1,168], CoO/ZnO, and CoO/TiO_2 [169]. The large bandgap MO in each system is considered as an insulator due weak visible absorption while the smaller bandgap material can be considered as a semiconductor. Such semiconductor–insulator hybrids offer the opportunity to manipulate the band structure of the overall system for various applications of interest. Some of these systems could be considered as semiconductor–semiconductor hybrids as long as their electronic properties are concerned.

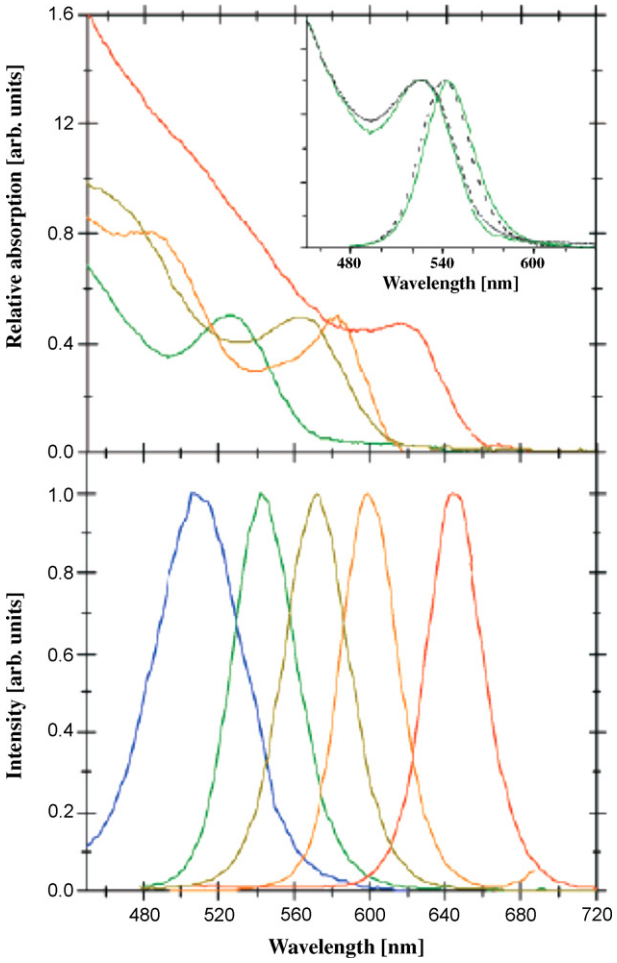

Fig. 4. Absorption (upper panel) and emission (lower panel) spectra of a series of silanized CdSe/ZnS in 10 mM PBS buffer, pH ~7. The data are normalized for the convenience of the display. From right to left, red, orange, yellow, green, and blue emitting nanocrystals are shown. For blue emitting particles, the absorption spectrum does not show features above 450 nm and is therefore omitted. Inset: Absorption and emission of silanized green nanocrystals in 10 mM PB (solid lines), and of the same green CdSe/ZnS particles in toluene (dashed lines). Reproduced with permission from Ref. [102]. (For interpretation of the references to color in this figure legend, the reader is referred to the web version of the article.)

2.1.2. *Inorganic semiconductor–organic insulator*

Beside inorganic insulators, organic or biological molecules can play a similar role as the inorganic insulators. The primary purpose of using the insulators is usually to protect or passivate the inorganic semiconductor nanomaterial for chemical and/or photo stability or other functionalities such as surface modification or conjugation to other molecules. The optical properties are usually not affected substantially by the insulator, especially in terms of optical absorption. PL properties can be very sensitive to the insulator on the QD surface.

For example, both small and large organic molecules, such as polymers, have been used to modify the surface of inorganic semiconductor NCs to create essentially inorganic–organic composite materials. There are two different classes of organic molecules: conjugated (aromatic with extended π-bonding) and non-conjugated, that have quite different optical and electronic properties. Gen-

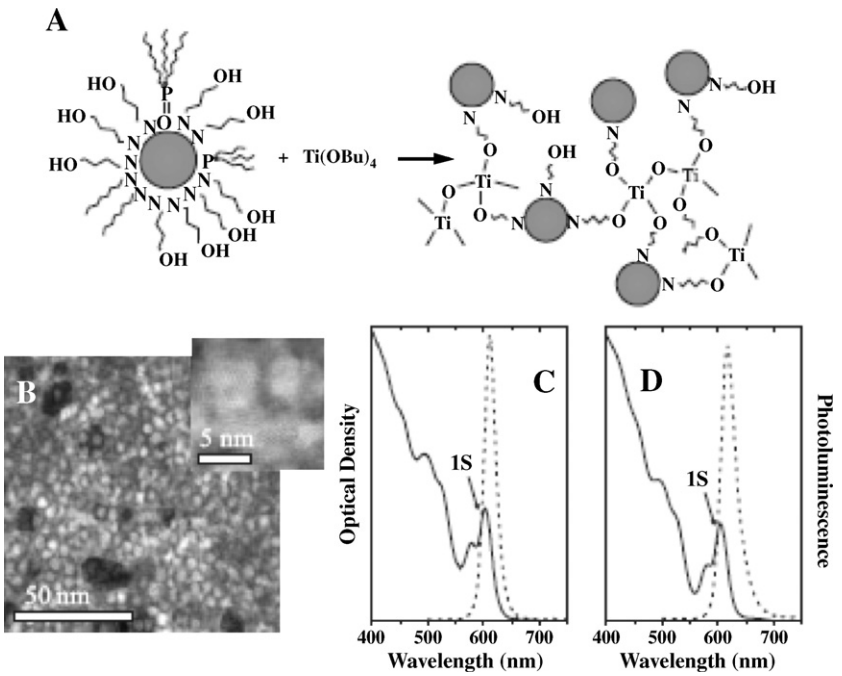

Fig. 5. (A) Schematic illustration of the pathway via which CdSe QDs are incorporated into a TiO_2 matrix. (B) Low and high (inset) resolution STEM of a thin sol–gel film containing CdSe QDs (white area). (C) UV–vis (solid line) and PL (dashed line) spectra of as-prepared CdSe QDs (R = 2.5 nm) in a hexane solution (the arrow indicates the lowest energy 1S exciton absorption resonance). (D) UV–vis and PL spectra of the same QDs incorporated into TiO_2. In this system, TiO_2 essentially functions as an insulator since the optical properties are dominated by the CdSe QDs. Reproduced with permission from Ref. [156].

erally, for non-conjugated organic molecules hybridized with inorganic, their influence on the properties of the inorganic is small, especially for metal and semiconductor materials. This is mainly because such organic molecules typically have no or weak visible absorption and their energy levels are not near those of the semiconductor or metal nanostructures, and thereby there is little energy level mixing or interaction. Their effect on optical properties of the metal or semiconductor is thus weak. In this situation, the effect of the organic molecules is similar to that of inorganic insulators.

Organic molecules can be small molecules or polymers. Many small molecules have been used to passivate inorganic semiconductor nanomaterials. For example, one of the most popular organic molecules used for surface passivation is trioctylphosphine oxide (TOPO) [13]. TOPO molecules provide good surface coverage and passivation of II–VI semiconductor QDs and afford the QDs high PL yield and stability. Similarly, a variety of organic polymers, mostly non-conjugated, have been used as matrix for creating composite nanostructures or for passivating the particle surface to stabilize their structures and optical properties, including semiconductor nanomaterials [170–180]. Interaction between the polymers and nanoparticles is often through functional groups such as –SH, –OH, $–NH_2$, and –COOH. Polymers have advantages such as low cost, flexible and large possible variations in structures, and ease to use. However, the nature of interaction between nanoparticles and the polymers tends to be complex and the surface passivation is usually not complete, resulting in a high density of surface trap states on the nanoparticle surface, as indicated by low PL yield and trap state PL in semiconductor nanoparticles.

2.1.3. Inorganic semiconductor–biological insulator

We will discuss semiconductor–biological hybrid nanomaterials that involve at least an inorganic, nanocrystalline semiconductor as the primary system and biological molecules as the secondary system. Such composites could form based on electrostatic interaction or mechanical force. However, in general, since most inorganic and biological systems are not naturally compatible, it is often necessary to provide a bridge or linker between the two components. A specific example is II–VI semiconductor QDs coated with bifunctional linker molecules for conjugating to protein or DNA molecules. The PL from QDs can be used for detection or imaging applications. For instance, if the conjugated protein is an antibody, the system can be used for detecting the corresponding antigen of interest. Likewise, a single strand DNA conjugated to the QDs can be used to detect the complementary DNA.

In the context of this article, semiconductor–biomolecule conjugates can be considered as hybrid nanomaterials. Similar to QD-non-conjugated polymers, as long as the biological molecules do not contain chromophores that cause absorption in the visible region of the spectrum, the QDs with strong visible absorption will dominate the optical properties of the composite system in the visible region. Indeed, in many respects, many biomolecules such as DNA, RNA, and proteins are non-conjugated polymers. The change to the optical properties of the QDs due to the biological molecules is usually small, at least in terms of spectroscopic features. The same is true for other non-conjugated or non-aromatic linker molecules, if present in the system.

However, in many cases the linker molecule and/or biological molecule could have substantial influence on the PL yield, and to a lesser degree, of PL spectrum, due to changes of the surface properties as a result of their presence on the QD surface. In some other cases, PL enhancement was observed, possibly due to better surface passivation when the biological or linker molecules are present. This is true for biological or linker molecules that are chemically and photochemically unreactive with the QDs, i.e. the molecules are stable on the QD surface with or without light. If the molecules are reactive, more significant changes, e.g. QD degradation, could occur.

Many QD-biomolecule conjugates have been designed and studied for bio detection applications. It is usually necessary to have the outer surface rendered hydrophilic for biological applications due to the aqueous environment. One example is CdSe/ZnS core/shell QDs [181], which are designed to create hydrophilic surface for bio detection and to enhance the chemical and optical stability of the QDs. Because of the CdSe core is well protected by the ZnS

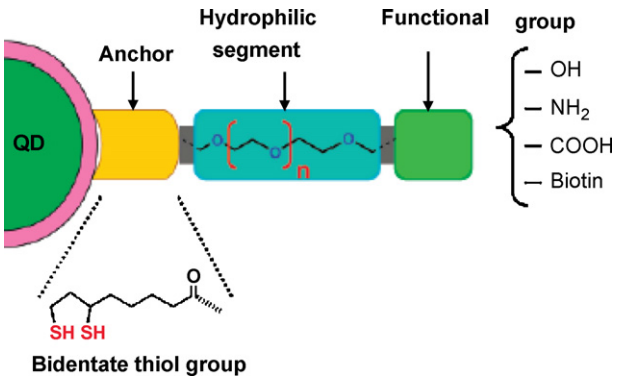

Fig. 6. An example of modular design of hydrophilic ligands with terminal functional groups. Dihydrolipoic acid (DHLA) is used, with one end, to cap CdSe/ZnS core/shell QDs and is linked, from the other end, to poly(ethylene glycol) (PEG). The out-pointing end of PEG is coupled with functional terminal groups to promote water-solubility and biocompatibility of the QDs. In this system, the QD is the primary inorganic semiconductor, labeled as component (A), and the rest of the components are considered as secondary, labeled as (B). In other words, this system contains more than two material components. Reproduced with permission from Ref. [181].

shell, the optical properties of such core/shell QDs are not sensitive to the surface molecular modification. As shown in Fig. 6, the modular ligands based on poly(ethylene glycol) (PEG) coupled with functional terminal groups have been found to promote water-solubility and biocompatibility of QDs. The overall nanostructures are stable over a broad pH range in aqueous solution and have been demonstrated to be useful for conjugation to a variety of biological molecules.

2.2. Inorganic semiconductor–semiconductor

2.2.1. Inorganic semiconductor–inorganic semiconductor

The situation for two semiconductors hybridized together is very similar to that of hybridized semiconductor–insulator with the main difference in the bandgap of the secondary semiconductor vs. that of the insulator. Core/shell structures such as CdSe/ZnS is essentially a semiconductor–semiconductor hybrid nanostructures. The properties of such structures strongly depend on their relative bandgap energies and interaction. Their interaction could depend sensitively on their structural and interfacial characteristics. In the case of CdSe/ZnS core/shell, the optical properties in the visible region are dominated by CdSe since its bandgap is smaller than that of ZnS. Fig. 7 shows UV and PL spectra of CdSe QDs passivated with TOPO or ZnS [73]. The ZnS passivation significantly enhances the yield and stability of the CdSe. Some of the hybrid systems discussed in Section 2.1.1, e.g. TiO_2/CdS [159,161], TiO_2/CdSe [162], ZnO/CdS [163], SnO_2/TiO_2 [164], SnO_2/ZnO [165,166], SnO_2/CdSe [167], TiO_2/ZnO [1,168], CoO/ZnO [169] could also be considered as inorganic semiconductor–inorganic semiconductor, especially if one focuses on their electrical or electronic properties.

2.2.2. Inorganic semiconductor–organic semiconductor

For conjugated organic molecules, including conjugated polymers with extended π-bonding, the energy level spacing between HOMO and LUMO is small, making them absorb visible light. Their energy levels are often close to those of inorganic semiconductors [180]. The conjugated polymers themselves behave like organic semiconductors. This makes it more likely to mix their energy levels, and their interaction is strong and can result in significant change in optical properties of the hybrid materials compared to their isolated components. The changes depend on the details of their energy levels with respect to each other.

For inorganic semiconductor–organic conjugated polymer hybrids, the situation resembles system composed of two different inorganic semiconductor nanomaterials since the conjugated polymer is practically a semiconductor. Their absorption spectra are often essentially a sum of the two materials while the PL of the hybrid system may differ substantially from those of the two isolated components because of expected strong interaction between the components. A number of studies have been done on semiconductor QD-conjugated polymer hybrid nanomaterials to gain a better understanding of their fundamental properties as well as to exploit their potential new properties for applications including sensors, light emitting diodes, and solar cells [182–191]. The change of optical properties of the composite as compared to the isolated QD or conjugated polymer depends sensitively on the relative electronic energy levels of the two components as well as how strongly they interact. Their electronic interaction also depends on their structural and interfacial characteristics. For example, in the hybrid system composed of CdS QDs and polyfluorene copolymers, CdS QDs enhance the PL as well as electroluminescence (EL) of the polyfluorene copolymer [188]. In the case of InP QDs with polythio-

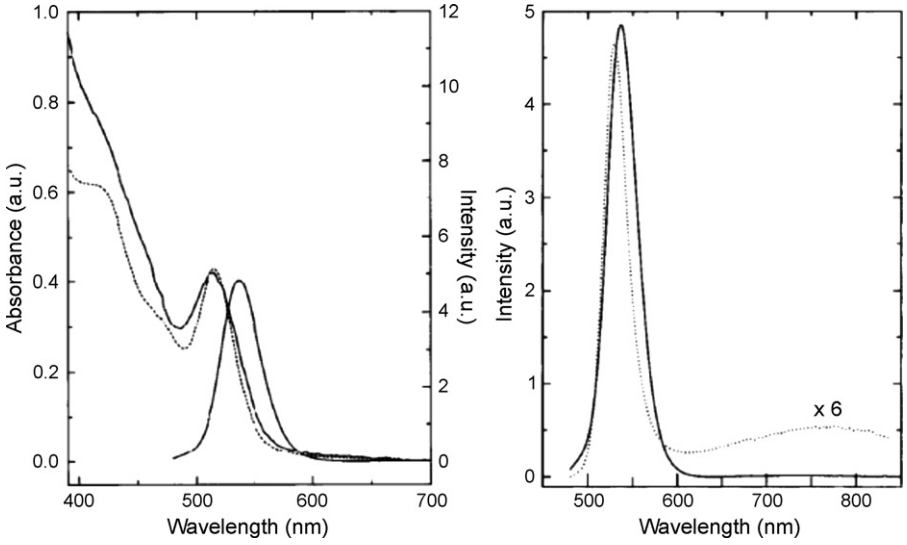

Fig. 7. (Left) Absorption spectrum of the (CdSe)TOPO (dotted line) and the (CdSe)ZnS nanocrystals (solid line). The fluorescence of the (CdSe)ZnS is also shown (solid line). (Right) Fluorescence of the (CdSe)TOPO (dotted line) and (CdSe)–ZnS (solid line) nanocrystals normalized by their absorption at the excitation wavelength (470 nm).

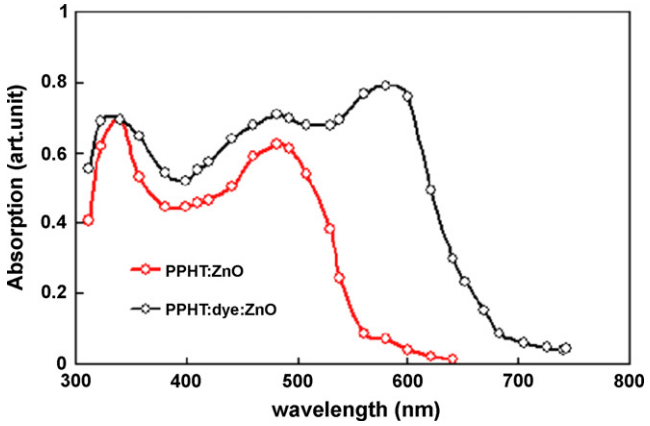

Fig. 8. UV–vis absorption spectra of PPHT:ZnO (lower) and PPHT:dye:ZnO (upper) thin films. The dye is safarine–O (SAF). Reproduced with permission from Ref. [191].

phene, the PL of the QDs is quenched by the conjugated polymer [186]. The PL quenching is attributed to photoinduced hole transfer from the QD to the conjugated polymer due to strong interaction between them. This finding has interesting implications in solar cell applications of this type of HSNs.

A similar system studied recently is ZnO with poly(3-phenyl hydrazone thiophene), PPHT, that was investigated for dye-sensitized solar cell applications [191]. Fig. 8 shows the electronic absorption spectra of PPHT:ZnO and PPHT:dye:ZnO thin films, with dye being safarine–O (SAF). The major absorption bands in the spectra can be easily correlated with ZnO (peaked ~425 nm), PPHT (~480 nm), and safarine–O dye (~680) and are not shifted noticeably from the peaks of the individual components. This indicates that there is no strong interaction or charge transfer in the ground state. However, PL of PPHT was found to be efficiently quenched by ZnO and further by the dye, attributed to charge and energy transfer from PPHT to the dye and ZnO [191].

2.3. Inorganic semiconductor–metal

Both semiconductor and metal are usually considered as active both optically and electronically since they usually have visible absorption due to electronic transitions in the relatively low energy region (1–3 eV). Their composites can have interesting and varied optical properties depending on the nature of the two components, their relative energy levels, their interactions, as well as the ratio between the two components. Their interactions are expected to depend on the details of their structures and the interface between them. Semiconductor–metal hybrid nanomaterials are generally more complex than their semiconductor–insulator or metal–insulator counterparts.

While the absorption spectrum of semiconductor–metal hybrid nanomaterials tend to be close to the simple sum of the spectra of the two individual components, at least when their electronic interaction is not strong, their PL properties often change significantly, especially in terms of intensity, either quenched or enhanced depending on the interaction and distance between the two components, compared to that of the semiconductor (metal usually with no or very weak PL). When one component is substantially dominant in size or weight over the other, the optical properties of the hybrid system tend to be primarily determined by the predominant component.

For example, Fig. 9 shows the UV–vis absorption and PL spectra of CdTe-Ag hybrid nanomaterials formed mainly through electrostatic interaction based on opposite charges on the Ag (negatively charged) and CdTe (positively charged) nanoparticles [192]. As can be seen, the absorption spectra exhibit an excitonic absorption band peaked around 433 nm typical for spherical CdTe nanocrystals. Upon addition of Ag nanoparticles, the CdTe excitonic absorption band red-shifted by 2.5 nm and the full width at half-maximum (FWHM) became wider. The surface plasmon band around 400 nm characteristic of Ag nanoparticles is not noticeable due to the strong absorption of CdTe QDs in the region and the fact that Ag nanoparticles are the minor component. However, the PL of CdTe QDs is strongly influenced by the presence of Ag nanoparticles. The CdTe PL is significantly quenched with increasing Ag nanoparticle content, attributed to non-radiative photoinduced electron transfer to Ag nanoparticles. Similar observations have been reported for analogous systems such as Au–CdS [193] and Au–CdSe nanocomposites [194]. While the QD PL intensity is quenched significantly by the metal nanoparticle, the PL spectrum does not change much. This suggests that the bandedges of the QDs are not affected substantially by the presence of the metal nanoparticles.

In a different scenario, PL from the semiconductor can be enhanced by metal nanoparticles at appropriate distance or with appropriate interaction. For example, enhancement of luminescence of CdSe/ZnS core/shell QDs by gold nanoparticles was studied as a function of distance between the QDs and gold nanoparticles [195]. This distance is controlled using a layer-by-layer polyelectrolyte deposition technique to insert well-defined spacer layers between gold nanoparticles and QDs. The maximum enhance-

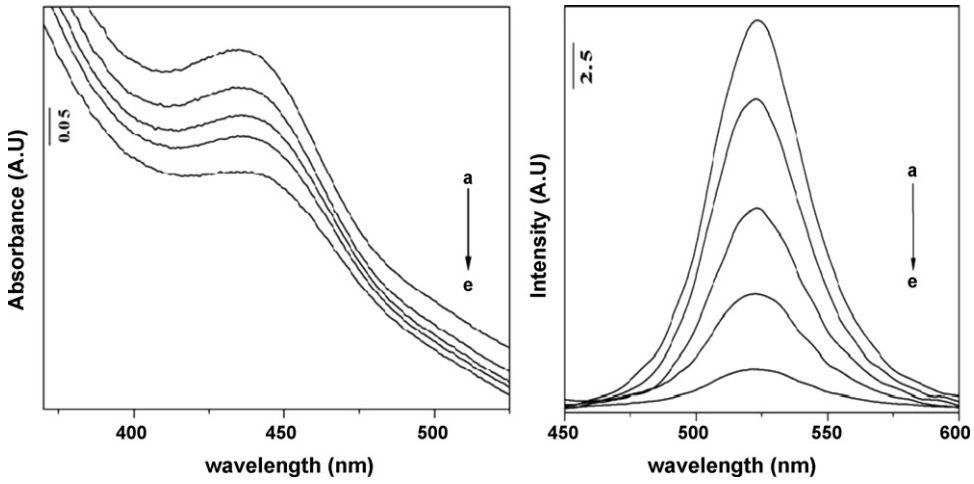

Fig. 9. UV–vis (left) and PL (right) spectra of Ag–CdTe hybrid nanomaterial in water with increasing Ag ratio compared to the original CdTe nanocrystals template: (a) CdTe template; (b) 1:50; (c) 1:20; (d) 1:10; (e) 1:5. Reproduced with permission from Ref. [192].

ment by a factor of 5 is achieved for a distance around 11 nm. The PL enhancement is attributed to enhanced QD excitation within the locally enhanced electromagnetic field produced by the gold nanoparticles. This is somewhat similar to the EM enhancement mechanism responsible for surface enhanced Raman scattering (SERS) [196]. Quenching or enhancement of PL of the semiconductor by the metal nanoparticles depends sensitively on the distance or interaction. In the same study, PL quenching was observed at distances of 3 and 19 nm. This non-monotonic distance dependence is suggested to arise from a competition between EM field enhancement and resonant energy transfer (RET) as well as possibly electron transfer to the gold nanoparticles. RET is strongly dependent on distance and expected to be particularly effective at short distance. A related technique, FRET (fluorescence or Foster resonance energy transfer), will be discussed later.

A relevant theoretical study of exciton-plasmon interaction in hybrid semiconductor QD and metal nanoparticle complex, e.g. CdTe QDs and Au nanorods (NRs), has shown that both the radiative rate of exciton in the QD and the non-radiative energy transfer rate from the QD to the Au NRs vary significantly with the distance between them and the orientation of the NRs [197]. Generally, both rates increase quickly as the distance between the QD and NR decreases. Quantitative experimental verification of the theoretical results is yet to be conducted.

Other common semiconductor–metal hybrid nanomaterials include Ag–ZnO, Pt–TiO_2 and Au–TiO_2 that are important for catalytic, photocatalytic, antibacteria, and photoelectrochemical applications [198–201]. In such systems, the optical properties, e.g. UV–vis absorption, in the visible is dominated by the metal nanoparticles due to weak absorption of the MO, e.g. TiO_2. There is usually no appearance of new absorption bands, indicating weak or moderate interaction between the metal and MO. However, there is evidence of improved photoinduced charge separation due to the presence of the metal nanoparticles, which is useful for photocatalytic and other reactions [199].

Another example of metal–semiconductor hybrid nanomaterials is Co–CdSe core/shell structures that exhibit magnetic, due to Co, and optical, due to CdSe properties [202]. In this system, the optical properties, absorption and PL, in the visible are dominated by CdSe due to weak absorption of Co. Such bifunctional nanostructures, magnetic and optical, are potentially useful for sensing and other magneto-optical applications. Hybrid nanostructures are particularly suitable for introducing multiple functionalities.

2.4. Doped semiconductor nanomaterials

Doped semiconductor nanomaterials (DSNs) are a class of semiconductor nanomaterials important to a number of technologies including laser, sensing, display, solid state lighting, imaging, and light energy conversion. DSNs can be considered as a special case of HSNs. The host semiconductor is the primary semiconductor, denoted as A, while the dopant, denoted as B, is the secondary component that is used to modify the property and functionality of the primary semiconductor. This is similar to the two-component systems discussed above. Compared to undoped semiconductors, doped materials offer the possibility of using the dopant to tune their electronic, magnetic and optical properties. Therefore, in addition to existing advantages nanomaterials offer in terms of controllable parameters such as size, shape, and surface, dopants offer the additional flexibility for designing new functionalities and for altering their properties.

Doped luminescent semiconductor nanoparticles are of strong interest for possible use in opto-electronics such as LEDs and lasers or as novel phosphors because of their interesting magnetic [203–206] and electro-optical properties [207–211]. A classic example is Mn^{2+}-doped ZnS nanoparticles, commonly denoted as ZnS:Mn that has received considerable attention. Bulk or powdered (micron-sized) ZnS:Mn have already been used as phosphors and in electroluminescence [212]. In these materials, a small amount of transition metal ions, such as Mn^{2+}, is incorporated into the nanocrystalline lattice of the ZnS host semiconductor. The host semiconductor usually absorbs light and transfers energy to the dopant metal ion that emits photons with energies characteristic of the metal ion. Luminescence can also result from direct photoexcitation through transitions of the metal ions.

Fig. 10 shows a schematic diagram of energy levels associated with semiconductor nanoparticles, including conduction band (CB), valence band (VB), and shallow trap (ST) and deep trap (DT) states, as well as dopant excited state (DE) and dopant ground state (DG). The right hand side of the figure illustrates the issues related to the number and location of the dopant ions in the nanoparticles. In the ideal case, each doped nanoparticle should have the same number of dopant ions in the same location in order for them to have the same or very similar properties, since the properties will depend on the number and locations of the dopants [213]. This is an important issue particularly for single nanostructure devices. For instance, for a nanoparticle with 100 atoms, a variation from 1 to 2 dopant ions can make a major difference in the property of the nanoparticles. Other possible complications involve aggregation or clustering of the dopants if more than one is present per nanostructure. The dopant ions often exist in substitutional or interstitial sites. Substitutional doping of a crystalline host material is often desired. Difference in the location of the dopant will affect its energy levels and spectroscopic signatures.

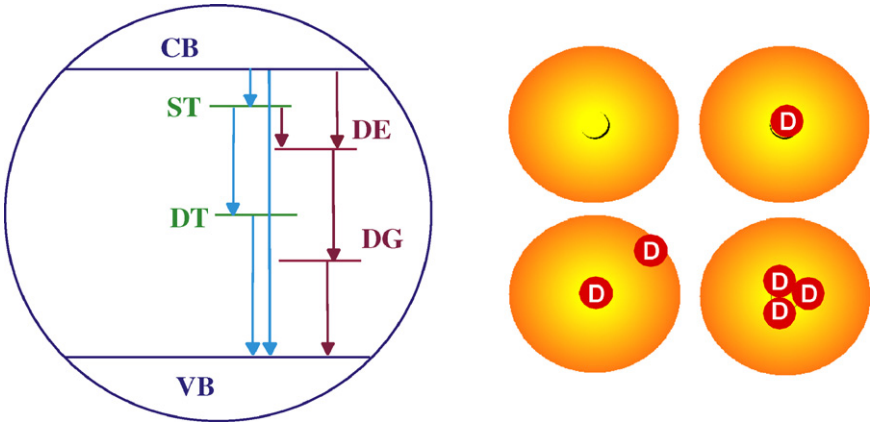

Fig. 10. (Left) Schematic illustration of energy levels of shallow trap (ST), deep trap (DT), dopant excited state (DE) and dopant ground state (DG) in a doped semiconductor nanoparticle with respect to the band edges of the valence band (VB) and conduction band (CB). (Right) Illustration of nanoparticles with different numbers of dopant ions per particles as well as different locations of the dopant ions in the nanoparticles. Reproduced from Ref. [214].

In practice, most samples contain NPs with a distribution in the number and location of the dopants in them. It is very challenging to control the number of dopants per NP and the locations of the dopants. This is an area that clearly needs further research.

One primary interest in doped semiconductor nanomaterials is their luminescence properties. For example, the PL and EL of Mn^{2+}-, Cu^{2+}-, and Er^{3+}-doped ZnS nanoparticles as free colloids [210,211,215] and in polymer matrices and thin films [209,216–219] have been extensively studied. As in bulk Mn^{2+}-doped ZnS, the Mn^{2+} ion acts as a luminescence color center, emitting near 585 nm as a result of $^4T_1$ to $^6A_1$ transition [205,210,215,220,221]. Mn^{2+}-doped ZnS NP was first reported by Becker and Bard in 1983 [222]. It was found that the Mn^{2+} emission at 538 nm with a quantum yield of about 8% was sensitive to chemical species on the particle surface and that the emission can be enhanced with photoirradiation in the presence of oxygen, which was attributed to photoinduced adsorption of O_2. In 1994, Bhargava et al. made the claim that the luminescence yield is much higher and the emission lifetime is much shorter in ZnS:Mn NPs than in bulk [207]. There were later some debate over whether the emission quantum yield is indeed higher in ZnS:Mn NPs relative to bulk. Several subsequent studies [223–228], including a theoretical study [229], made claims of enhancement that seem to support the original claim of enhanced luminescence by Bhargava et al. [207]. However, most of the studies failed to provide a calibrated, quantitative measure of the luminescence quantum yield in comparison to bulk ZnS:Mn. Several recent time-resolved studies have found that the emission lifetime in ZnS:Mn NPs is the same as in bulk, ~2 ms [111,230,231]. These lifetime studies seem to suggest that the luminescence yield in NPs should not be higher than that of bulk.

Besides ZnS:Mn, Cu-doped ZnS is another important phosphor material with strong emission in the blue region of the visible spectrum. Extensive studies on bulk and powdered (micron-sized) ZnS:Cu have been conducted over the years. Bulk ZnS doped with copper is known to have three PL emission bands: blue, green, and red [212,232]. Polarization experiments showed that the blue and red copper luminescent center had lower symmetry than the host lattice, indicating that they must be associated centers [233,234]. The green peak was found to not have lower symmetry than the lattice, hence not be spatially associated with the co-activator such as Cl^- [235]. The appearance of the three peaks was dependent on the ratio of activator to co-activator, e.g. Cu^+/Cl^- [236,237]. In particular, the blue peak was present when the concentration of Cu^+ was greater than the concentration of Cl^-. Recently, interests in nanosized ZnS:Cu have been on the rise due to the anticipation of potentially improved optical properties [218,219,238–242]. There seems to be some inconsistency in previous literatures in assigning the oxidation state of copper in ZnS:Cu, +1 vs. +2. A very recent study based on combined structural (EXAFS) and optical (PL) studies has found that copper exists primarily as Cu^{+1} in ZnS nanocrystals and is located in the interior but near the surface of the NCs [243]. Fig. 11 shows representative PL spectra of undoped and Cu-doped ZnS NCs. The PL peak in undoped ZnS NCs is due to electron–hole recombination from trap states while the PL for Cu-doped ZnS NCs with high doping level is mainly from shallow electron trap states to Cu^+ energy levels. For moderate doping level, the PL spectrum is clearly composed of both emission bands, one from ZnS and another associated with the Cu^+ dopant.

Doping is also used as a means to manipulate the bandgap states of semiconductors including metal oxide nanomaterials and thus the optical properties for other applications as discussed in the following section.

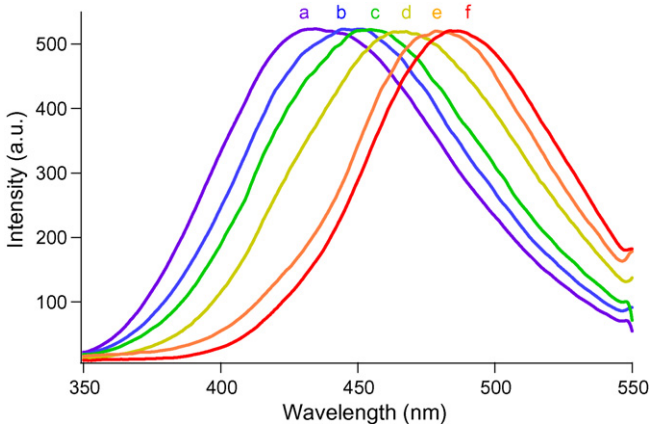

Fig. 11. PL spectra of ZnS NCs with different Cu dopant concentrations (λ_{ex} = 280 nm): (a) 0%; (b) 0.2%; (c) 0.5%; (d) 1%; (e) 2%; (f) 3% (from left to right). Reproduced with permission from Ref. [243].

3. Optical functionalities and applications of HSNs

The optical properties and associated functionalities of hybrid nanostructures have many important applications in various technologies. We will review some examples of applications including energy conversion, sensing, photonics, environmental protection, and biomedical detection, imaging, and therapy.

3.1. Light energy conversion

3.1.1. Photovoltaic (PV) solar cells

Conversion of solar energy into electrical energy using photovoltaic cells (PVC) is arguably one of the most successful and environmentally friendly technologies for energy generation [244]. To increase solar cell efficiency while maintaining a low production cost has been the primary objective of solar energy conversion. Thick single- and multi-crystalline silicon structures have been the dominant technology in the photovoltaic industry. Commercially available single-junction, single crystalline silicon cells offer 13% conversion efficiency while $GaInP_2$/GaAs-based multiple-junction solar cells have reached 27%, and InGaAsN-based solar cell systems have achieved 30% efficiency [245]. Although these devices exhibit impressive efficiencies, the process of material synthesis is often complex, resulting in low throughput and high production costs.

Conventional silicon solar cells make use of semiconductor diodes based on p–n junctions. Photogenerated electron and holes are driven to separation by a built-in electrical field and then collected as electrical current. Besides Si, other semiconductor materials, e.g. CdTe, CuInSe, and GaAs, have used for solar cells in bulk crystalline, thin film, or polycrystalline forms. These materials tend to be more costly even though some of them have demonstrated better efficiency than Si solar cells [246–248]. The relatively high cost of manufacturing commercial silicon cells and use of toxic chemicals in their manufacturing have limited them from widespread use. These aspects have prompted the search for environmentally friendly and potentially low cost materials.

Towards this goal, nanomaterials have been investigated as alternatives for bulk materials such as Si. Nanostructured materials offer some unique advantages that are ideal for applications in future generation PV devices. Their small size affords a large effective surface area, and thereby potentially low weight cells; quantum confinement effects lead to size-dependent and readily controllable material properties; nano-engineering and synthesis techniques may enable the design of sophisticated nanostructures at low cost and with improved properties. Nanostructured materials also lend

themselves conveniently for large area fabrication, including on flexible substrates.

Two general types of nanomaterial-based solar cells have been studied, dye-sensitized solar cells [249] and quantum dot solar cells [182]. In the original dye-sensitized solar cell (DSSC) developed in 1991 by O'Regan and Gratzel [249], TiO_2 nanoparticle films were sensitized with the N3 dye [250]. The nanocrystalline nature of the materials provides significantly increased surface area relative to volume as compared to bulk materials. In such a solar cell, dye molecules are adsorbed onto the surface of the nanoparticles. Photoexcitation of the dye molecules results in injection of electrons into the conduction band of TiO_2. The resulting oxidized dye is reduced by electron transfer from a redox couple such as I^-/I^{3-}, for the dye to be regenerated. Charge transport occurs through particles that are interconnected and collected by electrodes. These types of cells have reached solar power conversion efficiencies of 7–10% under full sun conditions [249–251]. Recently, there has been increasing research effort to use inorganic semiconductor QDs as sensitizers for large bandgap metal oxide nanostructures for solar cell applications [157,158,252,253]. In these cases, the QDs replace organic dye molecules and potential advantages include thermal stability and color tunability by controlling nanoparticle size and shape. All these solar cells are based on hybrid nanomaterials with the MO such as TiO_2 as the primary semiconductor and the secondary components such as dyes, QDs, or polymer as sensitizers. Organic conjugated polymers can function both as a hole transporter as well as a sensitizer for such nanocrystalline solar cells [254–258]. In another study, surface plasmon resonance from Au nanoparticle in a hybrid Au–TiO_2 system was found to improve the photoresponse of TiO_2 due to enhanced charge separation [259]. In spite of the potential advantages of nanomaterials, to date, solar cells based on nanomaterials generally show lower efficiency than the conventional solar cells based on bulk materials such as Si.

The relatively low efficiency is partly due to poor charge transport properties caused by grain boundaries or trap states. One possible solution to this problem, while maintaining the advantages of nanomaterials for solar cells, is to use 1D nanostructures such as nanowires and nanorods that are expected to have better transport properties than nanoparticles [125,260–271]. The 1D nanostructures still have large surface area and are suitable for large area processing. Solar cells based on 1D MO nanostructures have started to be investigated recently, e.g. Nd-doped TiO_2 nanorods [272] and ZnO nanorods [265].

In parallel, efforts have been made to enhance the visible absorption of MO by doping with elements such as N [120,122,273–281]. A recent study has also demonstrated the use of combining QD sensitization *and* N-doping to enhance visible absorption and facilitate charge transfer/transport in TiO_2 nanoparticle solar cells [158]. Fig. 12 shows the proposed energy diagram to explain the observed results. It was suggested that the electron occupied N energy level can donate the electron to the hole created in CdSe QD after photoexcitation, thereby facilitating the hole transport that is often a bottle-neck for charge transport in such nanocrystalline solar cells. This strategy points to the importance of using hybrid nanomaterial to manipulate the energy levels or improving the PV performance.

3.1.2. *Photoelectrochemical and photocatalytic hydrogen generation from water splitting*

Photoelectrochemical cells provide a powerful means for converting light energy into chemical energy that can be stored in molecules, such as hydrogen, through electrochemical reactions, e.g. water splitting [282,283]. Besides electrolytes, the key components in a PEC are the electrodes (cathode and anode) on which redox chemical reactions involving electron transfer take place. Fig. 13 shows a simple schematic of a typical PEC device. A conventional PEC is established with the semiconductor electrode as

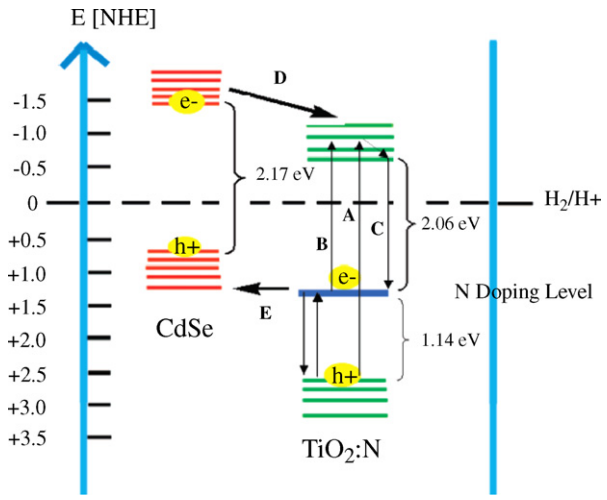

Fig. 12. Schematic electronic band structure of 3.5 nm CdSe with an effective bandgap of 2.17 eV and nanocrystalline TiO_2:N with a 3.2 eV bandgap, associated with normal TiO_2 and a N dopant state approximately 1.14 eV above the valence band. Different electron and hole creation, relaxation, and recombination pathways are illustrated, including (A) photoexcitation of an electron from the valence band (VB) to the conduction band (CB) of TiO_2, (B) transition or photoexcitation of an electron from the N energy level to the CB of TiO_2, (C) recombination of an electron in the CB of TiO_2 with a hole in the N energy level, (D) electron transfer or injection from the CB of a CdSe QD to the CB of TiO_2, and (E) hole transfer from the VB of a CdSe QD to the N energy level. Note that not all of these processes can happen simultaneously, and many of these are competing processes. Reproduced with permission from Ref. [158].

the photoanode and Pt electrode as the cathode in the electrolyte. Under irradiation with the photon energy equals to or exceeds the bandgap of the semiconductor photoanode, the electrons are excited and prompted from the valance band to the unoccupied conduction band. The electrons transport to the cathode and react with protons to generate hydrogen while the holes in the photoanode react with water molecule to produce oxygen.

For most materials, an external bias or potential needs to be applied to facilitate the photochemical reactions, and the overall process is named *photoelectrochemical*. If no external potential is applied or needed and the photoreduction and photooxidation occur on the same material or photoelectrode, the process is termed

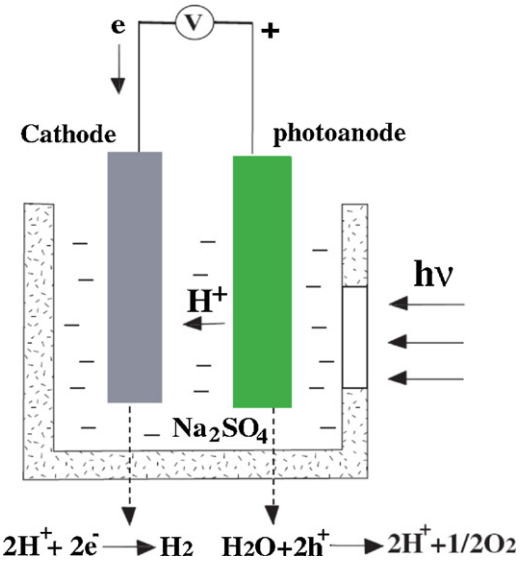

Fig. 13. Schematic of a typical PEC device and its basic operation mechanism for hydrogen generation from water splitting.

photocatalytic as long as the photoelectrode is not irreversibly changed. If permanent changes occur in the process, the reaction is *photochemical* in nature with the photoelectrode as part of the reactant involved. Both photoelectrochemical and photocatalytic processes have been frequently explored for hydrogen generation applications from water splitting, an attractive potential method for producing clean and renewable energy.

Most photoelectrodes for PEC are based on bulk materials. However, photoelectrodes based on nanostructured materials have been explored for a number of systems, usually single component nanomaterials such as CdS [284], Bi_2S_3 [285], Sb_2S_3 [286], WO_3 [58,287–292], and more commonly TiO_2 [293–299]. Similar to nanomaterials used for solar cells, nanomaterials offer some potential advantages for photoelectrodes in PEC, including large surface area, fast diffusion and reaction time, ease of surface modifications, and possibility for manipulating materials properties by structural control.

As mentioned above, 1D nanostructures such as nanowires and nanorods are expected to exhibit much improved transport properties than 0D nanoparticles. However, to date, only limited PEC studies based on 1D nanostructures, e.g. TiO_2 nanotubes and nanorods, have been reported [125,270,300]. PEC performance depends strongly on the properties of the photoanode, especially the bandgap and bandedge positions [301]. HSNs offer the possibility to manipulate the band structures for improved PEC performance.

To achieve effective splitting of water, the semiconductor photoelectrode should meet the following criteria [302,303]: (i) photochemical stability, (ii) low cost, (iii) with a conduction band edge higher than the H_2 evolution level and a valence band edge lower than the O_2 evolution level, and (iv) strong absorption in the solar spectrum region. Among the various candidates for the photoanodes, metal oxide semiconductors are inexpensive and stable, and many have bandedge energies matching the H_2 and O_2 evolution reactions [304]. Thus, most investigations have focused on TiO_2 and considerable progress has been made [305,306]. However, in terms of the wide bandgap (3.2 eV for anatase phase and 3.0 eV for rutile phase), TiO_2 is a poor absorber in the solar spectrum, and its efficiency in photosplitting can hardly exceed 10%, which hinders its application and commercialization [305].

Major efforts have been focused on attaining a broad photoresponse range and achieving better efficiency in water splitting by wide bandgap semiconductors, such as TiO_2 and ZnO. Among the strategies, combining semiconductors with other elements or compounds to form HSNs is considered as promising. In these cases, HSNs not only show higher efficiency in light absorption, but also suppress the recombination of the photogenerated electrons and holes, thus demonstrating notable improvement in the performance in water splitting compared to the single component semiconductors.

One approach in the design of HSNs is doping semiconductor nanomaterials with metal ions [307–309] or nonmetal species such as nitrogen [310], phosphor [311], carbon [312], sulfur [313], and boron [314]. By doping with metal ions, semiconductors such as TiO_2 show much higher efficiency in the photoelectrochemical activities [307]. After the implantation of some ions including Ru^{3+} and Cr^{3+}, the bandgap energies of TiO_2 were decreased or intra-bandgap states were introduced, and thus the HSNs possessed visible light response [307,315]. However, most of the metal ions mainly act as traps of photogenerated carriers, and the enhancement in the photoactivity is largely attributed to the suppression of the recombination of the photogenerated charge carriers rather than the narrowing of the bandgap [307,316–318]. In Fe^{3+}-doped anatase TiO_2, the energy level for Fe^{3+}/Fe^{2+} is below the bottom of the CB (E_{CB}) of TiO_2 and the energy level for Fe^{3+}/Fe^{4+} is above the top of the VB (E_{VB}). Therefore, Fe^{3+} could act as a trap for electrons as well as holes, and inhibit the e^-/h^+ recombination, whereas no noticeable change in bandgap energy of n-TiO_2 was observed [302,307]. Moreover, HSNs with metal ion dopants also encountered problems such as the thermal stability, increase in carrier recombination centers, and requirement of an expensive ion-implantation facility [308].

In view of these obstacles, doping with anions, rather than cations, has attracted growing attention in recent years. For efficient doping to enhance photoactivity of HSNs, the following requirements need to be met [310]: (i) doping should produce states in the bandgap of semiconductors that absorb visible light; (ii) the E_{CB}, including subsequent impurity states, should be higher than the H_2 evolution level to ensure its photoreduction activity; (iii) the states in the bandgap should overlap sufficiently with the bandedge of semiconductors to transfer photoexcited carriers to reactive sites at the catalyst surface within their lifetime. Unlike metal cations, which often afford localized *d* states deep in the bandgap of the semiconductors and result in recombination centers of carriers, anionic species could meet the above requirements, especially (ii) and (iii), by mixing their p states with the corresponding states in the semiconductors. For instance, in the N-doped TiO_2 film (denoted as $TiO_{2-x}N_x$) prepared by sputtering the TiO_2 target in an N_2 (40%)/Ar gas mixture, the p states of N mix with the O 2*p* states in TiO_2 and contributed to the bandgap narrowing of TiO_2, as indicated by noticeable absorption of light up to 500 nm [310]. Similarly, C-doped TiO_2 prepared by flame pyrolysis of Ti metal sheet in the natural gas also showed lower bandgap energy and appreciable light absorption up to 535 nm [302]. Besides experimental studies, theoretical calculations of the densities of states (DOSs) by the full-potential linearized augmented plane wave (FLAPW) formalism revealed that among the substitutional doping of C, N, F, P, or S for O in anatase TiO_2 crystal, substitutional doping of N was the most effective in narrowing the TiO_2 bandgap because its p states have a good mix with the O 2*p* states of TiO_2 [319,320]. The S dopants exhibited a similar bandgap narrowing, however, it would be difficult for S to incorporate into the TiO_2 crystal in view of its large ionic radius. For C and P doping, the introduced states would be a little too deep in the bandgap.

Another approach to induce visible light water splitting by semiconductor is the coupling of two semiconductors with different energy levels for their corresponding conduction and valence bands. Various studies have shown improved visible light photoactivity with coupled semiconductors of TiO_2/CdS [159–161], TiO_2/CdSe [162], ZnO/CdS [163], SnO_2/TiO_2 [164], SnO_2/ZnO [165], TiO2/ZnO [1], and SnO_2/CdSe [167]. For most HSNs composed of two semiconductors, a wide bandgap semiconductor is combined with another one with small bandgap energy. The visible light can directly excite an electron from the VB to the CB of the small bandgap semiconductor. Thereafter, the generated electrons can be injected into the wider bandgap materials and facilitate visible light photosplitting of water, as long as the bottom of the CB of the small bandgap semiconductor is above the bottom of the CB of the large bandgap semiconductor [163,321–323]. Moreover, electron transfer between the two portions of the HSNs enhances the charge separation and inhibits recombination by forming a potential gradient at the interface. In the case of TiO_2/CdS, CdS acts as the visible light absorber and transfers the photoexited electrons to the CB of TiO_2. Due to formation of the potential gradient at the interface, the rate of photoinduced electron transfer at CdS increased tenfold in the presence of TiO_2 [324,325] and the overall rate of hydrogen generation under visible light irradiation increased by tens of times compared to CdS alone [159].

As discussed in Section 4.1.1, sensitizing semiconductors by dyes to achieve a better use of solar light have been intensely investigated in the field of photovoltaic devices. This surface modification strategy also plays an important role in visible light water

splitting by wide bandgap semiconductors. In one scenario, dye sensitization was used to improve photoelectrochemical reactions by enhancing visible light absorption and photoconversion [250]. In another scenario, dye sensitization was used to improve photocatalytic reactions under visible light irradiation. For example, phenolic hydroxyls are able to react with TiO_2 by chemical condensation of the Ti–OH hydroxyl groups present on the TiO_2 surface with the phenolic hydroxyl(s) to give an inorganic–organic hybrid material [326,327]. 2,6-Dihydroxyantraquinone (DHA) functionalized TiO_2 nanotubes annealed in N_2 (denoted as N_2–TiO_2–DHA) exhibited a 140 nm red-shift in optical absorption compared with the native TiO_2 nanotubes, which was attributed to intramolecular ligand-to-metal charge transfer transitions [327–329]. Similarly, 1,1-binaphthalene-2,2-diol modified TiO_2 showed noticeable H_2 evolution under visible light, whereas bare TiO_2 did not.

One limitation with semiconductor oxide photoanodes is that they do not have sufficiently negative photocurrent onset potential to allow for direct water splitting in the presence of a metal cathode due to the overpotential and Ohmic drop losses [330,331]. To solve the problem, different approaches have been explored. One strategy is the PEC/PV tandem cell, which is composed of the photoelectrochemical cell (PEC) coupled with a photovoltaic cell. The PV cell is intended to provide the bias voltage required for the photoelectrolysis of water in the photoelectrolysis cell [331]. Another approach is integration of several semiconductors with different bandgaps in a single cell to make better use of broad solar light. It was calculated that single-gap electrodes have a solar conversion efficiency limit of 32%, whereas tandem-junction devices have an efficiency limit of 42% [332,333]. With a tandem cell based on $GaInP_2$/GaAs p/n, p/n multiple bandgap structures, and an efficiency of 12.4% for the H_2 generation was achieved [303].

3.1.3. Photoassisted direct methanol fuel cells

Among the various devices, fuel cells have been widely recognized as an attractive strategy to obtain direct electric energy from combustion of chemical fuels. So far, the most promising materials developed for the direct methanol fuel cells (DMFCs) are Pt–Ru bimetallic catalysts anchored on carbon materials [334,335]. A proton exchange membrane (PEM) separates the Pt–Ru/C anode and Pt/C cathode and allows ion transport between the two cell compartments [336–338]. However, these catalysts are easily poisoned by CO and require high loading of expensive metals [339], which causes performance losses and adds to the cost of DMFCs. In order to solve these problems, several strategies have been adopted, including reconfiguration of Pt-M alloy electrode [340–342] and introduction of oxides to increase the CO tolerance [343,344]. Until now, limited investigation has been focused on the HSNs in the DMFCs such as Pt/TiO_2/C [345] It was reported that introduction of TiO_2 into Pt significantly increased the surface area and thus enhanced the cell performance, due to altered electron density in the *d*-orbitals of Pt caused by interaction with TiO_2 [346].

However, in these studies the photoelectrochemical properties of TiO_2 were hardly utilized. Recently, the effect of irradiation on the performance of the TiO_2/Pt–Ru was investigated [347]. In the study, TiO_2 nanoparticles were incorporated into the electrode along with the Pt–Ru catalyst and methanol oxidation was carried out both electrocatalytically and photocatalytically in a synergetic way. As expected, the photocatalytical activity of TiO_2 enhanced the current generated from oxidation of methanol in the Pt–Ru catalyst system, and the output power of the hybrid cell increased by 30% with UV irradiation. For carbon supported hybrid anode of TiO_2/Pt–Ru, the introduction of TiO_2 not only reduced the use of noble metal and minimized the poisoning effect, but also contributed to the photooxidation of methanol under irradiation and delivered higher efficiency compared to bare Pt–Ru/C.

3.1.4. Thermophotovoltaic energy conversion

Thermophotovoltaics (TPVs) convert thermal radiation emitted from a high-temperature source into electricity by means of a photovoltaic diode, as solar photovoltaic systems convert solar radiation into electricity [348]. Compared to the photovoltaics, TPVs have a major advantage in certain settings: a generator can operate at night or when the sky is overcast, thereby eliminating any need for batteries to store electricity [349]. The two main approaches to TPVs are selective emitters/filters and TPV converter cell. Selective emitters/filters allow the use of more moderate temperatures, while in the latter approach very high temperatures are needed to achieve good conversion efficiencies.

TPVs materials convert thermal energy into electricity by absorbing electromagnetic radiation from black-body sources and creating electron–hole pairs. For the purpose to achieve higher energy efficiency, TPVs devices are intended to absorb radiation from sources with lower temperatures, requiring the semiconductor absorbing materials with bandgaps in the range of 0.4–0.7 eV. Silicon and germanium were first tried as TPVs converters but were eventually abandoned because of their low efficiency below 1700 °C [350]. Thereafter, the development of narrow-gap III–V materials within optimum bandgap values for TPVs applications (hybrid semiconducting materials such as GaSb, InGaAs, and InGaAsSb) has become popular. To obtain good quality thick absorbers, the film needs to be lattice matched to a substrate. Meanwhile, the compatibility of the TPVs requires the absorber to have the desired target bandgap value and strong direct transition. It is often challenging to simultaneously satisfy these requirements [351]. Two groups of materials have been studied: (i) InGaAsSb/GaSb with GaSb as the substrate materials [352], and (ii) InGaAs/InP with InP as the based materials [353]. Recently, photonic crystals, especially 1D structures such as Si/SiO_2, have been used to improve the efficiency of TPVs in the form of filberts or dielectric layers [348]. Both the quantum wells as active materials for TPVs and the photonic crystals as peripheral components to TPV devices are hybrid semiconductor nanomaterials.

3.2. Photocatalysis and application

3.2.1. Photocatalytic reactions

Nanomaterials have played a critical role in many important chemical reactions as reactants, catalysts, or photocatalysts. In relation to optical properties, nanomaterials have been used in photochemical and photocatalytic reactions. Their reactivities are often altered or enhanced due to size-dependent changes in their redox potentials and high density of active surface states associated with a very large surface-to-volume ratio.

Photocatalysis based on semiconductors plays an important role in chemical reactions of small inorganic, large organic, and biological molecules [354,355]. Photocatalytic reactivities are strongly dependent on the nature and properties of the photocatalysts, including particle size, shape, and surface characteristics [356]. These properties are sensitive to preparation methods [356]. Impurities or dopants can significantly alter these properties as well as reactivities [310,357]. For example, selectively doped nanoparticles have a much greater photoreactivity as measured by their quantum efficiency for oxidation and reduction than their undoped counterparts [307]. A systematic study of the effects of over 20 different metal ion dopants on the photochemical reactivity of TiO_2 colloids with respect to both chloroform oxidation and carbon tetrachloride reduction was conducted [307,358]. A maximum enhancement of 18-fold for CCl_4 reduction and 15-fold for $CHCl_3$ oxidation in quantum efficiency for Fe(III)-doped TiO_2 colloids were observed [359]. As discussed before, such doped MO nanostructures are hybrid systems with the MO as the primary component and the dopants as the secondary component.

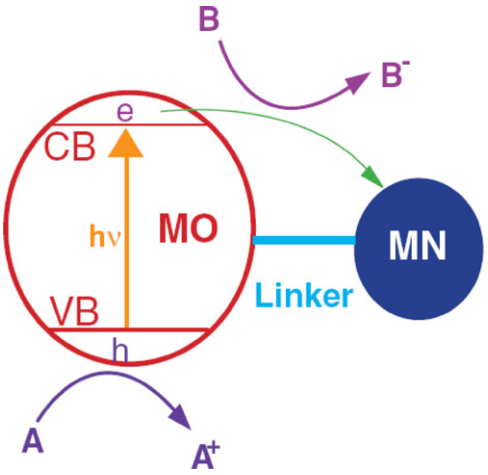

Fig. 14. Illustration of the basic principle of photocatalysis based on a hybrid semiconductor quantum dots (QDs)-metal nanoparticle (MNP) system. The linker may or may not be needed.

Another hybrid system related to photocatalysis is composites based on semiconductor and metal nanomaterials. Fig. 14 shows a schematic illustration of the basic principle of photocatalytic reactions involving a hybrid semiconductor QD–metal nanoparticle (MNP) system as a photocatalyst. The photogenerated electron in the CB of the QD is trapped by the MNP and results in reduction of B into B^- before, during, or after trapping, while the photogenerated hole in the VB participates in oxidation of A into A^+. When both photooxidation and photoreduction are complete, the QD recovers to its original state and it is thus acting as a photocatalyst. If only one of the two reactions take place, the QD will not recover to its original state and a net photochemical reaction has taken place. The MNP can be directly deposited onto the QD and in such a case no linker molecule is needed. The use of MNP generally enhances the photocatalytic efficiency [359].

Photocatalytic oxidation of organic and biological molecules is of great interest for environmental applications, especially in the destruction of hazardous wastes or pollutants. The ideal outcome is complete mineralization of the organic or biological compounds, including aliphatic and aromatic chlorinated hydrocarbons, into small inorganic, non- or less-hazardous molecules, such as CO_2, H_2O, HCl, HBr, SO_4^{2-}, and NO_3^-. Compounds that have been degraded by semiconductor photocatalysis include alkanes, haloalkanes, aliphatic alcohols, carboxylic acids, alkenes, aromatics, haloaromatics, herbicides, and pesticides [359]. In many cases the colloidal particles show new or improved photocatalytic reactivities over their bulk counterparts.

In general, the details of the surface morphology, crystal structure, and chemical composition critically influence the photocatalytic performance of the photocatalysts [360–364]. Therefore, these parameters need to be carefully controlled and evaluated when comparing photocatalytic activities of different materials. Hybrid nanomaterials, based on doping or composites, offer the possibility to control some of these parameters. The following few subsections will provide some specific examples of important applications of photocatalysis with emphasis on hybrid semiconductor nanomaterials as photocatalysts.

3.2.2. *Photochemical transformation of specific compounds*

Heterogeneous photocatalysis based on semiconductor nanomaterials dispersed in liquids or solutions provides the possibility of using the semiconductor/liquid junction as a site for light-stimulated redox reactions toward efficient and selective photochemical transformation [365]. These photocatalytic redox reactions require little or no harmful or dangerous chemical reagents and produce little harmful byproducts. In addition, many conventional multistep reactions can be substantially simplified [366].

Semiconductor-sensitized photosynthetic reactions include oxidation and oxidative cleavage, reduction, isomerization, substitution, and polymerization, and these reactions can be carried out in inert solvents [367]. The proposed mechanism for these reactions can be described as following: with the separation and migration of photogenerated electron–hole (e^-–h^+) pair to the surface of the irradiated semiconductor, the separated photogenerated electron or hole can potentially function as an effective reductant or oxidant, followed by the capture of reducible, adsorbed species or oxidizable, adsorbed species, respectively. The reduced or oxidized species then undergo a series of rapid chemical reactions. Subsequent formation of the final products and desorption from the surface completes the usual photoinduced reaction sequence. In the photocatalytic oxidation reactions, the general classes of organic compounds involved include alkanes, haloalkanes, aliphatic alcohols, carboxylic acids, alkenes, aromatics, haloaromatics, polymers, surfactants, herbicides, pesticides, and dyes [359,366,368–370]. For example, a silica catalyst containing isolated Cr-oxide species (Cr amount: 0.1%) showed excellent catalytic performance in cyclohexane oxidation [371,372]. It was found that visible light irradiation to an acetonitrile solution containing cyclohexane with Cr-containing silica and O_2 produced cyclohexanone with high selectivity (68%), and only trace amount of CO_2 was formed during the reaction. Recently, visible light induced solid state polymerization of diacetylene in nanostructured TiO_2 was reported and attributed to the photocatalytic effect of TiO_2 upon absorption of radiation [373]. In addition to organic compounds, various inorganic compounds are also sensitive to photochemical oxidative transformation on semiconductor surfaces, such as ammonia [374], chromium species [375], copper [376,377], gold [378], nitrates and nitrites [379], and sulfur species [380].

Among the photocatalytic reduction reactions, CO_2 and nitrogen-containing compounds are studied most extensively. Photocatalytic CO_2 reduction is a powerful method for transforming CO_2 to useful chemicals and decreasing the amount of CO_2 in the atmosphere. A recent exciting development in this area is the design of novel photocatalysts for the photocatalytic transformation of CO_2 with high efficiency. Silica containing highly dispersed Ti-oxide species could promote highly selective and efficient photoreduction of CO_2 for the production of methanol and methane, and the selective methanol formation could be further promoted by means of hydrophobic treatment of the catalysts [381,382]. With 3 wt.% CuO-doped TiO_2, photoirradiation to a CO_2-saturated water shows the best photocatalytic reductive activity for methanol production [383]. In such a reduction reaction, CuO is considered to behave as an efficient electron trap and is able to suppress the recombination of the electron–hole pairs, thus leading to the improvement of photocatalytic efficiency [383]. For the photocatalytic reduction of nitrogen-containing compounds, the reaction rates and selectivities generally can be enhanced by the addition of alcohols and the removal of O_2 from the reaction mixture [366,384]. This is because alcohols behave as an electron donor to scavenge the photogenerated hole formed on the TiO_2 surface for the suppression of electron–hole recombination and the elimination of the undesirable side reactions, while O_2 behaves as a competitive scavenger of the electron (e_{cb}^+) on the TiO_2 surface for the formation of reactive oxygen radical ($O_2^{\bullet -}$) [366,384]. For example, 4-nitrophenol could be successfully reduced to 4-aminophenol in various alcohols with irradiated TiO_2 semiconductor and the polarity of alcohols plays very important roles in the photocatalytic reduction reaction rate [385].

Furthermore, with separation of photogenerated electron–hole pairs on the surface of the irradiated semiconductor, both reduction and oxidation centers are created, making it possible to use these coupled redox processes for the synthesis of specific organic compounds. In fact, several organic compounds were synthesized in "one-pot" by using this coupling reaction, especially through C–N or C–C coupling reactions [386–389]. Photoirradiation to an aqueous solution containing primary amines in the presence of a powdered mixture of TiO_2 with Pt black (Pt/TiO_2 catalyst) gives rise to the corresponding secondary amines via C–N coupling reaction, involving a single electron transfer from one reaction center to another [386].

3.2.3. Environmental applications: water and air purification

The global industries and agricultures release large quantities of wastewater, on the order of millions of cubic meters every day. Generally, toxic organic compounds, hazardous inorganic constituents and bacteria in wastewater cause pollution to surroundings and pose severe ecological problems. Thus, the control and destruction of pollutants in wastewater is a major issue facing the world.

Traditional techniques for treating and disposing wastewater, including biological treatment, adsorption, and coagulation, are often inefficient and result in secondary pollution [390–396]. For example, conventional biological treatment of dyes does not lead to their complete degradation [397]. As a result, advanced oxidation processes (AOPs) based on the generation of reactive species, such as hydroxy radicals ($^{\bullet}OH$), are gaining attention for the oxidative degradation of pollutants.

Among AOPs, heterogeneous photocatalysis using semiconductor nanomaterials for the wastewater purification appears to be the most promising technology, because the photoactivated semiconductors can completely decompose (mineralize) various kinds of pollutants that are refractory, toxic, and non-biodegradable, to CO_2, water and mineral acids under mild conditions (room temperature and atmospheric pressure) [304,359,398–402]. Water treatment based on photocatalysis provides an important alternative to other advanced oxidation technologies such as UV-H_2O_2 and UV-O_3 for oxidative mineralization. The photocatalytic mineralization of organic compounds in aqueous media typically proceeds through the formation of a series of intermediates of progressively higher oxygen to carbon ratios [403,404]. Heterogeneous photocatalysis involves generation of electrons and holes by light and their subsequent reaction with chemicals in water, resulting in the ultimate degradation of pollutants to the ideal final products of CO_2 and H_2O. The hydroxyl radicals and superoxide radical anions are suggested to be the primary oxidizing species in the photocatalytic oxidation processes. The photocatalytic activity can be significantly suppressed by the absence of oxygen, possibly because of back-electron transfer from active species present on photocatalyst surface.

An ideal photocatalyst should be photostable, chemically and biologically inert, abundant and inexpensive, have strong visible absorption, and exhibit properties that can be controlled by changing size, doping, or sensitization [368,405]. For organic compound degradation, the redox potential of the $H_2O/^{\bullet}OH$ ($OH^- = {}^{\bullet}OH + e^-$; $E^\circ = -2.8$ V) couple need to lie within the bandgap of the semiconductor [10]. Many semiconductors, such as TiO_2, SnO_2, ZnO, ZrO_2, $SrTiO_3$, CdS, MoS_2, Fe_2O_3 and WO_3, have been examined as dynamic photocatalysts for the degradation of organic contaminants [406,407]. However, most of these semiconductor photocatalysts have bandgap in the ultraviolet (UV) region, i.e., >3.2 eV ($\lambda = 387$ nm) and require UV radiation, which is not ideal for practical applications [408–410]. In addition, surface and volumetric charge recombination is another obstacle that hinders heterogeneous photocatalysis to becoming an efficient purification method.

Various attempts have been made to suppress electron–hole recombination and to enhance the photosensitivity of photocatalysts for applications in wastewater treatment using visible light. HSNs are promising for this purpose because of the possibility of controlling and altering their optical properties, which could lead to enhanced photocatalytic properties compared to pure or single component semiconductor nanomaterials. One approach is chemical doping of semiconductor nanomaterials with different metal or nonmetal ions [316,411–413]. The main objective of doping is to reduce the effective bandgap or introduce bandgap states in the semiconductor, leading to enhanced visible light absorption and interfacial charge transfer [368]. Dominant doping parameters include the nature and concentration of dopants as well as the doping method used [414]. On one hand, doping can result in narrowing of the semiconductor's space-charge region and lead to more efficient separation of the electron–hole pairs within the region by the large electric field before recombination. On the other hand, at high level of doping, dopants can act as trapping sites and enhance electron–hole recombination. Consequently, there is an optimal concentration of dopants in terms of photon-to-charge conversion efficiency of the doped semiconductor [415].

There is strong evidence attesting to the positive influence of dopants on semiconductor photocatalytic activity. For example, the doping of TiO_2 with metal ions, such as V, Cr, Mn, Fe, and Nd, results in red-shift in the absorption spectrum into the range of 400–600 nm, which shows efficient photocatalytic activities in the visible [416–419]. Anionic nonmetal dopants such as C [276,420], N [310,421–424], S [425], B [426], and F [427], were also successfully used to extend the semiconductor's photocatalytic activity into the visible region. Films and powders of N-doped TiO_2 have shown improved visible light absorption and photocatalytic activity over bare TiO_2 in aqueous media [428]. In addition, co-doping represents another viable method to improve the charge separation and enhance the photocatalytic activity in the visible region. Several studies were reported on co-doped materials such as C and N [429], S and N [430], F and N [431,432], C and S [433], N and a variety of metal ions [434,435], and the synergetic effect of co-doping on photocatalytic activities was also investigated. By co-doping with Eu^{3+} and Fe^{3+} in an optimal concentration, TiO_2 shows significantly increase in photocatalytic degradation of chloroform in solution compared to separate doping with Fe^{3+} or Er^{3+} [436].

Another approach to enhance photocatalysis in the visible is to deposit metal on the semiconductor nanoparticle surface, resulting in semiconductor–metal HSNs. This results in the formation of a Schottky barrier at the metal–semiconductor interface, leading to a decrease in electron–hole recombination. For example, it was reported that Pd-, Cu-, Pt-coated photocatalysts (Pd/TiO_2, $Pd–Cu/TiO_2$, Cu/TiO_2, $Pd–Cu–Pt/TiO_2$) showed a higher activity in the photodecomposition of 2,4-dinitrophenol, trichloroethylene, and especially formaldehyde (up to five times) in aqueous solutions [437]. Similarly, the coupling of two semiconductors, possessing different energy levels for their corresponding CB and VB, can also be used to enhance photocatalysis. The enhancement is explained as a result of vectorial transfer of photogenerated electrons and holes from one semiconductor to another, e.g. WO_3/TiO_2 [438], SnO_2/TiO_2 [439–441], ZnO/TiO_2 [442,443], and CdS/TiO_2 [444]. For instance, a combination of CdS/TiO_2 leads to an enhancement in the degradation of 2-chlorophenol and pentachlorophenol by a factor greater than two, consistent with the notion that photogenerated CdS electrons are vectorially transferred towards TiO_2 particles [444]. In addition, dye sensitization has also been explored for improving photocatalysis of semiconductors in the visible [445–450]. In this case, the dye sensitizer is anchored onto the semiconductor surface and absorbs visible light that results in

electron injection into the semiconductor [451]. Subsequent photochemical reactions can lead to degradation of the dye. This method is useful for removal of colored pollutants in wastewater generated by the textile industry [405,452–454]. The same approach can also be used to assist photodegradation of various colorless organic pollutants [416,417,455].

Another important application of photocatalytic reactions involving semiconductor nanomaterials is air purification. In general, air pollutants mainly include nitrogen oxides (NO_x), carbon oxides (CO and CO_2), volatile organic compounds (VOCs), and particulates, and many of them are known to be toxic and considered to be carcinogenic, mutagenic, or teratogenic [456]. These pollutants are emitted from different sources such as tobacco smoke, vehicular emissions, combustion by-products, cooking, construction materials, office equipment, and consumer products. The conventional techniques for air purification generally employ filters to remove particulate matters or use sorption materials (e.g., granular activated carbon) to absorb the pollutants, which only transfer, rather than eliminate, the contaminants and thereby requires additional steps for disposal or handling [457].

Semiconductor photocatalysis is emerging as a promising alternative technology for efficient air purification at room temperature and ambient pressure, because the semiconductor catalysts are inexpensive and capable of mineralizing most organic compounds effectively. The process has many merits over conventional processes, such as the ability to degrade a broad range of pollutants, suitability for both liquid and gaseous fluids, and the potential utilization of sun power. As already mentioned, semiconductor photocatalysts can absorb photons under solar irradiation to generate excited pairs of electrons and holes, which can be further converted to hydroxyl radicals ($^{\bullet}OH$) or superoxide radical anions ($^{\bullet}O_2^-$). These radicals so produced are highly reactive and work together to completely oxidize the organic species, leading to the final mineralization of air pollutants. The use of illuminated TiO_2 can result in the overall degradation of VOCs together with nitrogen oxides and sulfur oxides in air [458–460]. However, most of conventional semiconductor photocatalysts are utilized only under UV light due to its wide bandgap and therefore their applications have been limited to a great extent.

HSNs are potentially useful for efficient photodegradation of air pollutants under visible light. Several investigations have described enhanced visible light induced photocatalytic properties of semiconductors by doping with transition metal ions (such as V, Cr, Mn, Fe, Ni) or anions (such as N^{3-}, C^{4-}, S^{4-}) or halides (F^-, Cl^-, Br^-, I^-) or lanthanide ions (such as La^{3+}, Nd^{3+}) [30,82]. For example, several groups reported the visible light photocatalysis of various TiO_2–xN_x for VOC decomposition, and found that these catalysts could photodegrade gaseous acetaldehyde [310], 2-propanol [461], acetone [462], and methylcyclohexene [463] upon irradiation with visible light. A highly selective photoreduction of NO to N_2O and N_2 was reported on metal-implanted TiO_2 [464], and TiO_2 photoactivity on photoreduction of NO could also be improved by the addition of an adsorbate such as zeolites (A and Y), which could concentrate NO on the surface [465]. Nanosized Ti–W mixed oxides were effective in photocatalytic degradation of toluene using sunlight-type excitation [466], and the photoactivity increased with W content and was much better than TiO_2 itself and TiO_2 P25. Recently, Ln^{3+}-doped TiO_2 catalysts for enhanced photocatalytic oxidation of benzene, toluene, ethylbenzene and o-xylene (BTEX) for indoor air purification was reported [467]. The enhanced photodegradation of BTEX was proposed to be due to the improved adsorption ability and the enhanced electron–hole pairs separation caused by the presence of Ti^{3+} on the surface of La^{3+}–TiO_2 catalysts and the electron transfer between the conduction band/defect level and lanthanide crystal field state.

3.2.4. Other applications: self-cleaning, anti-fogging, and disinfection

Self-cleaning and anti-fogging applications using semiconductor powders or thin films have become a subject of increasing interest. The primary principles behind are photocatalysis and hydrophilicity. Photocatalysis decomposes organic substances that come into contact with the surface and thus prevent them from building up. The hydrophilicity makes the cleaning more effective as the water spread over the surface rather than remains as droplets, facilitating faster drying of water and preventing undesirable water streaking or spotting on the surface [468,469]. TiO_2 is one of the most widely used materials for self-cleaning application for its thermal stability and photocatalytic properties [470–475]. Moreover, the ability to tune TiO_2 between superhydrophilic and superhydrophobic on surfaces by UV illumination is another advantage. The existence of hydrophilic sites was explained in terms of photoreduction of Ti^{4+} to Ti^{3+} on the hydrophobic TiO_2 surface [470].

Although building materials coated with photoactive TiO_2 show substantial self-cleaning and anti-fogging effects outdoors by absorbing UV light from the sun, they do not function indoors. This is because the UV light intensity indoors is too weak for a simple TiO_2 coating to exhibit either photocatalysis or photoinduced hydrophilicity. In order to obtain indoor photoactive materials, three different types of hybrid semiconductor nanomaterials based on TiO_2 have been investigated [476] The first one is the TiO_2 film deposited with Cu or Ag [477,478], which is harmless to human body, and shows a remarkable antibacterial effect since the TiO_2 photocatalytic reaction assists the intrusion of antibacterial copper or silver ions into cells. Thus, even very weak UV light is sufficient to lower cell activity. The second one is layered heterogeneous film of TiO_2/WO_3 [479] or TiO_2/SiO_2 [480], which becomes highly hydrophilic even under weak light since the photogenerated holes produced in WO_3 by UV light are transferred to the TiO_2 side due to the interfacial potential gradient and then used for hydrophilic conversion. The last one is TiO_2 film doped with anions, including nitrogen, sulfur, and carbon [476], which can be highly hydrophilic by absorbing visible light.

Disinfection or inactivation of biological species such as bacteria is of strong interest for many applications. Photocatalysis has been introduced as one of the promising processes in the inactivation of bacteria in water since 1985 [481]. Most reports with respect to inactivation of bacteria use UV light as the light source, [482–484], since the widely used TiO_2 photocatalyst is active only in the UV range. Under UV illumination, electron–hole pairs generated from TiO_2 are able to degrade chemicals and/or cell components of microorganisms into products such as water and CO_2 [359,368,485,486].

Although the bactericidal mode of TiO_2 photocatalysis has been investigated mostly with the use of fine TiO_2 particles, this type of photocatalytic systems is of limited practical importance because of the need of ultimately removing highly dispersed photocatalyst from the treated solution by filtration or centrifugation. To overcome this drawback, several approaches have been proposed, including fabrication of magnetic photocatalysts and combination of nanocrystalline titania with organic mesophases [487]. Another bottle-neck for titania is the limited efficiency, and numerous strategies have been investigated to improve the performance. The modification of titania particles or thin films with metal nanoparticles, especially particles of noble metals, is commonly used for enhancing the efficiency of photocatalysis. The metal deposits generally act as the sink for photoinduced charge carriers, thus promoting interfacial charge transfer reactions or improving the selectivity of the photoinduced reactions on the photocatalyst surface [488–490]. In these cases, TiO_2 photoactivity is strongly influenced by the presence of noble metals such as silver. Silver

is well-known for its bactericidal capability, whereas Ag^+ ion is a strong electron donor primarily involved in interaction with cell proteins through sulfydryl groups [481]. Silver nanoclusters release $Ag^{(0)}$ and both Ag^+ ion and $Ag^{(0)}$ atom have the ability to rapidly kill bacteria and fungi [491]. Moreover, silver metal on titania surface can strongly influence charge separation upon light absorption and thereby photochemical ctivity [492] Besides, metals like silver and copper can change the surface characteristics of titania at local level. For example, a loading of ca. 5 wt.% of Cu can induce measurable variations in the point of zero charge (PZC), altering the initial steps of microorganism interaction (adhesion) to catalyst surface [493]. It was reported that bactericidal activities of nanostructured TiO_2 films modified with Ag and bimetallic Ag/Ni nanoparticles as well as TiO_2/In_2O_3 films, introduced recently as a highly effective nanocomposite photocatalysts, are effective in killing both Gram-positive and Gram-negative bacteria with special reference on the role of the photoproduced reactive oxygen species of different types in the cell inactivation [494]. Similarly, Ag/ZnO nanocomposite has also been demonstrated to show antibacteria activity [201,495].

With developments of visible light n-TiO_2 photocatalyst by anionic doping, such as N, C, S, or F, a greater portion of the solar spectrum or just indoor light may be used to provide photocatalytic capability. However, one problem with the current anion-doped TiO_2 photocatalysts is that they lose their photocatalytic capability in the dark environment, where they could not produce electron and hole pairs. Therefore, it would be more desirable to design a visible light photocatalyst system which can provide enhanced photocatalytic efficiency by minimizing charge carrier recombination. It would be even better if the improved photocatalyst can store some of its photocatalytic activity in "memory" so that once the photoexcitation is turned off, the catalyst still remains active for an extended period of time. A visible light photocatalyst based on palladium oxide nanoparticles dispersed on N-doped n-TiO_2, hereafter referred to as TiON/PdO, demonstrated not only a much faster photocatalytic disinfection rate on *Escherichia coli* (*E. coli*) under visible light illumination than N-doped TiO_2 (TiON), but most strikingly, a "memory" catalytic disinfection capability after visible light illumination was turned off for extended periods of up to 8 h [496,497]. These unusual antimicrobial properties of TiON/PdO are derived from the optoelectronic coupling between PdO nanoparticles and TiON semiconductor, which promotes the charge carrier separation in TiON and results in the chemical reduction of PdO to Pd^0. While the separation of the charge carriers greatly enhances the visible light photocatalytic killing of *E. coli*, a "memory" antimicrobial effect results from the catalytic effect of Pd^0. The strong antimicrobial effects of TiON/PdO photocatalyst under visible light and their post-illumination activity open up the possibility of solar-powered disinfection during daytime and at night, for a broad range of environmental applications. In addition, HSNs, such as CdSe/ZnS–photosensitized nano-TiO_2 film (QDs-TiO_2 film) [498], ethylene–vinyl alcohol copolymer (EVOH)–TiO_2 nanoparticle composites [499], and $ZnIn_2S_4$ film electrode [500], have been used in disinfection under visible or UV light at low intensity.

3.3. Photonics: lasers, LEDs, solid state lighting, and displays

3.3.1. Lasing and lasers

One area of application of nanomaterials that has attracted considerable interest is lasers. It is in principle possible to built lasers with different wavelengths by changing the particle size. There are two practical problems with this idea. First, the spectrum of most nanoparticles is usually quite broad due to homogeneous and inhomogeneous broadening. Second, the high density of trap states leads to fast relaxation of the excited charge carrier, making it difficult to build up population inversion necessary for lasing. When the surface of the particles is clean and has little defects, the idea of lasing can indeed be realized. This has been demonstrated mostly for nanoparticles self-assembled in clean environments based on physical methods, e.g. molecular beam epitaxy (MBE) [501–504] or metal organic chemical vapor deposition (MOCVD) [505]. Examples of quantum dot lasers include InGaAs [501], InAs [503], AlInAs [502,504], and InP [506]. Stimulated emission was also observed in GaN quantum dots by optical pumping [505]. The lasing action or stimulated emission was observed mostly at low temperature [504,506]. However, room temperature lasing was also achieved [501,502].

Recently, lasing action was observed in colloidal QDs of CdSe based on wet chemistry synthesis and optical pumping [507]. It was found that, despite highly efficient intrinsic non-radiative Auger recombination, large optical gain can be developed at the wavelength of the emitting transition for close-packed solids of CdSe QDs. Narrow-band stimulated emission with a pronounced gain threshold at wavelengths tunable with size of the nanocrystal was observed. This work demonstrates the feasibility of nanocrystal quantum dot lasers based on wet chemistry synthesis. Whether real laser devices can be built based on this type of nanoparticles remains to be seen. Also, it is unclear if electrical pumping of such lasers can be realized. Likewise, nanoparticles can be potentially used for laser amplification and such application has yet to be explored. Nanoparticles such as TiO_2 have also been used to enhance stimulated emission for conjugated polymers based on multiple reflection effect [508].

3.3.2. Light emitting diodes (LEDs)

Nanoparticles have been used for LED application in two ways. First, they are used to enhance light emission of LED devices with other materials, e.g. conjugated polymers, as the active media. The role of the nanoparticles, such as TiO_2, is not completely clear but thought to enhance either charge injection or transport [509]. In some cases the presence of semiconductor nanocrystals in carrier-transporting polymers was found to not only enhance the photoinduced charge generation efficiency but also extends the sensitivity range of the polymers, while the polymer matrix is responsible for charge transport [510,511]. This type of polymer/nanocrystal composite materials can have improved properties over the individual constituent components and may have interesting applications.

Second, the nanoparticles are used as the active materials for light generation directly [182,504,512–516]. In this case, the electron and hole are injected directly into the CB and VB, respectively, of the NPs and the recombination of the electron and hole results in light emission. Fig. 15 shows the absorption, PL, and EL spectra of CdSe/ZnS core/shell quantum dots in multilayered LEDs [516].

Several studies have been reported with the goal to optimize injection and charge transport in such device structures using CdS [514] and CdSe nanoparticles [182,512]. Since the mobility of the charge carriers is usually much lower than in bulk single crystals, charge transport is one of the major limitations in efficient light generation in such devices. For example, photoconductivity and electric field induced photoluminescence quenching studies of close-packed CdSe quantum dot solids suggest that photoexcited, quantum confined excitons are ionized by the applied electric field with a rate dependent on both the size and surface passivation of the quantum dots [517,518]. Separation of electron–hole pairs confined to the core of the dot requires significantly more energy than separation of carriers trapped at the surface and occurs through tunneling processes. New nanostructures, such as nanowires [519,520], nanorods [51,521–523], and nanobelts [524], provide some interesting alternatives with better transport prop-

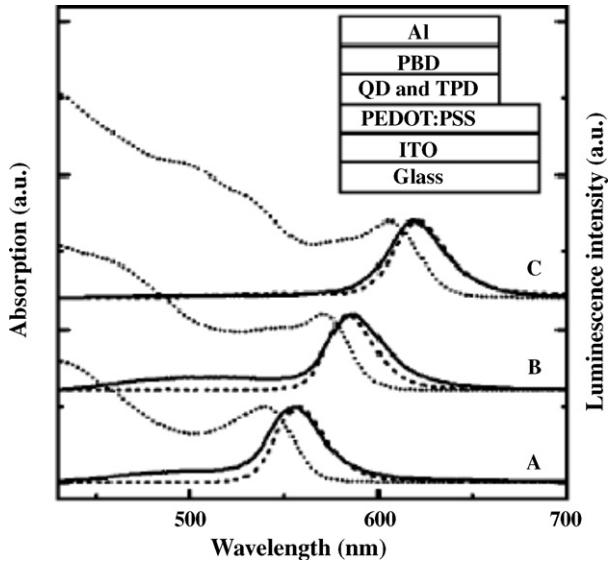

Fig. 15. Absorption (dotted lines), photo- (dashed lines), and electroluminescence (solid lines) spectra for 3.2 nm (A), 4.1 nm (B), and 5.4 nm (C) diameter CdSe QDs covered by 2 MLs of ZnS. Voltages and currents are: (A) 5.5 V, 0.11 mA; (B) 5.0 V, 0.08 mA; (C) 4.0 V, 0.06 mA, respectively. Schematic of the structure of the multilayered CdSe/ZnS QD LEDs is shown in the inset. Abbreviations: TPD for *N*,*N*′-diphenyl-*N*,*N*′-bis(3-methylphenyl)-1,1′-biphenyl-4,4′-diamine; PEDOT:PSS for poly(3,4-ethylenedioxythiophene):poly(styrenesulfonate); ITO for indium tin oxide; and PBD for 2-biphenyl-4-yl-5-(4-tert-butylphenyl)-1,3,4-oxadiazole. Reproduced with permission from Ref. [516].

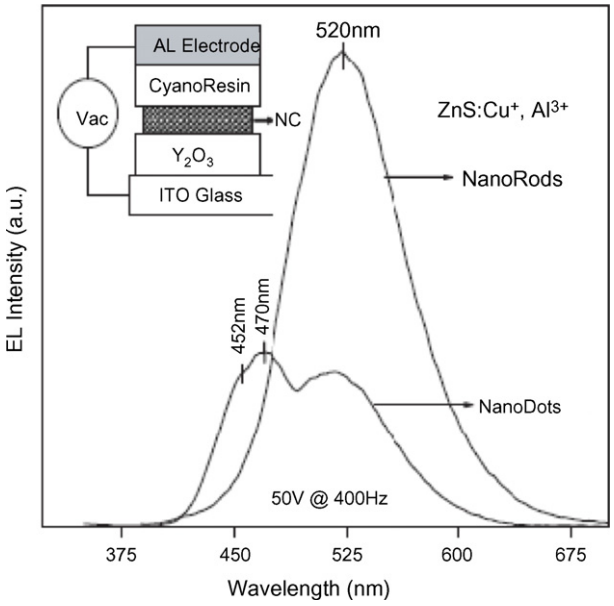

Fig. 16. EL spectra of ZnS:Cu^+,Al^{3+} nanodots and nanorods. (Inset) Schematic structure of AC EL device based on nanodots/nanorods. Reproduced with permission from Ref. [529].

erties than nanoparticles. Devices such as LEDs based on such nanostructures are starting to be developed.

3.3.3. Solid state lighting-AC powder electroluminescence (ACPEL)

One major photonics application of doped or hybrid semiconductor nanomaterials is solid state lighting. Solid state lighting is an area of fast growth. Approximately one-third of the United States electricity is consumed by lighting, an industry that is largely dominated by relatively old technologies such as the incandescent and fluorescent light bulb. New innovations in lower cost and higher efficiency solid state lighting are expected to significantly reduce our dependence on fossil fuels. A solid state lighting technology that is already compatible with low cost manufacturing is AC powder electroluminescence (ACPEL). Discovered in 1936 [525], powder electroluminescence utilizes emission from ~40 to 50 μm-sized-doped ZnS:Cu,Cl phosphor particles and requires relatively low applied electric fields (10^4 V/cm) compared to DC EL which requires electric fields near 10^6 V/cm. More recently, microencapsulation technology was successfully applied to ZnS:Cu,Cl powder phosphors so that the emissive particles can be deposited on plastic substrates under open air, non-clean-room conditions using low cost, large area print-based manufacturing. Consequently, ACPEL lights are one of the least expensive large area solid state lighting technologies, and the characteristic blue-green light can now be found in many products. Furthermore, fluorescent energy conversion and doping can readily be used to convert the blue-green light to the white light preferred for normal everyday lighting. Using a variety of dopants (I, Br, Al, Mn, Pr, Tm, etc.), other colors can also be obtained [526,527].

The mechanism for light emission from ZnS:Cu,Cl particles is thought to be due to localized electron and hole injection near Cu_xS inclusions which requires an alternating current (AC) to enable the frequency-dependent electron–hole recombination. While this process is highly efficient, the lifetime and power efficiency of ACPEL lights are heretofore too low to provide a replacement for white lights. The power efficiency is limited by the large ZnS:Cu,Cl particle size (>20 μm) over which the electric field is dropped, resulting in the need for higher voltages, ~120 V, to achieve the brightness needed for solid state lighting. Research on phosphor nanoparticles has attempted to address the voltage issue; however, these systems typically have significantly reduced lifetime and quantum efficiency due to poor charge transport and/or trapping. For example, an EXAFS study was conducted to understand how the degradation depends on the local microstructure about Cu in doped ZnS:Cu,Cl and have found that the degradation process is reversible through modest application of elevated temperatures (~200 °C) [528]. Note that although the particle size is large (typically 20–50 μm), the active regions within each particle are near Cu_xS precipitates a few nm in size; hence it is essential to understand the Cu_xS nanoparticle precipitates within the ZnS host and how they interact with other optically active centers. Nanoparticle and nanorod systems exhibiting AC EL have been reported recently [527,529]. Fig. 16 shows EL spectra of ZnS:Cu^+,Al^{3+} nanodot and nanorods that clearly exhibit different radiative recombination pathways based on their different EL spectroscopic features [529].

A recent study of ZnS:Cu NPs using combined PL and EXAFS studies has found that the Cu exists in the +1 oxidation state and the Cu dopant ions are in the interior but near the surface of the host ZnS NPs [243]. Further research is needed to better understand the local atomic structure of dopants and its correlation to the PL and EL properties relevant to solid state lighting applications.

3.3.4. Photochromic and electrochromic displays

Photochromism refers to the reversible transformation of a chemical species between two forms, e.g. isomers, by the absorption of light [530]. The two forms usually have quite different absorption spectra in the visible, and therefore photoinduced transformation from one form to another results in color changes. If the transformation is induced electrically, the process is called *electrochromism*. These phenomena have found applications in light attenuation, data storage, sunglasses, switchable windows, and sensors [530,531]. They have been observed mostly in organic molecules, such as spiropyrans and sprioxazines, azobenzenes, and quinones, or inorganic substances such as silver chloride and other metal halides [532–534].

Photochromism and electrochromism have also been reported for semiconductor nanomaterials including HSNs [535,536]. For example, a transparent working electrode coated with Ag–TiO_2 nanocomposite exhibits multicolor photochromism [537]. Similarly, photochromic properties of MoO_3 and Au nanocomposite think films have been demonstrated [536]. Inorganic transition metal oxides, such as WO_3, MoO_3 and V_2O_5, are used as the electrochromic materials [537]. For example, when WO_3 was electrochemically reduced in the presence of cations small enough to penetrate into the oxide lattice, a bluish-colored tungsten bronze could be formed [538]. The electrochromic process was highly reversible and lifetimes of over 10^7 cycles have been achieved in display applications [538]. During the process, W^{6+} was reduced to W^{5+}, and the color was considered to be resulted from an intervalence charge transfer process between W^{5+} and W^{6+} sites [539]. Another example is TiO_2 based HSNs, in which 3-methylthiophene (MeT) was electrochemically incorporated with nano- and mesoporous TiO_2 films to form poly(3-methylthiophene) (PMeT)/TiO_2 nanocomposite electrochromic electrodes with enhanced long-term stability [540].

In addition, photoelectrochromic (PE) devices based on a combination of dye-sensitized solar cells [249,250] and electrochromic layers [531] have been reported. In contrast to electrochromic devices, the coloring in PE devices is induced by light illumination and no external bias is needed [291]. The transmittance decreases under light illumination and can be reverted in the dark. Furthermore, in contrast to photochromic devices, the system is externally switchable [291]. As an example of PE application based on HSNs, WO_3–TiO_2 hybrid layers were used to assemble PE devices that allow high optical modulation with the visible transmittance changes from 62% to 1.6%. The coloring and bleaching processes were finished within 10 min, while self-bleaching extended beyond 100 h [291]. Applications of PE devices include switchable sunroofs in cars or smart windows in buildings [541].

3.4. Chemical sensing and biomedical detection, imaging, and therapy

Semiconductor nanomaterials have optical properties useful for chemical and biomedical applications, including detection, imaging, and therapeutic treatment. Detection, analysis and sensing of chemicals and biochemicals are important to a number of industrial and technological applications ranging from medicine to food, electronics, security, and chemical industry. Equipment or devices used for such analytical purposes operate based on different mechanisms. The basic idea is that signal detected contains information about the target analyte and can thus be used for its identification. The signal is generated when the analyzer or sensor interacts with the target analyte and the interaction usually needs to be triggered by a stimuli or source of energy. The source stimuli and the signal detected can come in many forms, e.g. light, heat, current or voltage, magnetic, mechanical, or sound. Among these, optical stimulation and detection are the most common and have the advantage of low cost and non-invasiveness.

We will focus our discussion on optical sensing and detection using HSNs. Optical sensors are analyzers that involve light as the stimuli and/or the signal for detection. For instance, light can be used to excite an analyte, and optical signal can be detected in terms of fluorescence or Raman scattering. Both semiconductor and metal nanostructures have been used extensively for chemical and biomedical detection by taking advantage of their unique optical properties. The detection scheme usually makes use of their absorption, scattering, or other effects such as photothermal conversion [542–546]. In this section, we will concentrate on a few specific application examples.

3.4.1. Luminescence-based detection

The basic mechanism behind many optical sensors is the detection of changes of optical signatures of nanomaterials when they interact with target analyte molecules. The optical signature could be absorption, luminescence, or Raman scattering. Among these, luminescence is the most popular for the reason that it is highly sensitive, ubiquitous, and easy to detect. Almost all semiconductors and insulators are luminescent to different degrees at the appropriate excitation wavelength. Metal are often non-luminescent or very weakly luminescent, but can be strongly luminescent when inter-band transitions are involved with appropriate excitation wavelength.

QDs have been widely used, in place of dye molecules, as fluorescence labels in biomedical detection. Compared to dye molecules, QDs offer broader absorption and PL tunability, choice of multiple colors from the same chemical composition, flexibility for surface functionalization, and, in some cases, less photobleaching or higher stability [97,102,181,547–550]. The optical signal detected is usually fluorescence from the QDs conjugated to appropriate biomolecules of interest, e.g. DNA and proteins. In these systems, the QDs are the primary component while the biological molecules are the secondary component. Together, the QDs and biomolecule form a hybrid system.

In most cases, luminescence quenching or enhancement of a fluorophore is detected when the fluorophore interacts with a target analyte. The degree of luminescence quenching or enhancement should ideally be linearly proportional to the analyte concentration over a broad range (large dynamic range) and sensitive down to a very low concentration (sensitivity) with small background (low noise).

One of the most commonly encountered techniques based on photoluminescence is fluorescence or Förster resonance energy transfer (FRET). FRET is often used to determine the distance between two functional groups in a molecule [551]. FRET involves non-radiative transfer of energy from a donor molecule (or nanoparticle) to an acceptor molecule (or nanoparticle). Therefore, the signature of FRET is quenching of the donor fluorescence followed by lower energy or longer wavelength fluorescence of the acceptor. FRET efficiency, E_{FRET}, defined as the fraction of energy (in photons) absorbed by the donor that was subsequently transferred to the acceptor, is expressed as:

$$E_{FRET} = \frac{R_0^6}{R_0^6 + R^6} = \frac{1}{1 + (R/R_0)^6} \quad (3)$$

where R_0 is the Förster distance and R is the distance between the center of the donor and acceptable fluorophore dipole moments. From this equation, it is clear that, at the Förster distance, the FRET efficiency is 50%. The Förster distance R_0 is determined by the spectroscopic overlap between the donor fluorescence and acceptor absorption, fluorescence quantum yield of the donor in the absence of the acceptor, the refractive index of the medium, and the dipole orientation factor.

More relevant to experimental measurement is the expression:

$$E_{FRET} = 1 - \frac{F_{DA}}{F_D} = 1 - \frac{\tau_D}{\tau_{DA}} \quad (4)$$

where F_{DA} and τ_{DA} are, respectively, the fluorescence intensity and lifetime of the donor in the presence of the acceptor, F_D and τ_D are the fluorescence intensity and lifetime of the donor when the acceptor is far away or absent. Eq. (4) shows that the FRET efficiency ranges from zero when the acceptor is far away and $F_{DA} = F_D$ to 1 when the acceptor is very close to the donor and F_{DA} is near zero (complete quenching). By attaching appropriate donors and acceptors to functional groups of interest in a molecule and measuring the FRET efficiency, one can determine the distance between the functional groups. For FRET to work effectively, the donor fluores-

cence spectrum must overlap with the absorption spectrum of the acceptor. This is to ensure effective coupling or interaction between the donor and acceptor dipoles. In addition, the distance between the donor and acceptor cannot be too far, usually within 5 nm.

While most earlier studies of FRET are based on molecular systems, recent work on using semiconductor nanoparticles or QDs for FRET has been conducted successfully, often with QDs as donors [552–555] and, to a lesser degree, as acceptors [556–558], or both as donors and acceptors [559]. QDs are less ideal as acceptors due to their typically broad absorption that easily results in absorption of the light used to excite the donor. One limitation for QDs in FRET is their relatively large size compared to molecular systems. Their advantages include size-tunable absorption and emission as well as enhanced photostability when properly passivated.

As an example, FRET has been demonstrated between two different sized QDs, with the larger, red-emitting one conjugated to an antigen (bovine serum albumin) and the smaller green-emitting one attached to the corresponding anti-BSA antibody (IgG) [559]. The formation of BSA-IgG immuno-complex resulted in FRET between the two different QDs as evidenced by the quenching of the luminescence of green-emitting QDs and simultaneous enhancement of the emission of the red-emitting QDs. This study shows that FRET based on QDs can be potentially useful for detection of antigens using corresponding known antibodies. Besides FRET, QDs have been used in direct detection of biological molecules such as DNA [560–562] as well as imaging [563] based on fluorescence from the QDs. They have also been utilized for detection of metal ions [564,565] as well as radicals [566].

3.4.2. Chemical and biochemical imaging

Imaging is attractive since it provides spatial information besides spectroscopic information compared to conventional opti-

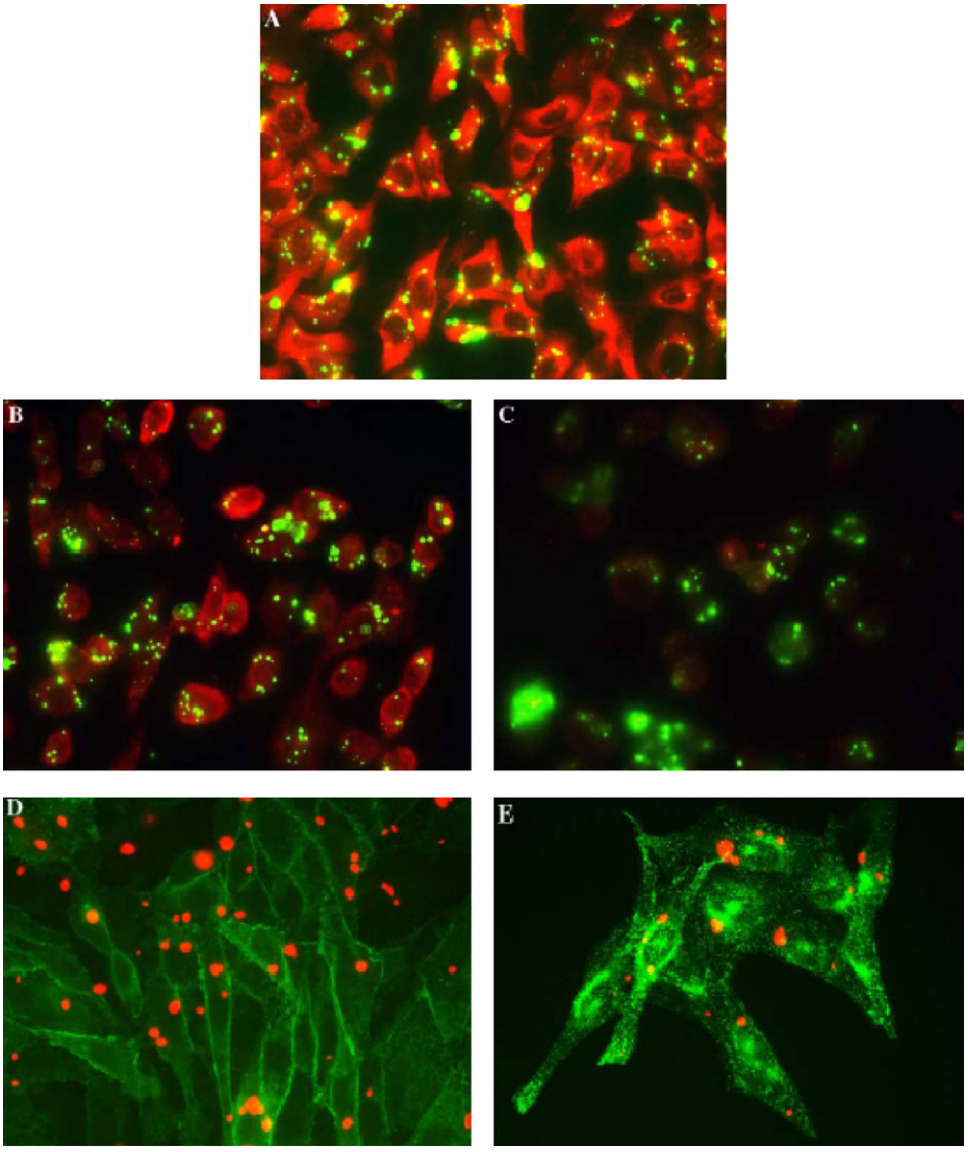

Fig. 17. Fluorescent microscopy images of encoded cells in various cellular assays. (A) Immunostaining of tubulin in Chinese hamster ovary (CHO) cells. Cells were encoded with 530 nm QDs and fixed for immunostaining using rabbit antitubulin IgG fraction, biotinylated goat anti-rabbit IgG, and streptavidin-conjugated Cy3 (a cyanine dye). Shown is a composite of the Cy3 and QD images. (B and C) Binding of CGP-12177 (a fluorescent ligand) to CHO cells expressing the 2-adrenergic receptor. CHO cells were encoded with 530 nm QDs and incubated with 250 nM BODIPY TMR (±) CGP-12177 (a long-acting fluorescent beta$_2$-adrenoceptor agonist) in the absence (B) or presence (C) of 1 μM unlabeled CGP-12177 (a beta$_3$-receptor agonist). Shown are composites of the QD and BODIPY images. Binding was measured as total pixel intensity of CGP-12177 fluorescence. (D and E) Agonist-induced internalization of the β_2-adrenergic receptor. CHO cells expressing HA-tagged β_2-adrenergic receptor were encoded with 608 nm QDs and incubated in the absence (D) or presence (E) of 10 μM isoproterenol. The cells were assayed for receptor internalization. Shown is a composite of the fluorescein isothiocyanate (FITC) and QD images. Reproduced with permission from Ref. [570].

cal detection based on spectroscopy. However, it is understandably more involved in terms of instrumentation as well as signal processing and data analysis. Optical imaging is a 2D display of optical signal, usually emitted or scattered photons, containing 3D information. Usually the vertical axis represents the optical signal intensity while the two axes in the plane represent a combination of space and/or spectroscopic frequency.

QDs have been successfully used for imaging in cell biology and animal biology. In cell biology applications, QDs are used as immunolabels and offer potential advantages over conventional organic dye molecule in terms of stability against photobleaching, tunable and broad absorption, tunable and narrow PL band, possibility for multiplexing, and flexibility for surface modification [97,101,104,567–569]. QDs have been used not only to label cellular structures and receptors and to incorporate into living cells but also to track the path and fate of individual cells including stems cells [100,549,568,570]. For example, different QDs have been used to label various subpopulations of Chinese hamster ovary (CHO) carcinoma cells on a substrate [570]. Fig. 17 shows representative fluorescent microscopy images of encoded cells in different cellular assays [570]. This study demonstrates the usefulness of multicolored QDs in cell labeling applications.

In live animal imaging applications, the surface of QDs is very important for toxicity and other considerations such as binding or accumulation in different organs. For example, surface modification of QDs with high molecular weight polyethylene glycol (PEG) molecules is effective in reducing undesired accumulation in the liver and bone marrow [105]. Compared to visible light, near IR light penetrates deeper into tissues and has less scattering. Therefore, near IR emitting QDs are desired for animal imaging applications, as has been demonstrated using small bandgap CdTe/CdSe core/shell QDs [571]. It is clear that both the optical and surface properties of QDs are critical for animal imaging applications. More research is needed to better understand some of the fundamental issues including interaction between QDs and different cells, toxicity, and mechanism of biodegradation of the QDs. The QDs used in imaging are passivated with or conjugated to organic and/or biological molecules. The overall systems are therefore HSNs.

3.4.3. *Biomedical therapy*

Besides detection and imaging applications, some nanomaterials have also been explored as therapeutic agents. In relation to optical properties, one interesting application is the use of nanomaterials as photosensitizer in a process called *photodynamic therapy* (*PDT*). PDT is a medical technique for cancer treatment that uses a combination of light, photosensitizers, and oxygen [572]. The basic mechanism is that photoexcitation of the photosensitizer leads to generation of radical and/or singlet oxygen that results in cancer cell necrosis. Most photosensitizers are molecules with strong visible or near IR absorption, e.g. porphyrins [573]. Ideal photosensitizers should have low dark toxicity and strong light absorption, can selectively localize onto cancer tissues, are stable and efficient in generating useful singlet oxygen and/or radicals.

Semiconductor nanoparticles have been exploited and successfully demonstrated to be potentially useful for PDT applications. For example, Si nanocrystals are effective in singlet oxygen generation via an exchange of electrons with mutually opposite spins between the photoexcited Si nanocrystal and ground state (triplet) oxygen [574]. Supporting evidence includes PL quenching of Si NC by O_2 and light emission from the singlet oxygen at 0.98 eV [575]. Similarly, CdSe QDs were explored for PDT application and found to be able to generate singlet oxygen directly via a triplet energy transfer mechanism [576]. Nanoparticles, such as gold and silica, have been used for photosensitizer delivery in PDT applications [577–579]. In these cases, the QDs or nanoparticles are the primary system while the surface capping molecules or photosensitizers to be delivered are the secondary system for such effective HSNs.

4. Summary

A number of hybrid semiconductor nanomaterial (HSN) systems have been discussed with their optical properties highlighted. Besides the systems presented, there are many other hybrid nanostructures that we did not cover, including inorganic metal–metal, that tend to have strong interaction between their constituent components and thereby complex optical properties. The examples covered illustrate the diversity and usefulness of hybrid materials. There are practically unlimited possibilities for generating composite materials due to the many parameters and material components one can choose and vary. New hybrid nanomaterials are expected to continue to be developed and studied, and new applications are to be exploited for emerging technologies.

Acknowledgements

We are grateful to financial support by the Basic Energy Sciences Division of the US DOE (DE-FG02-05ER46232-A002 and DE-FG02-07ER46388-A002), the US NSF (ECCS-0823921), National Natural Science Foundation of China (No. 20675044, No. 20628303) and National Basic Research Program of China (No. 2007CB310500).

References

[1] J. Wang, Z. Jiang, L.Q. Zhang, P.L. Kang, Y.P. Xie, Y.H. Lv, R. Xu, X.D. Zhang, Ultrasonics Sonochem. 16 (2009) 225.
[2] J. Wang, M. Nozaki, M. Lachab, R.S.Q. Fareed, Y. Ishikawa, T. Wang, Y. Naoi, S. Sakai, J. Cryst. Growth 200 (1999) 85.
[3] S.Y. Lu, S.W. Chen, J. Am. Ceram. Soc. 83 (2000) 709.
[4] J.W. Wang, Y.P. Sun, Z.H. Liang, H.P. Xu, C.M. Fan, X.M. Chen, Rare Met. Mater. Eng. 33 (2004) 478.
[5] Y.J. Li, P.B. Shi, R. Duan, B.R. Zhang, Y.P. Qiao, G.G. Qin, L. Huang, J. Infrared Millimeter Waves 23 (2004) 176.
[6] M. Sacilotti, J. Decobert, H. Sik, G. Post, C. Dumas, P. Viste, G. Patriarche, J. Cryst. Growth 272 (2004) 198.
[7] H.T. Lin, J.L. Huang, S.C. Wang, C.F. Lin, J. Alloys Compd. 417 (2006) 214.
[8] D.Y. He, X.Q. Wang, Q. Chen, J.S. Li, M. Yin, A.V. Karabutov, A.G. Kazanskii, Chin. Sci. Bull. 51 (2006) 510.
[9] Z.Z. Ye, J.Y. Huang, W.Z. Xu, J. Zhou, Z.L. Wang, Solid State Commun. 141 (2007) 464.
[10] J.Y. Wang, T. Ito, Diam. Relat. Mater. 16 (2007) 589.
[11] J. Huerta, M. Lopez, O. Zelaya-Angel, J. Vac. Sci. Technol. B 18 (2000) 1716.
[12] J. Huerta-Ruelas, M. Lopez-Lopez, O. Zelaya-Angel, Jpn. J. Appl. Phys. Part 1: Regul. Papers Short Notes Rev. Papers 39 (2000) 1701.
[13] C.B. Murray, C.R. Kagan, M.G. Bawendi, Ann. Rev. Mater. Sci. 30 (2000) 545.
[14] J. Turkevich, P.C. Stevenson, J. Hiller, Discuss. Faraday Soc. 11 (1951) 55.
[15] G. Frens, Nat. Phys. Sci. 241 (1973) 20.
[16] P.C. Lee, D. Meisel, J. Phys. Chem. 86 (1982) 3391.
[17] A. Henglein, Israel J. Chem. 33 (1993) 77.
[18] F. Silly, A.O. Gusev, A. Taleb, F. Charra, M.P. Pileni, Phys. Rev. Lett. 84 (2000) 5840.
[19] J. Kimling, M. Maier, B. Okenve, V. Kotaidis, H. Ballot, A. Plech, J. Phys. Chem. B 110 (2006) 15700.
[20] X.H. Ji, X.N. Song, J. Li, Y.B. Bai, W.S. Yang, X.G. Peng, J. Am. Chem. Soc. 129 (2007) 13939.
[21] N.R. Jana, L. Gearheart, C.J. Murphy, J. Phys. Chem. B 105 (2001) 4065.
[22] N.R. Jana, L. Gearheart, C.J. Murphy, Chem. Commun. (2001) 617.
[23] K.R. Brown, D.G. Walter, M.J. Natan, Chem. Mater. 12 (2000) 306.
[24] K.R. Brown, L.A. Lyon, A.P. Fox, B.D. Reiss, M.J. Natan, Chem. Mater. 12 (2000) 314.
[25] J. Rodriguez-Fernandez, J. Perez-Juste, F.J.G. de Abajo, L.M. Liz-Marzan, Langmuir 22 (2006) 7007.
[26] C.J. Johnson, E. Dujardin, S.A. Davis, C.J. Murphy, S. Mann, J. Mater. Chem. 12 (2002) 1765.
[27] A. Gole, C.J. Murphy, Chem. Mater. 16 (2004) 3633.
[28] C.J. Murphy, T.K. San, A.M. Gole, C.J. Orendorff, J.X. Gao, L. Gou, S.E. Hunyadi, T. Li, J. Phys. Chem. B 109 (2005) 13857.
[29] L.F. Gou, C.J. Murphy, Chem. Mater. 17 (2005) 3668.
[30] C.J. Murphy, T.K. Sau, A. Gole, C.J. Orendorff, Mrs Bull. 30 (2005) 349.
[31] B. Nikoobakht, M.A. El-Sayed, Chem. Mater. 15 (2003) 1957.
[32] Y.G. Sun, B. Mayers, Y.N. Xia, Adv. Mater. 15 (2003) 641.
[33] Y.G. Sun, B. Wiley, Z.Y. Li, Y.N. Xia, J. Am. Chem. Soc. 126 (2004) 9399.
[34] C.H. Wang, D.C. Sun, X.H. Xia, Nanotechnology 17 (2006) 651.

[35] Y.G. Sun, B.T. Mayers, Y.N. Xia, Nano Lett. 2 (2002) 481.
[36] A.M. Schwartzberg, T.Y. Olson, C.E. Talley, J.Z. Zhang, J. Phys. Chem. B 110 (2006) 19935.
[37] A.M. Schwartzberg, C.D. Grant, T. van Buuren, J.Z. Zhang, J. Phys. Chem. C 111 (2007) 8892.
[38] R.A. Bley, S.M. Kauzlarich, J.E. Davis, H.W.H. Lee, Chem. Mater. 8 (1996) 1881.
[39] R.K. Baldwin, K.A. Pettigrew, E. Ratai, M.P. Augustine, S.M. Kauzlarich, Chem. Commun. (2002) 1822.
[40] J.R. Heath, J.J. Shiang, A.P. Alivisatos, J. Chem. Phys. 101 (1994) 1607.
[41] B.R. Taylor, S.M. Kauzlarich, G.R. Delgado, H.W.H. Lee, Chem. Mater. 11 (1999) 2493.
[42] N. Zaitseva, Z.R. Dai, C.D. Grant, J. Harper, C. Saw, Chem. Mater. 19 (2007) 5174.
[43] C.B. Murray, D.J. Norris, M.G. Bawendi, J. Am. Chem. Soc. 115 (1993) 8706.
[44] C.B. Murray, M. Nirmal, D.J. Norris, M.G. Bawendi, Zeitschrift Fur Physik D: Atoms Mol. Clusters 26 (1993) S231.
[45] A.P. Alivisatos, Science 271 (1996) 933.
[46] A.A. Guzelian, J.E.B. Katari, A.V. Kadavanich, U. Banin, K. Hamad, E. Juban, A.P. Alivisatos, R.H. Wolters, C.C. Arnold, J.R. Heath, J. Phys. Chem. 100 (1996) 7212.
[47] X.G. Peng, M.C. Schlamp, A.V. Kadavanich, A.P. Alivisatos, J. Am. Chem. Soc. 119 (1997) 7019.
[48] X.G. Peng, Chem. A: Eur. J. 8 (2002) 335.
[49] J. Joo, H.B. Na, T. Yu, J.H. Yu, Y.W. Kim, F. Wu, J.Z. Zhang, T. Hyeon, J. Am. Chem. Soc. 125 (2003) 11100.
[50] A.Y. Nazzal, X.Y. Wang, L.H. Qu, W. Yu, Y.J. Wang, X.G. Peng, M. Xiao, J. Phys. Chem. B 108 (2004) 5507.
[51] L. Manna, E.C. Scher, A.P. Alivisatos, J. Am. Chem. Soc. 122 (2000) 12700.
[52] F. Wu, J.Z. Zhang, R. Kho, R.K. Mehra, Chem. Phys. Lett. 330 (2000) 237.
[53] J. Moser, M. Grätzel, J. Am. Chem. Soc. 106 (1984) 6557.
[54] L. Spanhel, A. Henglein, H. Weller, Ber. Bunsen-Ges. Phys. Chem. 91 (1987) 1359.
[55] W.Y. Zhou, Y. Zhou, S.Q. Tang, Mater. Lett. 59 (2005) 3115.
[56] J.J. Qiu, W.D. Yu, X.D. Gao, X.M. Li, Nanotechnology 17 (2006) 4695.
[57] G. Oskam, F.D.P. Poot, J. Sol–Gel Sci. Technol. 37 (2006) 157.
[58] A. Wolcott, T.R. Kuykendall, W. Chen, S.W. Chen, J.Z. Zhang, J. Phys. Chem. B 110 (2006) 25288.
[59] Z.H. Zhang, Y. Yuan, Y.J. Fang, L.H. Liang, H.C. Ding, L.T. Jin, Talanta 73 (2007) 523.
[60] H.M. Cheng, J.M. Ma, Z.G. Zhao, L.M. Qi, Chem. J. Chin. Univ. 17 (1996) 833 (in Chinese).
[61] S.W. Lu, B.I. Lee, Z.L. Wang, W.D. Samuels, J. Cryst. Growth 219 (2000) 269.
[62] S. Jeon, P.V. Braun, Chem. Mater. 15 (2003) 1256.
[63] X. Wang, Y.D. Li, Mater. Chem. Phys. 82 (2003) 419.
[64] K. Lee, N.H. Leea, S.H. Shin, H.G. Lee, S.J. Kim, Mater. Sci. Eng. B: Solid State Mater. Adv. Technol. 129 (2006) 109.
[65] Y. Ding, Y. Wan, Y.L. Min, W. Zhang, S.H. Yu, Inorg. Chem. 47 (2008) 7813.
[66] H.F. Wang, Y.Q. Ma, G.S. Yi, D.P. Chen, Mater. Chem. Phys. 82 (2003) 414.
[67] J. Yang, C.K. Lin, Z.L. Wang, J. Lin, Inorg. Chem. 45 (2006) 8973.
[68] J.X. Wang, X.W. Sun, Y. Yang, H. Huang, Y.C. Lee, O.K. Tan, L. Vayssieres, Nanotechnology 17 (2006) 4995.
[69] N. Baccile, A. Fischer, B. Julian-Lopez, D. Grosso, C. Sanchez, J. Sol–Gel Sci. Technol. 47 (2008) 119.
[70] T. Wetz, K. Soulantica, A. Talqui, M. Respaud, E. Snoeck, B. Chaudret, Angew. Chem. Int. Ed. 46 (2007) 7079.
[71] S. Jansat, K. Pelzer, J. Garcia-Anton, R. Raucoules, K. Philippot, A. Maisonnat, B. Chaudret, Y. Guari, A. Mehdi, C. Reye, R.J.R. Corriu, Adv. Funct. Mater. 17 (2007) 3339.
[72] A.R. Kortan, R. Hull, R.L. Opila, M.G. Bawendi, M.L. Steigerwald, P.J. Carroll, L.E. Brus, J. Am. Chem. Soc. 112 (1990) 1327.
[73] M.A. Hines, P. Guyot-Sionnest, J. Phys. Chem. 100 (1996) 468.
[74] B.O. Dabbousi, J. RodriguezViejo, F.V. Mikulec, J.R. Heine, H. Mattoussi, R. Ober, K.F. Jensen, M.G. Bawendi, J. Phys. Chem. B 101 (1997) 9463.
[75] S.L. Cumberland, K.M. Hanif, A. Javier, G.A. Khitrov, G.F. Strouse, S.M. Woessner, C.S. Yun, Chem. Mater. 14 (2002) 1576.
[76] A.R. Clapp, E.R. Goldman, H. Mattoussi, Nat. Protoc. 1 (2006) 1258.
[77] M. Dybiec, G. Chornokur, S. Ostapenko, A. Wolcott, J.Z. Zhang, A. Zajac, C. Phelan, T. Sellers, D. Gerion, Appl. Phys. Lett. 90 (2007) 263112.
[78] R.E. Anderson, W.C.W. Chan, ACS Nano 2 (2008) 1341.
[79] M. Danek, K.F. Jensen, C.B. Murray, M.G. Bawendi, Chem. Mater. 8 (1996) 173.
[80] J. Tang, H. Birkedal, E.W. McFarland, G.D. Stucky, Chem. Commun. (2003) 2278.
[81] A. Mews, A.V. Kadavanich, U. Banin, A.P. Alivisatos, Phys. Rev. B: Condens. Matter 53 (1996) 13242.
[82] M. Braun, C. Burda, M.A. El-Sayed, J. Phys. Chem. A 105 (2001) 5548.
[83] H. Fujii, K. Inata, M. Ohtaki, K. Eguchi, H. Arai, J. Mater. Sci. 36 (2001) 527.
[84] S.L. Cumberland, M.G. Berrettini, A. Javier, G.F. Strouse, Chem. Mater. 15 (2003) 1047.
[85] Y.M. Wang, X.J. Li, S.J. Zheng, J. Inorg. Mater. 22 (2007) 729.
[86] M.G. Manera, J. Spadavecchia, D. Buso, C.D. Fernandez, G. Mattei, A. Martucci, P. Mulvaney, J. Perez-Juste, R. Rella, L. Vasanelli, P. Mazzoldi, Sens. Actuators B: Chem. 132 (2008) 107.
[87] L.J. Diguna, Q. Shen, A. Sato, K. Katayama, T. Sawada, T. Toyoda, Mater. Sci. Eng. C: Biomim. Supramol. Syst. 27 (2007) 1514.
[88] J.P. Ge, S. Xu, J. Zhuang, X. Wang, Q. Peng, Y.D. Li, Inorg. Chem. 45 (2006) 4922.
[89] A. Wolcott, D. Gerion, M. Visconte, J. Sun, A. Schwartzberg, S.W. Chen, J.Z. Zhang, J. Phys. Chem. B 110 (2006) 5779.
[90] L.M. Liz-Marzan, P. Mulvaney, New J. Chem. 22 (1998) 1285.
[91] B.P. Zhang, H. Masumoto, Y. Someno, T. Goto, Mater. Trans. 44 (2003) 215.
[92] H.W. Lee, S. Cho, S. Lee, F. Rotermund, J. Lee, H. Lim, J. Kor. Phys. Soc. 51 (2007) 390.
[93] E. Mine, A. Yamada, Y. Kobayashi, M. Konno, L.M. Liz-Marzan, J. Colloid Interf. Sci. 264 (2003) 385.
[94] Y.S. Park, L.M. Liz-Marzan, A. Kasuya, Y. Kobayashi, D. Nagao, M. Konno, S. Mamykin, A. Dmytruk, M. Takeda, N. Ohuchi, J. Nanosci. Nanotechnol. 6 (2006) 3503.
[95] I. Pastoriza-Santos, J. Perez-Juste, L.M. Liz-Marzan, Chem. Mater. 18 (2006) 2465.
[96] M. Sangermano, S. Perruchas, T. Gacoin, G. Rizza, Macromol. Chem. Phys. 209 (2008) 2343.
[97] W.C.W. Chan, S.M. Nie, Science 281 (1998) 2016.
[98] C.Y. Zhang, H. Ma, S.M. Nie, Y. Ding, L. Jin, D.Y. Chen, Analyst 125 (2000) 1029.
[99] J.O. Winter, T.Y. Liu, B.A. Korgel, C.E. Schmidt, Adv. Mater. 13 (2001) 1673.
[100] J.A. Kloepfer, R.E. Mielke, M.S. Wong, K.H. Nealson, G. Stucky, J.L. Nadeau, Appl. Environ. Microbiol. 69 (2003) 4205.
[101] M. Bruchez, M. Moronne, P. Gin, S. Weiss, A.P. Alivisatos, Science 281 (1998) 2013.
[102] D. Gerion, F. Pinaud, S.C. Williams, W.J. Parak, D. Zanchet, S. Weiss, A.P. Alivisatos, J. Phys. Chem. B 105 (2001) 8861.
[103] W.J. Parak, D. Gerion, D. Zanchet, A.S. Woerz, T. Pellegrino, C. Micheel, S.C. Williams, M. Seitz, R.E. Bruehl, Z. Bryant, C. Bustamante, C.R. Bertozzi, A.P. Alivisatos, Chem. Mater. 14 (2002) 2113.
[104] X.Y. Wu, H.J. Liu, J.Q. Liu, K.N. Haley, J.A. Treadway, J.P. Larson, N.F. Ge, F. Peale, M.P. Bruchez, Nat. Biotechnol. 21 (2003) 41.
[105] B. Ballou, B.C. Lagerholm, L.A. Ernst, M.P. Bruchez, A.S. Waggoner, Bioconjug. Chem. 15 (2004) 79.
[106] X.H. Gao, Y.Y. Cui, R.M. Levenson, L.W.K. Chung, S.M. Nie, Nat. Biotechnol. 22 (2004) 969.
[107] C.-A. Lin, J.K. Li, R.A. Sperling, L. Manna, W.J. Parak, W.H. Chang, in: G.Z. Cao, C.J. Brinker (Eds.), Annual Rev. Nano Research, World Scientific, Singapore, 2007, p. 467.
[108] W. Chen, J.Z. Zhang, A. Joly, J. Nanosci. Nanotechnol. 4 (2004) 919.
[109] M.C. Deng, T.S. Chin, F.R. Chen, J. Appl. Phys. 75 (1994) 5888.
[110] S. Kishimoto, T. Hasegawa, H. Kinto, O. Matsumoto, S. Iida, J. Cryst. Growth 214 (2000) 556.
[111] B.A. Smith, J.Z. Zhang, A. Joly, J. Liu, Phys. Rev. B 62 (2000) 2021.
[112] H.S. Yang, P.H. Holloway, B.B. Ratna, J. Appl. Phys. 93 (2003) 586.
[113] W.G. Lu, P.X. Gao, W. Bin Jian, Z.L. Wang, J.Y. Fang, J. Am. Chem. Soc. 126 (2004) 14816.
[114] R. Viswanatha, S. Sapra, S. Sen Gupta, B. Satpati, P.V. Satyam, B.N. Dev, D.D. Sarma, J. Phys. Chem. B 108 (2004) 6303.
[115] M. Ghosh, R. Seshadri, C.N.R. Rao, J. Nanosci. Nanotechnol. 4 (2004) 136.
[116] N.S. Norberg, G.L. Parks, G.M. Salley, D.R. Gamelin, J. Am. Chem. Soc. 128 (2006) 13195.
[117] N. Pradhan, D.M. Battaglia, Y.C. Liu, X.G. Peng, Nano Lett. 7 (2007) 312.
[118] N. Janssen, K.M. Whitaker, D.R. Gamelin, R. Bratschitsch, Nano Lett. 8 (2008) 1991.
[119] R. Beaulac, P.I. Archer, D.R. Gamelin, J. Solid State Chem. 181 (2008) 1582.
[120] J.L. Gole, J.D. Stout, C. Burda, Y.B. Lou, X.B. Chen, J. Phys. Chem. B 108 (2004) 1230.
[121] H. Tokudome, M. Miyauchi, Chem. Lett. 33 (2004) 1108.
[122] M. Sathish, B. Viswanathan, R.P. Viswanath, C.S. Gopinath, Chem. Mater. 17 (2005) 6349.
[123] C. Burda, J. Gole, J. Phys. Chem. B 110 (2006) 7081.
[124] H.Y. Chen, A. Nambu, W. Wen, J. Graciani, Z. Zhong, J.C. Hanson, E. Fujita, J.A. Rodriguez, J. Phys. Chem. C 111 (2007) 1366.
[125] J.H. Park, S. Kim, A.J. Bard, Nano Lett. 6 (2006) 24.
[126] M.G. Ou, B. Mutelet, M. Martini, R. Bazzi, S. Roux, G. Ledoux, O. Tillement, P. Perriat, J. Colloid Interf. Sci. 333 (2009) 684.
[127] R. Viswanatha, S. Chakraborty, S. Basu, D.D. Sarma, J. Phys. Chem. B 110 (2006) 22310.
[128] J.Z. Zhang, Z.L. Wang, J. Liu, S. Chen, G.-Y. Liu, Self-assembled Nanostructures. Nanoscale Science and Technology, Kluwer Academic/Plenum Publishers, New York, 2003, p. 316.
[129] S. Besson, T. Gacoin, C. Ricolleau, J.P. Boilot, Chem. Commun. (2003) 360.
[130] I. Lisiecki, M. Walls, D. Parker, M.P. Pileni, Langmuir 24 (2008) 4295.
[131] C. Sanchez, C. Boissiere, D. Grosso, C. Laberty, L. Nicole, Chem. Mater. 20 (2008) 682.
[132] J. Maynadie, A. Salant, A. Falqui, M. Respaud, E. Shaviv, U. Banin, K. Soulantica, B. Chaudret, Angew. Chem. Int. Ed. 48 (2009) 1814.
[133] J.Z. Zhang, Optical Properties and Spectroscopy of Nanomaterials, World Scientifc Publisher, Singapore, 2009, p. 383.
[134] J.Z. Zhang, J. Phys. Chem. B 104 (2000) 7239.
[135] R.L. Whetten, J.T. Khoury, M.M. Alvarez, S. Murthy, I. Vezmar, Z.L. Wang, P.W. Stephens, C.L. Cleveland, W.D. Luedtke, U. Landman, Adv. Mater. 8 (1996) 428.
[136] C.B. Murray, C.R. Kagan, M.G. Bawendi, Science 270 (1995) 1335.
[137] G.Y. Liu, S. Xu, Y.L. Qian, Accounts Chem. Res. 33 (2000) 457.
[138] Z.L. Wang, J. Phys. Chem. B 104 (2000) 1153.
[139] Z.L. Wang, P. Poncharal, W.A. de Heer, Microsc. Microanal. 6 (2000) 224.
[140] G. Cao, Nanostructures & Nanomaterials: Synthesis, Properties & Applications, Imperial College Press, London, 2004, p. 433.
[141] F.J. Giessibl, S. Hembacher, H. Bielefeldt, J. Mannhart, Science 289 (2000) 422.

[142] D. Bonnell, Scanning Probe Microscopy and Spectroscopy: Theory, Techniques, and Applications, Wiley-VCH, New York, 2000.
[143] E. Meyer, Atomic Force Microscopy: Fundamentals to Most Advanced Applications, vol. 1, Springer-Verlag TELOS, New York, 2007, p. 250.
[144] G. Binnig, C.F. Quate, C. Gerber, Phys. Rev. Lett. 56 (1986) 930.
[145] H.J. Guntherodt, D. Anselmetti, E. Meyer (Eds.), NATO ASI series. Series E, Applied sciences, vol. 286, Kluwer Academic, 1995, p. 644.
[146] T.L. Barr, Modern ESCA: The Principles and Practice of X-Ray Photoelectron Spectroscopy, CRC Press, New York, 1994, p. 384.
[147] D.C. Koningsberger, R. Prins (Eds.), A Series of Monographs on Anal. Chem. and Its Applications, Wiley-Interscience, New York, 1988, p. 688.
[148] O. Glatter, O. Kratky (Eds.), Small Angle X-ray Scattering, Academic Press, New York, 1982, p. 515.
[149] A. Balerna, L. Liotta, A. Longo, A. Martorana, C. Meneghini, S. Mobilio, G. Pipitone, Eur. Phys. J. D 7 (1999) 89.
[150] A. Plech, V. Kotaidis, M. Lorenc, M. Wulff, Chem. Phys. Lett. 401 (2005) 565.
[151] E. Meyer, H.J. Hug, R. Bennewitz, Scanning Probe Microscopy: The Lab on a Chip, Springer, New York, 2003, p. 210.
[152] J.I. Goldstein, D.E. Newbury, P. Echlin, D.C. Joy, J. Romig, A.D.C.E. Lyman, C. Fiori, E. Lifshin, Scanning Electron Microscopy and X-ray Microanalysis, 2nd ed., Plenum Press, New York, 1992, p. 820.
[153] W. Zhou, Z.L. Wang, Scanning Microscopy for Nanotechnology, 1st ed., Springer, New York, 2006, p. 522.
[154] Z.L. Wang (Ed.), Characterization of Nanophase Materials, Wiley–VCH, New York, 2000, p. 406.
[155] Z.L. Wang, Adv. Mater. 10 (1998) 13.
[156] M.A. Petruska, A.V. Malko, P.M. Voyles, V.I. Klimov, Adv. Mater. 15 (2003) 610.
[157] A. Kongkanand, K. Tvrdy, K. Takechi, M. Kuno, P.V. Kamat, J. Am. Chem. Soc. 130 (2008) 4007.
[158] T. Lopez-Luke, A. Wolcott, L.-P. Xu, S. Chen, Z. Wen, J.H. Li, E. De La Rosa, J.Z. Zhang, J. Phys. Chem. C 112 (2008) 1282.
[159] H. Park, W. Choi, M.R. Hoffmann, J. Mater. Chem. 18 (2008) 2379.
[160] R. Vogel, K. Pohl, H. Weller, Chem. Phys. Lett. 174 (1990) 241.
[161] S. Kohtani, A. Kudo, T. Sakata, Chem. Phys. Lett. 206 (1993) 166.
[162] D. Liu, P.V. Kamat, J. Phys. Chem. 97 (1993) 10769.
[163] S. Hotchandani, P.V. Kamat, J. Phys. Chem. 96 (1992) 6834.
[164] C. Nasr, P.V. Kamat, S. Hotchandani, J. Phys. Chem. B 102 (1998) 10047.
[165] G. Kumara, K. Tennakone, I.R.M. Kottegoda, P.K.M. Bandaranayake, A. Konno, M. Okuya, S. Kaneko, K. Murakami, Semicond. Sci. Technol. 18 (2003) 312.
[166] Y. Wang, S. Zhang, X.H. Wu, Q.J. Liu, Mater. Chem. Phys. 98 (2006) 121.
[167] C. Nasr, P.V. Kamat, S. Hotchandani, J. Electroanal. Chem. 420 (1997) 201.
[168] M.R. Vaezi, J. Mater. Process. Technol. 205 (2008) 332.
[169] L.H. Van, M.H. Hong, J. Ding, Solid State Phenomena 111 (2006) 131.
[170] R.E. Schwerzel, K.B. Spahr, J.P. Kurmer, V.E. Wood, J.A. Jenkins, J. Phys. Chem. A 102 (1998) 5622.
[171] J.H. Zhan, X.G. Yang, D.W. Wang, S.D. Li, Y. Xie, Y. Xia, Y.T. Qian, Adv. Mater. 12 (2000) 1348.
[172] Y. Gotoh, Y. Ohkoshi, M. Nagura, Polym. J. 33 (2001) 303.
[173] S.H. Yu, M. Yoshimura, J.M.C. Moreno, T. Fujiwara, T. Fujino, R. Teranishi, Langmuir 17 (2001) 1700.
[174] S.Y. Lu, M.L. Wu, H.L. Chen, J. Appl. Phys. 93 (2003) 5789.
[175] M.Z. Rong, M.Q. Zhang, H.C. Liang, H.M. Zeng, Chem. Phys. 286 (2003) 267.
[176] I.V. Klimenko, E.P. Krinichnaya, T.S. Zhuravleva, S.A. Zav'yalov, E.I. Grigor'ev, I.A. Misurkin, S.V. Titov, B.A. Loginov, Russ. J. Phys. Chem. 80 (2006) 2041.
[177] J.F. Zhu, Y.J. Zhu, M.G. Ma, L.X. Yang, L. Gao, J. Phys. Chem. C 111 (2007) 3920.
[178] Y.B. Zhao, F. Wang, Q. Fu, W.F. Shi, Polymer 48 (2007) 2853.
[179] C. Inui, H. Kura, T. Sato, Y. Tsuge, S. Shiratori, H. Ohkita, A. Tagaya, Y. Koike, J. Mater. Sci. 42 (2007) 8144.
[180] E. Holder, N. Tessler, A.L. Rogach, J. Mater. Chem. 18 (2008) 1064.
[181] K. Susumu, H.T. Uyeda, I.L. Medintz, T. Pons, J.B. Delehanty, H. Mattoussi, J. Am. Chem. Soc. 129 (2007) 13987.
[182] N.C. Greenham, X.G. Peng, A.P. Alivisatos, Phys. Rev. B: Condens. Matter 54 (1996) 17628.
[183] N.C. Greenham, X.G. Peng, A.P. Alivisatos, Synth. Met. 84 (1997) 545.
[184] H. Skaff, K. Sill, T. Emrick, J. Am. Chem. Soc. 126 (2004) 11322.
[185] S.K. Hong, K.H. Yeon, J. Kor. Phys. Soc. 45 (2004) 1568.
[186] D. Selmarten, M. Jones, G. Rumbles, P.R. Yu, J. Nedeljkovic, S. Shaheen, J. Phys. Chem. B 109 (2005) 15927.
[187] S.H. Choi, H.J. Song, I.K. Park, J.H. Yum, S.S. Kim, S.H. Lee, Y.E. Sung, J. Photochem. Photobiol. A: Chem. 179 (2006) 135.
[188] C.H. Chou, H.S. Wang, K.H. Wei, J.Y. Huang, Adv. Funct. Mater. 16 (2006) 909.
[189] R. van Beek, A.P. Zoombelt, L.W. Jenneskens, C.A. van Walree, C.D. Donega, D. Veldman, R.A.J. Janssen, Chem. Eur. J. 12 (2006) 8075.
[190] N.I. Hammer, T. Emrick, M.D. Barnes, Nanoscale Res. Lett. 2 (2007) 282.
[191] P. Suresh, P. Balaraju, S.K. Sharma, M.S. Roy, G.D. Sharma, Solar Energy Mater. Solar Cells 92 (2008) 900.
[192] Y.F. Wang, M.J. Li, H.Y. Jia, W. Song, X.X. Han, J.H. Zhang, B. Yang, W.Q. Xu, B. Zhao, Spectrochim. Acta A: Mol. Biomol. Spec. 64 (2006) 101.
[193] P.V. Kamat, B. Shanghavi, J. Phys. Chem. B 101 (1997) 7675.
[194] T. Mokari, E. Rothenberg, I. Popov, R. Costi, U. Banin, Science 304 (2004) 1787.
[195] O. Kulakovich, N. Strekal, A. Yaroshevich, S. Maskevich, S. Gaponenko, I. Nabiev, U. Woggon, M. Artemyev, Nano Lett. 2 (2002) 1449.
[196] M. Moskovits, Rev. Modern Phys. 57 (1985) 783.
[197] M.T. Cheng, S.D. Liu, H.J. Zhou, Z.H. Hao, Q.Q. Wang, Optics Lett. 32 (2007) 2125.
[198] V. Subramanian, E.E. Wolf, P.V. Kamat, Langmuir 19 (2003) 469.
[199] M. Jakob, H. Levanon, P.V. Kamat, Nano Lett. 3 (2003) 353.
[200] T. Sasaki, N. Koshizaki, J.W. Yoon, S. Yamada, M. Koinuma, M. Noguchi, Y. Matsumoto, Electrochemistry 72 (2004) 443.
[201] A. Meng, W. Cen, Z.J. Li, F. Guo, Z.D. Geng, Z.H. Zhang, Rare Met. Mater. Eng. 38 (2009) 358.
[202] H. Kim, M. Achermann, L.P. Balet, J.A. Hollingsworth, V.I. Klimov, J. Am. Chem. Soc. 127 (2005) 544.
[203] T.A. Kennedy, E.R. Glaser, P.B. Klein, R.N. Bhargava, Phys. Rev. B: Condens. Matter 52 (1995) 14356.
[204] G. Counio, S. Esnouf, T. Gacoin, J.P. Boilot, J. Phys. Chem. 100 (1996) 20021.
[205] T. Igarashi, T. Isobe, M. Senna, Phys. Rev. B: Condens. Matter 56 (1997) 6444.
[206] N. Feltin, L. Levy, D. Ingert, M.P. Pileni, J. Phys. Chem. B 103 (1999) 4.
[207] R.N. Bhargava, D. Gallagher, T. Welker, J. Lumin. 60–61 (1994) 275.
[208] U.W. Pohl, H.E. Gumlich, Phys. Rev. B: Condens. Matter 40 (1989) 1194.
[209] P. Devisschere, K. Neyts, D. Corlatan, J. Vandenbossche, C. Barthou, P. Benalloul, J. Benoit, J. Lumin. 65 (1995) 211.
[210] R.N. Bhargava, J. Lumin. 70 (1996) 85.
[211] J.Q. Yu, H.M. Liu, Y.Y. Wang, W.Y. Jia, J. Lumin. 79 (1998) 191.
[212] S. Shionoya, W.M. Yen (Eds.), Phosphor Handbook, CRC Press, New York, 1999.
[213] T.J. Norman, D. Magana, T. Wilson, C. Burns, J.Z. Zhang, D. Cao, F. Bridges, J. Phys. Chem. B 107 (2003) 6309.
[214] J.Z. Zhang, C.D. Grant, in: G. Cao, C.J. Brinker (Eds.), Annual Review of Nano Research, World Scientific, Singapore, 2008, p. 1.
[215] K. Sooklal, B.S. Cullum, S.M. Angel, C.J. Murphy, J. Phys. Chem. 100 (1996) 4551.
[216] L.D. Sun, C.H. Yan, C.H. Liu, C.S. Liao, D. Li, J.Q. Yu, J. Alloys Compd. 277 (1998) 234.
[217] D.D. Papakonstantinou, J. Huang, P. Lianos, J. Mater. Sci. Lett. 17 (1998) 1571.
[218] A.A. Khosravi, M. Kundu, L. Jatwa, S.K. Deshpande, U.A. Bhagwat, M. Sastry, S.K. Kulkarni, Appl. Phys. Lett. 67 (1995) 2702.
[219] J.M. Huang, Y. Yang, S.H. Xue, B. Yang, S.Y. Liu, J.C. Shen, Appl. Phys. Lett. 70 (1997) 2335.
[220] C.M. Jin, J.Q. Yu, L.D. Sun, K. Dou, S.G. Hou, J.L. Zhao, Y.M. Chen, S.H. Huang, J. Lumin. 66–67 (1995) 315.
[221] R.N. Bhargava, D. Gallagher, X. Hong, A. Nurmikko, Phys. Rev. Lett. 72 (1994) 416.
[222] W.G. Becker, A.J. Bard, J. Phys. Chem. 87 (1983) 4888.
[223] G. Counio, T. Gacoin, J.P. Boilot, J. Phys. Chem. B 102 (1998) 5257.
[224] J.Q. Yu, H.M. Liu, Y.Y. Wang, F.E. Fernandez, W.Y. Jia, J. Lumin. 76–77 (1998) 252.
[225] A.D. Dinsmore, D.S. Hsu, H.F. Gray, S.B. Qadri, Y. Tian, B.R. Ratna, Appl. Phys. Lett. 75 (1999) 802.
[226] W. Chen, R. Sammynaiken, Y.N. Huang, J. Appl. Phys. 88 (2000) 5188.
[227] W. Chen, R. Sammynaiken, Y.N. Huang, J.O. Malm, R. Wallenberg, J.O. Bovin, V. Zwiller, N.A. Kotov, J. Appl. Phys. 89 (2001) 1120.
[228] M. Konishi, T. Isobe, M. Senna, J. Lumin. 93 (2001) 1.
[229] K. Yan, C.K. Duan, Y. Ma, S.D. Xia, J.C. Krupa, Phys. Rev. B: Condens. Matter 58 (1998) 13585.
[230] A.A. Bol, A. Meijerink, Phys. Rev. B: Condens. Matter 58 (1998) R15997.
[231] J.H. Chung, C.S. Ah, D.-J. Jang, J. Phys. Chem. B 105 (2001) 4128.
[232] R. Bowers, N.T. Melamed, Phys. Rev. 99 (1955) 1781.
[233] K. Urabe, S. Shionoya, J. Appl. Phys. Jpn. 24 (1968) 543.
[234] A. Suzuki, S. Shionoya, J. Phys. Soc. Jpn. 31 (1971) 1462.
[235] A. Suzuki, S. Shionoya, J. Appl. Phys. Jpn. 31 (1971) 1719.
[236] C.S. Kang, P. Beverley, P. Phipps, R.H. Bube, Phys. Rev. 156 (1967) 998.
[237] W. Van Gool, in Philips Res. Rept., Suppl.; No. 3; Thesis; Amsterdam, Universiteit, 1961, p. 122.
[238] M. Wang, L. Sun, X. Fu, C. Liao, C. Yan, Solid State Commun. 115 (2000) 493.
[239] W. Sang, Y. Qian, J. Min, D. Li, L. Wang, W. Shi, L. Yinfeng, Solid State Commun. 121 (2002) 475.
[240] A.A. Bol, J. Lumin. 99 (2002) 325.
[241] K. Manzoor, S.R. Vadera, N. Kumar, T.R.N. Kutty, Mater. Chem. Phys. 82 (2003) 718.
[242] W.Q. Peng, G.W. Cong, S.C. Qu, Z.G. Wang, Opt. Mater. 29 (2006) 313.
[243] C. Corrado, Y. Jiang, F. Oba, M. Kozina, F. Bridges, J.Z. Zhang, J. Phys. Chem. A 113 (2009) 3830.
[244] M.A. Green, Third Generation Photovoltaics: Advanced Solar Energy Conversion, Springer, Berlin–New York, 2003, xi.
[245] L.L. Kazmerski, The 29th IEEE PV Specialists Conference, NREL, New Orleans, LA, 2002.
[246] M.S. Tomar, F.J. Garcia, Thin Solid Films 90 (1982) 419.
[247] M. Alonealaluf, J. Appelbaum, N. Croitoru, Thin Solid Films 320 (1998) 159.
[248] K.D. Dobson, I. Visoly-Fisher, G. Hodes, D. Cahen, Solar Energy Mater. Solar Cells 62 (2000) 295.
[249] B. Oregan, M. Gratzel, Nature 353 (1991) 737.
[250] M.K. Nazeeruddin, A. Kay, I. Rodicio, R. Humphrybaker, E. Muller, P. Liska, N. Vlachopoulos, M. Gratzel, J. Am. Chem. Soc. 115 (1993) 6382.
[251] P. Prene, E. Lancelle-Beltran, C. Boscher, P. Belleville, P. Buvat, C. Sanchez, Adv. Mater. 18 (2006) 2579.
[252] P.V. Kamat, J. Phys. Chem. C 112 (2008) 18737.
[253] S. Biswas, M.F. Hossain, T. Takahashi, Thin Solid Films 517 (2008) 1284.
[254] T.J. Savenije, J.M. Warman, A. Goossens, Chem. Phys. Lett. 287 (1998) 148.
[255] D. Godovsky, L.C. Chen, L. Pettersson, O. Inganas, M.R. Andersson, J.C. Hummelen, Adv. Mater. Opt. Electron. 10 (2000) 47.
[256] S. Spiekermann, G. Smestad, J. Kowalik, L.M. Tolbert, M. Gratzel, Synth. Met. 121 (2001) 1603.

[257] C.D. Grant, A.M. Schwartzberg, G.P. Smestad, J. Kowalik, L.M. Tolbert, J.Z. Zhang, J. Electroanal. Chem. 522 (2002) 40.
[258] C.D. Grant, A.M. Schwartzberg, G.P. Smestad, J. Kowalik, L.M. Tolbert, J.Z. Zhang, Synth. Met. 132 (2003) 197.
[259] Y. Tian, T. Tatsuma, J. Am. Chem. Soc. 127 (2005) 7632.
[260] N. Beermann, L. Vayssieres, S.E. Lindquist, A. Hagfeldt, J. Electrochem. Soc. 147 (2000) 2456.
[261] T. Lindgren, H.L. Wang, N. Beermann, L. Vayssieres, A. Hagfeldt, S.E. Lindquist, Solar Energy Mater. Solar Cells 71 (2002) 231.
[262] W.U. Huynh, J.J. Dittmer, A.P. Alivisatos, Science 295 (2002) 2425.
[263] S. Uchida, R. Chiba, M. Tomiha, N. Masaki, M. Shirai, Nanotechnology in Mesostructured Materials, 2003, p. 791.
[264] S. Ngamsinlapasathian, S. Sakulkhaemaruethai, S. Pavasupree, A. Kitiyanan, T. Sreethawong, Y. Suzuki, S. Yoshikawa, J. Photochem. Photobiol. A: Chem. 164 (2004) 145.
[265] M. Law, L.E. Greene, J.C. Johnson, R. Saykally, P.D. Yang, Nat. Mater. 4 (2005) 455.
[266] B.R. Mehta, F.E. Kruis, Solar Energy Mater. Solar Cells 85 (2005) 107.
[267] S. Pavasupree, S. Ngamsinlapasathian, M. Nakajima, Y. Suzuki, S. Yoshikawa, J. Photochem. Photobiol. A: Chem. 184 (2006) 163.
[268] H.M. Jia, H. Xu, Y. Hu, Y.W. Tang, L.Z. Zhang, Electrochem. Commun. 9 (2007) 354.
[269] K.S. Kim, Y.S. Kang, J.H. Lee, Y.J. Shin, N.G. Park, K.S. Ryu, S.H. Chang, Bull. Kor. Chem. Soc. 27 (2006) 295.
[270] K. Pan, Q.L. Zhang, Q. Wang, Z.Y. Liu, D.J. Wang, J.H. Li, Y.B. Bai, Thin Solid Films 515 (2007) 4085.
[271] Y.B. Liu, B.X. Zhou, B.T. Xiong, J. Bai, L.H. Li, Chin. Sci. Bull. 52 (2007) 1585.
[272] Q.H. Yao, J.F. Liu, Q. Peng, X. Wang, Y.D. Li, Chem.: Asian J. 1 (2006) 737.
[273] C. Burda, Y.B. Lou, X.B. Chen, A.C.S. Samia, J. Stout, J.L. Gole, Nano Lett. 3 (2003) 1049.
[274] X.B. Chen, C. Burda, J. Phys. Chem. B 108 (2004) 15446.
[275] K. Kobayakawa, Y. Murakami, Y. Sato, J. Photochem. Photobiol. A: Chem. 170 (2005) 177.
[276] Y. Nakano, T. Morikawa, T. Ohwaki, Y. Taga, Appl. Phys. Lett. 86 (2005) 132104.
[277] S.W. Yang, L. Gao, J. Inorg. Mater. 20 (2005) 785.
[278] A.R. Gandhe, S.P. Naik, J.B. Fernandes, Micropor. Mesopor. Mater. 87 (2005) 103.
[279] K. Yamada, H. Nakamura, S. Matsushima, H. Yamane, T. Haishi, K. Ohira, K. Kumada, C. R. Chimie 9 (2006) 788.
[280] P. Xu, L. Mi, P.N. Wang, J. Cryst. Growth 289 (2006) 433.
[281] X. Yang, A. Wolcott, G. Wang, A. Sobo, R.C. Fitzmorriw, Q. Fang, J.Z. Zhang, Y. Li, Nano Letters 9 (2009) 2331.
[282] S. Licht, J. Phys. Chem. B 107 (2003) 4253.
[283] A. Fujishima, K. Honda, Nature 238 (1972) 37.
[284] B.H. Wang, D.J. Wang, Y. Cui, J. Zhang, X.D. Chai, T.J. Li, Synth. Met. 71 (1995) 2239.
[285] R.S. Mane, B.R. Sankapal, C.D. Lokhande, Mater. Chem. Phys. 60 (1999) 196.
[286] R.S. Mane, C.D. Lokhande, Mater. Chem. Phys. 78 (2002) 385.
[287] I. Bedja, S. Hotchandani, P.V. Kamat, J. Phys. Chem. 97 (1993) 11064.
[288] I. Bedja, S. Hotchandani, R. Carpentier, K. Vinodgopal, P.V. Kamat, Thin Solid Films 247 (1994) 195.
[289] I. Saeki, N. Okushi, H. Konno, R. Furuichi, J. Electrochem. Soc. 143 (1996) 2226.
[290] H.L. Wang, T. Lindgren, J.J. He, A. Hagfeldt, S.E. Lindquist, J. Phys. Chem. B 104 (2000) 5686.
[291] U.O. Krasovec, M. Topic, A. Georg, A. Georg, G. Drazic, J. Sol–Gel Sci. Technol. 36 (2005) 45.
[292] C.V. Ramana, S. Utsunomiya, R.C. Ewing, C.M. Julien, U. Becker, J. Phys. Chem. B 110 (2006) 10430.
[293] F. Cao, G. Oskam, G.J. Meyer, P.C. Searson, J. Phys. Chem. 100 (1996) 17021.
[294] E. Stathatos, P. Lianos, Int. J. Photoenergy 4 (2002) 11.
[295] T. Stergiopoulos, I.M. Arabatzis, G. Katsaros, P. Falaras, Nano Lett. 2 (2002) 1259.
[296] H. Saitoh, K. Takayama, H. Sugata, S. Ohshio, H. Takada, Y. Yamazaki, Y. Yamaguchi, Y. Ono, Jpn. J. Appl. Phys. Part 2: Lett. 41 (2002) L1250.
[297] P.R. Mishra, P.K. Shukla, O.N. Srivastava, Int. J. Hydrogen Energy 32 (2007) 1680.
[298] H.L. Zhao, D.L. Jiang, S.L. Zhang, W. Wen, J. Catal. 250 (2007) 102.
[299] D. Chen, Y.F. Gao, G. Wang, H. Zhang, W. Lu, J.H. Li, J. Phys. Chem. C 111 (2007) 13163.
[300] J. Knappenberger, K.L.D.B. Wong, W. Xu, A.M. Schwartzberg, A. Wolcott, J.Z. Zhang, S.R. Leone, ACS Nano 2 (2008) 2143.
[301] T. Bak, J. Nowotny, M. Rekas, C.C. Sorrell, Int. J. Hydrogen Energy 27 (2002) 991.
[302] S.U.M. Khan, M. Al-Shahry, I.J.W. B****al, Science 297 (2002) 2243.
[303] O. Khaselev, J.A. Turner, Science 280 (1998) 425.
[304] A.L. Linsebigler, G.Q. Lu, J.T. Yates, Chem. Rev. 95 (1995) 735.
[305] A.J. Bard, M.A. Fox, Acc. Chem. Res. 28 (1995) 141.
[306] J.R. Bolton, Solar Energy 57 (1996) 37.
[307] W.Y. Choi, A. Termin, M.R. Hoffmann, J. Phys. Chem. 98 (1994) 13669.
[308] M. Anpo, M. Matsuoka, H. Mishima, H. Yamashita, Res. Chem. Intermed. 23 (1997) 197.
[309] A.K. Ghosh, H.P. Maruska, J. Electrochem. Soc. 124 (1977) 1516.
[310] R. Asahi, T. Morikawa, T. Ohwaki, K. Aoki, Y. Taga, Science 293 (2001) 269.
[311] L. Lin, W. Lin, Y.X. Zhu, B.Y. Zhao, Y.C. Xie, Chem. Lett. 34 (2005) 284.
[312] S. Sakthivel, H. Kisch, Angew. Chem. Int. Ed. 42 (2003) 4908.
[313] T. Ohno, T. Mitsui, M. Matsumura, Chem. Lett. 32 (2003) 364.
[314] W. Zhao, W.H. Ma, C.C. Chen, J.C. Zhao, Z.G. Shuai, J. Am. Chem. Soc. 126 (2004) 4782.
[315] H. Kato, A. Kudo, J. Phys. Chem. B 106 (2002) 5029.
[316] M.I. Litter, J.A. Navio, J. Photochem. Photobiol. A: Chem. 84 (1994) 183.
[317] M. Gratzel, R.F. Howe, J. Phys. Chem. 94 (1990) 2566.
[318] Z.H. Luo, Q.H. Gao, J. Photochem. Photobiol. A: Chem. 63 (1992) 367.
[319] E. Wimmer, H. Krakauer, M. Weinert, A.J. Freeman, Phys. Rev. B 24 (1981) 864.
[320] H.J.F. Jansen, A.J. Freeman, Phys. Rev. B 30 (1984) 561.
[321] P.V. Kamat, J. Phys. Chem. C 111 (2007) 2834.
[322] E.C. Hao, X.M. Qian, B. Yang, D.J. Wang, J.C. Shen, Mol. Cryst. Liquid Cryst. Sci. Technol. A: Mol. Cryst. Liquid Cryst. 337 (1999) 181.
[323] J.H. Fang, J.W. Wu, X.M. Lu, Y.C. Shen, Z.H. Lu, Chem. Phys. Lett. 270 (1997) 145.
[324] L. Spanhel, H. Weller, A. Henglein, J. Am. Chem. Soc. 109 (1987) 6632.
[325] P.A. Sant, P.V. Kamat, Phys. Chem. Chem. Phys. 4 (2002) 198.
[326] A. Ghicov, J.M. Macak, H. Tsuchiya, J. Kunze, V. Haeublein, L. Frey, P. Schmuki, Nano Lett. 6 (2006) 1080.
[327] S.K. Mohapatra, M. Misra, J. Phys. Chem. C 111 (2007) 11506.
[328] J. Moser, S. Punchihewa, P.P. Infelta, M. Gratzel, Langmuir 7 (1991) 3012.
[329] H. Ohtake, S. Ono, Z.L. Liu, N. Sarukura, M. Ohta, K. Watanabe, Y. Matsumoto, Jpn. J. Appl. Phys. Part 2: Lett. 38 (1999) L1186.
[330] K. Rajeshwar, J. Appl. Electrochem. 37 (2007) 765.
[331] B.D. Alexander, P.J. Kulesza, L. Rutkowska, R. Solarska, J. Augustynski, J. Mater. Chem. 18 (2008) 2298.
[332] G. Yu, G. Srdanov, J. Wang, H. Wang, Y. Cao, A.J. Heeger, Synth. Met. 111 (2000) 133.
[333] S. Licht, J. Phys. Chem. B 105 (2001) 6281.
[334] R. Ganesan, A. Gedanken, Nanotechnology 19 (2008) 435709.
[335] S. Surampudi, S.R. Narayanan, E. Vamos, H. Frank, G. Halpert, A. Laconti, J. Kosek, G.K.S. Prakash, G.A. Olah, J. Power Sources 47 (1994) 377.
[336] Q.P. Wang, M. Eikerling, D.T. Song, Z.S. Liu, J. Electroanal. Chem. 573 (2004) 61.
[337] L. Carrette, K.A. Friedrich, U. Stimming, Chem. Phys. Chem. 1 (2000) 162.
[338] S. Wasmus, A. Kuver, J. Electroanal. Chem. 461 (1999) 14.
[339] X.M. Qian, X.T. Zhang, X. Ai, Y.Z. Hao, F.Q. Liu, S.M. Cai, Y.B. Bai, T.J. Li, X.Y. Tang, J.N. Yao, Mol. Cryst. Liquid Cryst. Sci. Technol. A: Mol. Cryst. Liquid Cryst. 337 (1999) 437.
[340] S. Mukerjee, S. Srinivasan, J. Electroanal. Chem. 357 (1993) 201.
[341] J.T. Hwang, J.S. Chung, Electrochim. Acta 38 (1993) 2715.
[342] S. Mukerjee, S. Srinivasan, M.P. Soriaga, J. McBreen, J. Electrochem. Soc. 142 (1995) 1409.
[343] F.A. Uribe, J.A. Valerio, F.H. Garzon, T.A. Zawodzinski, Electrochem. Solid State Lett. 7 (2004) A376.
[344] P.A. Adcock, S.V. Pacheco, K.M. Norman, F.A. Uribe, J. Electrochem. Soc. 152 (2005) A459.
[345] L. Xiong, A. Manthiram, Electrochim. Acta 49 (2004) 4163.
[346] J. Shim, C.R. Lee, H.K. Lee, J.S. Lee, E.J. Cairns, J. Power Sources 102 (2001) 172.
[347] K. Drew, G. Girishkumar, K. Vinodgopal, P.V. Kamat, J. Phys. Chem. B 109 (2005) 11851.
[348] F. O'Sullivan, I. Celanovic, N. Jovanovic, J. Kassakian, S. Akiyama, K. Wada, J. Appl. Phys. 97 (2005) 033529.
[349] D. Marti, C. Algora, V. Corregidor, A. Datas, J. Solar Energy Eng. Trans. ASME 129 (2007) 283.
[350] B. Bitnar, Semiconduct. Sci. Technol. 18 (2003) S221.
[351] P. Piquini, A. Zunger, Phys. Rev. B 78 (2008) 161302.
[352] M.W. Dashiell, J.E. Beausang, H. Ehsani, G.J. Nichols, D.M. Depoy, L.R. Danielson, P. Talamo, K.D. Rahner, E.J. Brown, S.R. Burger, P.M. Fourspring, W.E. Topper, P.F. Baldasaro, C.A. Wang, R.K. Huang, M.K. Connors, G.W. Turner, Z.A. Shellenbarger, G. Taylor, J.Z. Li, R. Martinelli, D. Donetski, S. Anikeev, G.L. Belenky, S. Luryi, IEEE Trans. Electron. Devices 53 (2006) 2879.
[353] C. Rohr, P. Abbott, I. Ballard, J.P. Connolly, K.W.J. Barnham, M. Mazzer, C. Button, L. Nasi, G. Hill, J.S. Roberts, G. Clarke, R. Ginige, J. Appl. Phys. 100 (2006).
[354] P. Pichat, M.-N. Mozzanega, H. Courbon, J. Chem. Soc., Faraday Trans. I 83 (1987) 697.
[355] P. Pichat, H. Khalaf, D. Tabet, M. Houari, M. Saidi, Environ. Chem. Lett. 2 (2005) 191.
[356] M.A. Fox, M.T. Dulay, Chem. Rev. 93 (1993) 341.
[357] D. Li, H. Haneda, S. Hishita, N. Ohashi, Mater. Sci. Eng. B: Solid State Mater. Adv. Technol. 117 (2005) 67.
[358] W.Y. Choi, A. Termin, M.R. Hoffmann, Angew. Chem. Int. Ed. 33 (1994) 1091 (in English).
[359] M.R. Hoffmann, S.T. Martin, W.Y. Choi, D.W. Bahnemann, Chem. Rev. 95 (1995) 69.
[360] C.H. Kwon, H.M. Shin, J.H. Kim, W.S. Choi, K.H. Yoon, Mater. Chem. Phys. 86 (2004) 78.
[361] Y. Nemoto, T. Hirai, Bull. Chem. Soc. Jpn. 77 (2004) 1033.
[362] Y. Jiang, P. Zhang, Z.W. Liu, F. Xu, Mater. Chem. Phys. 99 (2006) 498.
[363] Z.X. Wang, S.W. Ding, M.H. Zhang, Chin. J. Inorg. Chem. 21 (2005) 437.
[364] Y.C. Lee, S. Cheng, J. Chin. Chem. Soc. 53 (2006) 1355.
[365] M.A. Fox, Acc. Chem. Res. 16 (1983) 314.
[366] Y. Shiraishi, T. Hirai, J. Photochem. Photobiol. C: Photochem. Rev. 9 (2008) 157.
[367] R. Terzian, N. Serpone, C. Minero, E. Pelizzetti, H. Hidaka, J. Photochem. Photobiol. A: Chem. 55 (1990) 243.
[368] O. Carp, C.L. Huisman, A. Reller, Prog. Solid State Chem. 32 (2004) 33.
[369] O. Legrini, E. Oliveros, A.M. Braun, Chem. Rev. 93 (1993) 671.
[370] E. Pelizzetti, C. Minero, Electrochim. Acta 38 (1993) 47.
[371] Y. Shiraishi, Y. Teshima, T. Hirai, Chem. Commun. (2005) 4569.
[372] Y. Shiraishi, Y. Teshima, T. Hirai, J. Phys. Chem. B 110 (2006) 6257.

[373] Y. Wang, L. Li, K. Yang, L.A. Samuelson, J. Kumar, J. Am. Chem. Soc. 129 (2007) 7238.
[374] N.W. Cant, J.R. Cole, J. Catal. 134 (1992) 317.
[375] M.R. Prairie, L.R. Evans, B.M. Stange, S.L. Martinez, Environ. Sci. Technol. 27 (1993) 1776.
[376] K. Sayama, H. Arakawa, J. Phys. Chem. 97 (1993) 531.
[377] M. Bideau, B. Claudel, L. Faure, H. Kazouan, J. Photochem. Photobiol. A: Chem. 61 (1991) 269.
[378] G.R. Bamwenda, S. Tsubota, T. Kobayashi, M. Haruta, J. Photochem. Photobiol. A: Chem. 77 (1994) 59.
[379] A. Zafra, J. Garcia, A. Milis, X. Domenech, J. Mol. Catal. 70 (1991) 343.
[380] A.P. Hong, D.W. Bahnemann, M.R. Hoffmann, J. Phys. Chem. 91 (1987) 6245.
[381] H. Yamashita, Y. Fujii, Y. Ichihashi, S.G. Zhang, K. Ikeue, D.R. Park, K. Koyano, T. Tatsumi, M. Anpo, Catal. Today 45 (1998) 221.
[382] K. Ikeue, H. Yamashita, M. Anpo, T. Takewaki, J. Phys. Chem. B 105 (2001) 8350.
[383] H.W. Slamet, E. Nasution, S. Purnama, J. Kosela, Gunlazuardi, Catal. Commun. 6 (2005) 313.
[384] J.L. Ferry, W.H. Glaze, J. Phys. Chem. B 102 (1998) 2239.
[385] V. Brezova, A. Blazkova, I. Surina, B. Havlinova, J. Photochem. Photobiol. A: Chem. 107 (1997) 233.
[386] S.I. Nishimoto, B. Ohtani, T. Yoshikawa, T. Kagiya, J. Am. Chem. Soc. 105 (1983) 7180.
[387] B. Ohtani, S. Tsuru, S. Nishimoto, T. Kagiya, K. Izawa, J. Org. Chem. 55 (1990) 5551.
[388] K.V.S. Rao, B. Srinivas, A.R. Prasad, M. Subrahmanyam, Chem. Commun. (2000) 1533.
[389] A. Maldotti, R. Amadelli, L. Samiolo, A. Molinari, A. Penoni, S. Tollari, S. Cenini, Chem. Commun. (2005) 1749.
[390] S.S. Patil, V.M. Shinde, Environ. Sci. Technol. 22 (1988) 1160.
[391] A.T. Moore, A. Vira, S. Fogel, Environ. Sci. Technol. 23 (1989) 403.
[392] S.H. Lin, C.M. Lin, Water Res. 27 (1993) 1743.
[393] V. Meshko, L. Markovska, M. Mincheva, A.E. Rodrigues, Water Res. 35 (2001) 3357.
[394] M. Arami, N.Y. Limaee, N.M. Mahmoodi, N.S. Tabrizi, J. Colloid Interf. Sci. 288 (2005) 371.
[395] C. Galindo, P. Jacques, A. Kalt, Chemosphere 45 (2001) 997.
[396] W.S. Kuo, P.H. Ho, Chemosphere 45 (2001) 77.
[397] U. Pagga, K. Taeger, Water Res. 28 (1994) 1051.
[398] I.K. Konstantinou, T.A. Albanis, Appl. Catal. B: Environ. 49 (2004) 1.
[399] V. Augugliaro, M. Litter, L. Palmisano, J. Soria, J. Photochem. Photobiol. C: Photochem. Rev. 7 (2006) 127.
[400] D.F. Ollis, H. Al-Ekabi, Proceedings of the 1st International Conference on TiO* Photocatalytic Purification and Treatment of Water and Air, London, Ontario, Canada, November 8–13, 1992;
D.F. Ollis, H. Al-Ekabi, Trace Metals in the Environment, vol. 3, Elsevier, Amsterdam–New York, 1993, xiii.
[401] A. Mills, R.H. Davies, D. Worsley, Chem. Soc. Rev. 22 (1993) 417.
[402] N. Serpone, R.F. Khairutdinov, in: P.V. Kamat, D. Meisel (Eds.), Semiconductor Nanoclusters—Physical, Chemical, and Catalytic Aspects, Elsevier, New York, 1997, p. 417.
[403] K. Okamoto, Y. Yamamoto, H. Tanaka, M. Tanaka, A. Itaya, Bull. Chem. Soc. Jpn. 58 (1985) 2015.
[404] M. Andersson, L. Osterlund, S. Ljungstrom, A. Palmqvist, J. Phys. Chem. B 106 (2002) 10674.
[405] D. Chatterjee, S. Dasgupta, J. Photochem. Photobiol. C: Photochem. Rev. 6 (2005) 186.
[406] I.K. Konstantinou, V.A. Sakkas, T.A. Albanis, Water Res. 36 (2002) 2733.
[407] D.S. Bhatkhande, V.G. Pangarkar, A. Beenackers, J. Chem. Technol. Biotechnol. 77 (2002) 102.
[408] K. Wilke, H.D. Breuer, J. Photochem. Photobiol. A: Chem. 121 (1999) 49.
[409] R. Ullah, J. Dutta, J. Hazard. Mater. 156 (2008) 194.
[410] O.K. Dalrymple, D.H. Yeh, M.A. Trotz, J. Chem. Technol. Biotechnol. 82 (2007) 121.
[411] S.T. Martin, C.L. Morrison, M.R. Hoffmann, J. Phys. Chem. 98 (1994) 13695.
[412] N. Serpone, D. Lawless, J. Disdier, J.M. Herrmann, Langmuir 10 (1994) 643.
[413] Y.A. Cao, W.S. Yang, W.F. Zhang, G.Z. Liu, P.L. Yue, New J. Chem. 28 (2004) 218.
[414] J. Soria, J.C. Conesa, V. Augugliaro, L. Palmisano, M. Schiavello, A. Sclafani, J. Phys. Chem. 95 (1991) 274.
[415] K. Fujihara, S. Izumi, T. Ohno, M. Matsumura, J. Photochem. Photobiol. A: Chem. 132 (2000) 99.
[416] M. Anpo, M. Takeuchi, J. Catal. 216 (2003) 505.
[417] H. Yamashita, M. Harada, J. Misaka, M. Takeuchi, K. Ikeue, M. Anpo, J. Photochem. Photobiol. A: Chem. 148 (2002) 257.
[418] R.J. Tayade, R.G. Kulkarni, R.V. Jasra, Ind. Eng. Chem. Res. 45 (2006) 5231.
[419] F.B. Li, X.Z. Li, K.H. Ng, Ind. Eng. Chem. Res. 45 (2006) 1.
[420] C.K. Xu, S.U.M. Khan, Electrochem. Solid State Lett. 10 (2007) B56.
[421] O. Diwald, T.L. Thompson, T. Zubkov, E.G. Goralski, S.D. Walck, J.T. Yates, J. Phys. Chem. B 108 (2004) 6004.
[422] C. Di Valentin, G. Pacchioni, A. Selloni, Chem. Mater. 17 (2005) 6656.
[423] Y. Liu, X. Chen, J. Li, C. Burda, Chemosphere 61 (2005) 11.
[424] H. Irie, Y. Watanabe, K. Hashimoto, J. Phys. Chem. B 107 (2003) 5483.
[425] T. Umebayashi, T. Yamaki, H. Itoh, K. Asai, Appl. Phys. Lett. 81 (2002) 454.
[426] R. Khan, S.W. Kim, T.J. Kim, C.M. Nam, Mater. Chem. Phys. 112 (2008) 167.
[427] J.H. Pan, X.W. Zhang, A.J. Du, D.D. Sun, J.O. Leckie, J. Am. Chem. Soc. 130 (2008) 11256.
[428] T. Ihara, M. Miyoshi, M. Ando, S. Sugihara, Y. Iriyama, J. Mater. Sci. 36 (2001) 4201.
[429] D. Noguchi, Y. Kawamata, T. Nagatomo, J. Electrochem. Soc. 152 (2005) D124.
[430] H.Y. Liu, L. Gao, J. Am. Ceram. Soc. 87 (2004) 1582.
[431] D. Li, H. Haneda, S. Hishita, N. Ohashi, Chem. Mater. 17 (2005) 2596.
[432] D.G. Huang, S.J. Liao, J.M. Liu, Z. Dang, L. Petrik, J. Photochem. Photobiol. A: Chem. 184 (2006) 282.
[433] H.Q. Sun, Y. Bai, Y.P. Cheng, W.Q. Jin, N.P. Xu, Ind. Eng. Chem. Res. 45 (2006) 4971.
[434] H. Ozaki, S. Iwamoto, M. Inoue, Catal. Lett. 113 (2007) 95.
[435] M. Miyauchi, M. Takashio, H. Tobimatsu, Langmuir 20 (2004) 232.
[436] P. Yang, C. Lu, N.P. Hua, Y.K. Du, Mater. Lett. 57 (2002) 794.
[437] J. Chen, D.F. Ollis, W.H. Rulkens, H. Bruning, Water Res. 33 (1999) 661.
[438] Y.T. Kwon, K.Y. Song, W.I. Lee, G.J. Choi, Y.R. Do, J. Catal. 191 (2000) 192.
[439] H. Tada, A. Hattori, Y. Tokihisa, K. Imai, N. Tohge, S. Ito, J. Phys. Chem. B 104 (2000) 4585.
[440] K. Vinodgopal, P.V. Kamat, Environ. Sci. Technol. 29 (1995) 841.
[441] K. Vinodgopal, I. Bedja, P.V. Kamat, Chem. Mater. 8 (1996) 2180.
[442] G. Marci, V. Augugliaro, M.J. Lopez-Munoz, C. Martin, L. Palmisano, V. Rives, M. Schiavello, R.J.D. Tilley, A.M. Venezia, J. Phys. Chem. B 105 (2001) 1026.
[443] E.L.P. Larsen, L.L. Randeberg, O.A. Gederaas, C.J. Arum, A. Hjelde, C.M. Zhao, D. Chen, H.E. Krokan, L.O. Svaasand, J. Biomed. Optics 13 (2008) 044031.
[444] N. Serpone, P. Maruthamuthu, P. Pichat, E. Pelizzetti, H. Hidaka, J. Photochem. Photobiol. A: Chem. 85 (1995) 247.
[445] R. Memming, Prog. Surf. Sci. 17 (1984) 7.
[446] V.H. Houlding, M. Gratzel, J. Am. Chem. Soc. 105 (1983) 5695.
[447] M.A. Ryan, E.C. Fitzgerald, M.T. Spitler, J. Phys. Chem. 93 (1989) 6150.
[448] P.V. Kamat, Chem. Rev. 93 (1993) 267.
[449] V. Hequet, P. Le Cloirec, C. Gonzalez, B. Meunier, Chemosphere 41 (2000) 379.
[450] Y.M. Cho, W.Y. Choi, C.H. Lee, T. Hyeon, H.I. Lee, Environ. Sci. Technol. 35 (2001) 966.
[451] K. Kalyanasundaram, M. Gratzel, Coord. Chem. Rev. 177 (1998) 347.
[452] M. Bauer, C. Lei, K. Read, R. Tobey, J. Gland, M.M. Murnane, H.C. Kapteyn, Phys. Rev. Lett. 8702 (2001) 5501.
[453] F. Kiriakidou, D.I. Kondarides, X.E. Verykios, Catal. Today 54 (1999) 119.
[454] L. Lucarelli, V. Nadtochenko, J. Kiwi, Langmuir 16 (2000) 1102.
[455] C. Dominguez, J. Garcia, M.A. Pedraz, A. Torres, M.A. Galan, Catal. Today 40 (1998) 85.
[456] R.M. Alberici, W.E. Jardim, Appl. Catal. B: Environ. 14 (1997) 55.
[457] H. Yu, K. Zhang, C. Rossi, Indoor Built Environ. 16 (2007) 529.
[458] J. Peral, D.F. Ollis, J. Catal. 136 (1992) 554.
[459] T.N. Obee, R.T. Brown, Environ. Sci. Technol. 29 (1995) 1223.
[460] N.J. Lawryk, C.P. Weisel, Environ. Sci. Technol. 30 (1996) 810.
[461] M. Miyauchi, A. Ikezawa, H. Tobimatsu, H. Irie, K. Hashimoto, Phys. Chem. Chem. Phys. 6 (2004) 865.
[462] T. Ihara, M. Miyoshi, Y. Iriyama, O. Matsumoto, S. Sugihara, Appl. Catal. B: Environ. 42 (2003) 403.
[463] C. Belver, R. Bellod, S.J. Stewart, F.G. Requejo, M. Fernandez-Garcia, Appl. Catal. B: Environ. 65 (2006) 309.
[464] M. Anpo, M. Takeuchi, K. Ikeue, S. Dohshi, Curr. Opin. Solid State Mater. Sci. 6 (2002) 381.
[465] K. Hashimoto, K. Wasada, M. Osaki, E. Shono, K. Adachi, N. Toukai, H. Kominami, Y. Kera, Appl. Catal. B: Environ. 30 (2001) 429.
[466] A. Fuerte, M.D. Hernandez-Alonso, A.J. Maira, A. Martinez-Arias, M. Fernandez-Garcia, J.C. Conesa, J. Soria, G. Munuera, J. Catal. 212 (2002) 1.
[467] F.B. Li, X.Z. Li, C.H. Ao, S.C. Lee, M.F. Hou, Chemosphere 59 (2005) 787.
[468] Y.C. Lee, Y.P. Hong, H.Y. Lee, H. Kim, Y.J. Jung, K.H. Ko, H.S. Jung, K.S. Hong, J. Colloid Interf. Sci. 267 (2003) 127.
[469] C. Euvananont, C. Junin, K. Inpor, P. Limthongkul, C. Thanachayanont, Ceram. Int. 34 (2008) 1067.
[470] R. Wang, K. Hashimoto, A. Fujishima, M. Chikuni, E. Kojima, A. Kitamura, M. Shimohigoshi, T. Watanabe, Adv. Mater. 10 (1998) 135.
[471] R. Wang, K. Hashimoto, A. Fujishima, M. Chikuni, E. Kojima, A. Kitamura, M. Shimohigoshi, T. Watanabe, Nature 388 (1997) 431.
[472] J. Premkumar, Chem. Mater. 17 (2005) 944.
[473] X.T. Zhang, M. Jin, Z.Y. Liu, S. Nishimoto, H. Saito, T. Murakami, A. Fujishima, Langmuir 22 (2006) 9477.
[474] C.H. Ao, S.C. Lee, Chem. Eng. Sci. 60 (2005) 103.
[475] N. Sakai, R. Wang, A. Fujishima, T. Watanabe, K. Hashimoto, Langmuir 14 (1998) 5918.
[476] H. Irie, K. Sunada, K. Hashimoto, Electrochemistry 72 (2004) 807.
[477] K. Sunada, T. Watanabe, K. Hashimoto, Environ. Sci. Technol. 37 (2003) 4785.
[478] K. Sunada, T. Watanabe, K. Hashimoto, J. Photochem. Photobiol. A: Chem. 156 (2003) 227.
[479] M. Miyauchi, A. Nakajima, K. Hashimoto, T. Watanabe, Adv. Mater. 12 (2000) 1923.
[480] D. Lee, M.F. Rubner, R.E. Cohen, Nano Lett. 6 (2006) 2305.
[481] T. Matsunaga, R. Tomoda, T. Nakajima, H. Wake, FEMS Microbiol. Lett. 29 (1985) 211.
[482] C. Sichel, J. Tello, M. de Cara, P. Fernandez-Ibanez, Catal. Today 129 (2007) 152.
[483] T.A. Egerton, S.A.M. Kosa, P.A. Christensen, Phys. Chem. Chem. Phys. 8 (2006) 398.
[484] A.K. Benabbou, Z. Derriche, C. Felix, P. Lejeune, C. Guillard, Appl. Catal. B: Environ. 76 (2007) 257.
[485] A. Kubacka, M. Ferrer, A. Martinez-Arias, M. Fernandez-Garcia, Appl. Catal. B: Environ. 84 (2008) 87.

[486] D.G. Shchukin, A.I. Kulak, D.V. Sviridov, Photochem. Photobiol. Sci. 1 (2002) 742.
[487] D.G. Shchukin, E.A. Ustinovich, A.I. Kulak, D.V. Sviridov, Photochem. Photobiol. Sci. 3 (2004) 157.
[488] J.X. He, P.J. Yang, H. Sato, Y. Umemura, A. Yamagishi, J. Electroanal. Chem. 566 (2004) 227.
[489] S. Sen, S. Mahanty, S. Roy, O. Heintz, S. Bourgeois, D. Chaumont, Thin Solid Films 474 (2005) 245.
[490] D. Shchukin, E. Ustinovich, D. Sviridov, P. Pichat, Photochem. Photobiol. Sci. 3 (2004) 142.
[491] S.Y. Liau, D.C. Read, W.J. Pugh, J.R. Furr, A.D. Russell, Lett. Appl. Microbiol. 25 (1997) 279.
[492] P.V. Kamat, J. Phys. Chem. B 106 (2002) 7729.
[493] H. Tada, T. Ishida, A. Takao, S. Ito, Langmuir 20 (2004) 7898.
[494] E.V. Skorb, L.I. Antonouskaya, N.A. Belyasova, D.G. Shchukin, H. Mohwald, D.V. Sviridov, Appl. Catal. B: Environ. 84 (2008) 94.
[495] Z.J. Li, F. Guo, A. Meng, R.X. Li, K.M. Liang, Rare Met. Mater. Eng. 36 (2007) 293.
[496] Q. Li, Y.W. Li, P.G. Wu, R.C. Xie, J.K. Shang, Adv. Mater. 20 (2008) 3717.
[497] P.G. Wu, R.C. Xie, J.K. Shang, J. Am. Ceram. Soc. 91 (2008) 2957.
[498] X.C. Shen, Z.L. Zhang, B. Zhou, J. Peng, M. Xie, M. Zhang, D.W. Pang, Environ. Sci. Technol. 42 (2008) 5049.
[499] M.L. Cerrada, C. Serrano, M. Sanchez-Chaves, M. Fernandez-Garcia, F. Fernandez-Martin, A. de Andres, R.J.J. Rioboo, A. Kubacka, M. Ferrer, Adv. Funct. Mater. 18 (2008) 1949.
[500] H.T. Yu, X. Quan, Y.N. Zhang, N. Ma, S. Chen, H.M. Zhao, Langmuir 24 (2008) 7599.
[501] R. Mirin, A. Gossard, J. Bowers, Electron. Lett. 32 (1996) 1732.
[502] S. Fafard, K. Hinzer, A.J. Springthorpe, Y. Feng, J. McCaffrey, S. Charbonneau, E.M. Griswold, Mater. Sci. Eng. B: Solid State Mater. Adv. Technol. 51 (1998) 114.
[503] K. Hinzer, C.N. Allen, J. Lapointe, D. Picard, Z.R. Wasilewski, S. Fafard, A.J.S. Thorpe, J. Vac. Sci. Technol. A: Vac. Surf. Films 18 (2000) 578.
[504] K. Hinzer, J. Lapointe, Y. Feng, A. Delage, S. Fafard, A.J. SpringThorpe, E.M. Griswold, J. Appl. Phys. 87 (2000) 1496.
[505] S. Tanaka, H. Hirayama, Y. Aoyagi, Y. Narukawa, Y. Kawakami, S. Fujita, Appl. Phys. Lett. 71 (1997) 1299.
[506] M.K. Zundel, K. Eberl, N.Y. Jin-Phillipp, F. Phillipp, T. Riedl, E. Fehrenbacher, A. Hangleiter, J. Cryst. Growth 202 (1999) 1121.
[507] V.I. Klimov, A.A. Mikhailovsky, S. Xu, A. Malko, J.A. Hollingsworth, C.A. Leatherdale, H.J. Eisler, M.G. Bawendi, Science 290 (2000) 314.
[508] F. Hide, B.J. Schwartz, M.A. Diazgarcia, A.J. Heeger, Chem. Phys. Lett. 256 (1996) 424.
[509] S.A. Carter, J.C. Scott, P.J. Brock, Appl. Phys. Lett. 71 (1997) 1145.
[510] Y. Wang, N. Herron, J. Lumin. 70 (1996) 48.
[511] S. Chaudhary, M. Ozkan, W.C.W. Chan, Appl. Phys. Lett. 84 (2004) 2925.
[512] V.L. Colvin, M.C. Schlamp, A.P. Alivisatos, Nature 370 (1994) 354.
[513] M.C. Schlamp, X.G. Peng, A.P. Alivisatos, J. Appl. Phys. 82 (1997) 5837.
[514] S. Nakamura, K. Kitamura, H. Umeya, A. Jia, M. Kobayashi, A. Yoshikawa, M. Shimotomai, K. Takahashi, Electron. Lett. 34 (1998) 2435.
[515] V.V. Khorenko, S. Malzer, C. Bock, K.H. Schmidt, G.H. Dohler, Phys. Status Solidi B: Basic Res. 224 (2001) 129.
[516] J.L. Zhao, J.Y. Zhang, C.Y. Jiang, J. Bohnenberger, T. Basche, A. Mews, J. Appl. Phys. 96 (2004) 3206.
[517] C.A. Leatherdale, C.R. Kagan, N.Y. Morgan, S.A. Empedocles, M.A. Kastner, M.G. Bawendi, Phys. Rev. B 62 (2000) 2669.
[518] H. Mattoussi, A.W. Cumming, C.B. Murray, M.G. Bawendi, R. Ober, Phys. Rev. B: Condens. Matter 58 (1998) 7850.
[519] L. Brus, J. Phys. Chem. 98 (1994) 3575.
[520] M.H. Huang, S. Mao, H. Feick, H.Q. Yan, Y.Y. Wu, H. Kind, E. Weber, R. Russo, P.D. Yang, Science 292 (2001) 1897.
[521] Z.L. Wang, M.B. Mohamed, S. Link, M.A. El-Sayed, Surf. Sci. 440 (1999) L809.
[522] W.U. Huynh, X.G. Peng, A.P. Alivisatos, Adv. Mater. 11 (1999) 923.
[523] Z. Adam, X. Peng, J. Am. Chem. Soc. 123 (2001) 183.
[524] Z.W. Pan, Z.R. Dai, Z.L. Wang, Science 291 (2001) 1947.
[525] Y.A. Ono, Annu. Rev. Mater. Sci. 27 (1997) 283.
[526] S. Tanaka, H. Kobayashi, H. Sasakura, in: S. Shionoya, W.M. Yen (Eds.), Phosphor Handbook, CRC Press, New York, 1999, p. 601.
[527] K. Manzoor, S.R. Vadera, N. Kumar, T.R.N. Kutty, Appl. Phys. Lett. 84 (2004) 284.
[528] M. Warkentin, F. Bridges, S.A. Carter, M. Anderson, Phys. Rev. B 75 (2007) 075301.
[529] K. Manzoor, V. Aditya, S.R. Vadera, N. Kumar, T.R.N. Kutty, Solid State Commun. 135 (2005) 16.
[530] H. Durr, H. Bous-Laurent, Photochromism: Molecules and Systems, Elsevier Science, Netherland, 2003, p. 1044.
[531] C. Bechinger, S. Ferrer, A. Zaban, J. Sprague, B.A. Gregg, Nature 383 (1996) 608.
[532] F. Ribot, A. Lafuma, C. Eychenne-Baron, C. Sanchez, Adv. Mater. 14 (2002) 1496.
[533] M.Q. Zhu, L.Y. Zhu, J.J. Han, W.W. Wu, J.K. Hurst, A.D.Q. Li, J. Am. Chem. Soc. 128 (2006) 4303.
[534] I.K. Akopyan, V.V. Golubkov, O.A. Dyatlova, B.V. Novikov, A.N. Tsagan-Mandzhiev, Phys. Solid State 50 (2008) 1352.
[535] B. Ohtani, S. Adzuma, S. Nishimoto, T. Kagiya, J. Polym. Sci. Part C: Polym. Lett. 25 (1987) 383.
[536] T. He, Y.H. Yin, Y. Ma, P. Jiang, Y.A. Cao, J.N. Yao, Chem. J. Chin. Univ. 22 (2001) 824 (in Chinese).
[537] T. Tatsuma, K. Suzuki, Electrochem. Commun. 9 (2007) 574.
[538] S.K. Deb, Sol. Energy Mater. Sol. Cells 25 (1992) 327.
[539] B.A. Gregg, Endeavour 21 (1997) 52.
[540] L.J. Ma, Y.X. Li, X.F. Yu, N.F. Zhu, Q.B. Yang, C.H. Noh, J. Solid State Electrochem. 12 (2008) 1503.
[541] A. Hauch, A. Georg, U.O. Krasovec, B. Orel, J. Electrochem. Soc. 149 (2002) H159.
[542] D. Dong, D. Zheng, F.Q. Wang, X.Q. Yang, N. Wang, Y.G. Li, L.H. Guo, J. Cheng, Anal. Chem. 76 (2004) 499.
[543] P. Huh, S.C. Kim, Y. Kim, Y. Wang, J. Singh, J. Kumar, L.A. Samuelson, B.S. Kim, N.J. Jo, J.O. Lee, Biomacromolecules 8 (2007) 3602.
[544] A.M. Schwartzberg, T.Y. Oshiro, J.Z. Zhang, T. Huser, C.E. Talley, Anal. Chem. 78 (2006) 4732.
[545] M. Commandre, J.Y. Natoli, L. Gallais, Eur. Phys. J. Special Topics 153 (2008) 59.
[546] J.L. Bridot, D. Dayde, C. Riviere, C. Mandon, C. Billotey, S. Lerondel, R. Sabattier, G. Cartron, A. Le Pape, G. Blondiaux, M. Janier, P. Perriat, S. Roux, O. Tillement, J. Mater. Chem. 19 (2009) 2328.
[547] P. Alivisatos, Pure Appl. Chem. 72 (2000) 3.
[548] H. Mattoussi, J.M. Mauro, E.R. Goldman, G.P. Anderson, V.C. Sundar, F.V. Mikulec, M.G. Bawendi, J. Am. Chem. Soc. 122 (2000) 12142.
[549] J.K. Jaiswal, H. Mattoussi, J.M. Mauro, S.M. Simon, Nat. Biotechnol. 21 (2003) 47.
[550] W. Jiang, A. Singhal, J.N. Zheng, C. Wang, W.C.W. Chan, Chem. Mater. 18 (2006) 4845.
[551] J.R. Lakowicz, Principles of Fluorescence Spectroscopy, Kluwer, New York, 1999, p. 371.
[552] D.M. Willard, L.L. Carillo, J. Jung, A. Van Orden, Nano Lett. 1 (2001) 469.
[553] I.L. Medintz, A.R. Clapp, H. Mattoussi, E.R. Goldman, B. Fisher, J.M. Mauro, Nat. Mater. 2 (2003) 630.
[554] D.J. Zhou, J.D. Piper, C. Abell, D. Klenerman, D.J. Kang, L.M. Ying, Chem. Commun. (2005) 4807.
[555] J.M. Zhang, Z. Dai, N. Guo, S.C. Xu, Q.X. Dong, B. Sun, Chem. J. Chin. Univ. 28 (2007) 254 (in Chinese).
[556] C.R. Kagan, C.B. Murray, M. Nirmal, M.G. Bawendi, Phys. Rev. Lett. 76 (1996) 1517.
[557] C.R. Kagan, C.B. Murray, M.G. Bawendi, Phys. Rev. B: Condens. Matter 54 (1996) 8633.
[558] X.Y. Huang, L. Li, H.F. Qian, C.Q. Dong, J.C. Ren, Angew. Chem. Int. Ed. 45 (2006) 5140.
[559] S.P. Wang, N. Mamedova, N.A. Kotov, W. Chen, J. Studer, Nano Lett. 2 (2002) 817.
[560] R. Robelek, L.F. Niu, E.L. Schmid, W. Knoll, Anal. Chem. 76 (2004) 6160.
[561] L.A. Bentolila, S. Weiss, Cell Biochem. Biophys. 45 (2006) 59.
[562] L. Ma, S.M. Wu, J. Huang, Y. Ding, D.W. Pang, L.J. Li, Chromosoma 117 (2008) 181.
[563] D.R. Larson, W.R. Zipfel, R.M. Williams, S.W. Clark, M.P. Bruchez, F.W. Wise, W.W. Webb, Science 300 (2003) 1434.
[564] Y.F. Chen, Z. Rosenzweig, Anal. Chem. 74 (2002) 5132.
[565] C.Q. Dong, H.F. Qian, N.H. Fang, J.C. Ren, J. Phys. Chem. B 110 (2006) 11069.
[566] V. Maurel, M. Laferriere, P. Billone, R. Godin, J.C. Scaiano, J. Phys. Chem. B 110 (2006) 16353.
[567] A. Sukhanova, L. Venteo, J. Devy, M. Artemyev, V. Oleinikov, M. Pluot, I. Nabiev, Lab. Invest. 82 (2002) 1259.
[568] A.M. Derfus, W.C.W. Chan, S.N. Bhatia, Adv. Mater. 16 (2004) 961.
[569] A. Sukhanova, M. Devy, L. Venteo, H. Kaplan, M. Artemyev, V. Oleinikov, D. Klinov, M. Pluot, J.H.M. Cohen, I. Nabiev, Anal. Biochem. 324 (2004) 60.
[570] L.C. Mattheakis, J.M. Dias, Y.J. Choi, J. Gong, M.P. Bruchez, J.Q. Liu, E. Wang, Anal. Biochem. 327 (2004) 200.
[571] S. Kim, Y.T. Lim, E.G. Soltesz, A.M. De Grand, J. Lee, A. Nakayama, J.A. Parker, T. Mihaljevic, R.G. Laurence, D.M. Dor, L.H. Cohn, M.G. Bawendi, J.V. Frangioni, Nat. Biotechnol. 22 (2004) 93.
[572] T.J. Dougherty, J. Opt. Soc. Am. B: Opt. Phys. 1 (1984) 555.
[573] T.G. Truscott, A.J. McLean, A. Phillips, W.S. Foulds, Mol. Aspects Med. 11 (1990) 106.
[574] D. Kovalev, M. Fuji, in: G. Cao, C.J. Brinker (Eds.), Annual Review of Nano Research, World Scientific, Singapore, 2008, p. 159.
[575] D. Kovalev, E. Gross, N. Kunzner, F. Koch, V.Y. Timoshenko, M. Fujii, Phys. Rev. Lett. 89 (2002).
[576] A.C.S. Samia, X.B. Chen, C. Burda, J. Am. Chem. Soc. 125 (2003) 15736.
[577] M.E. Wieder, D.C. Hone, M.J. Cook, M.M. Handsley, J. Gavrilovic, D.A. Russell, Photochem. Photobiol. Sci. 5 (2006) 727.
[578] T.Y. Hulchanskyy, I. Roy, L.N. Goswami, Y. Chen, E.J. Bergey, R.K. Pandey, A.R. Oseroff, P.N. Prasad, Nano Lett. 7 (2007) 2835.
[579] Y. Cheng, A.C. Samia, J.D. Meyers, I. Panagopoulos, B.W. Fei, C. Burda, J. Am. Chem. Soc. 130 (2008) 10643.